Lecture Notes on

3+1 Numerical Relativity

v0.1

S.Bernuzzi ©
sebastiano.benuzzi@uni-jena.de
Jena FSU

Last update: July 8, 2021

Contents

1. About

Numerical relativity (NR) is the art of solving Einstein Field Equations (EFEs) with computers. These lecture notes focus on the 3+1 formalism for NR; they do not substitute books and papers. Here, intuitive or simplified arguments are preferred to more rigorous but lenghtly mathematical definitions. The reader is referred to the literature for the latter. For a historical perspective, I recommend to read the abstract/content of the original articles listed in the resources cited in the main text.

These notes follow rather closely Gourgoulhon's 2006 lecture notes and the Baumgarte&Shapiro's 2003 review (and the following book) but are more compact/essential, thus less complete. I learnt NR myself from those references in years 2005/2006. Baumgarte&Shapiro's notes were one of the best reviews on the 3+1 formalism. Later, I had the luck to attend Gourgoulhon's lectures at IHP Paris in 2006. The book of Alcubierre (2008) covers some additional key aspects (hyperbolicity, punctures, etc) and it is the main source for the (1+1)D and (1+2)D numerics tutorials associated to these lectures.

The lectures notes cover about 12-14 lectures of 1.5-2 hours. The lectures are to be complemented by tutorials during which some calculations are presented in detail (Gauss-Codazzi-Ricci equations, slicings of Schwarzschild spacetime, etc) and basic numerical aspects/computer experiments are discussed (function approximation, solution of wave and Poisson equations, symbolic calculations, etc). Please visit

`http://sbernuzzi.gitpages.tpi.uni-jena.de/nr/`

for an updated list of references and other material.

The spacetime and the metric are indicated as $(\mathcal{M}, g_{ab})$ and the notation mostly follows Wald's book: signature convention $(-,+,+,+)$, $a, b, ...$ indexes in abstract notation, $\alpha, \beta, ...$ indexes of tensor components, $i, j, ...$ spatial coordinate indexes, etc. Vector and tensors are sometimes indicated as $\boldsymbol{v}$ and $\boldsymbol{g}$, i.e. avoiding the abstract notation, to stress the geometrical meaning of the equations. Coordinate basis of the tange vector space $T_p(M)$ are indicated as $\boldsymbol{e}_\mu$; the natural basis of partial derivatives is $\boldsymbol{e}_\mu = \boldsymbol{\partial}_\mu$. The dual basis $\boldsymbol{e}^{*\nu}$ $(\boldsymbol{e}_\mu \boldsymbol{e}^{*\nu} = \delta^\nu_\mu)$ is constructed by the gradients of the coordinates is $\boldsymbol{e}^{*\mu} = \mathrm{d}x^\mu$. The exterior derivative of an n-form is indicated with $\mathbf{d}$; applied to scalars it reduces to the gradient (1-form) $\mathbf{d}f = \mathrm{d}f = \mathrm{grad}(f)$ with components $(\mathbf{d}f)_\mu = (\mathrm{d}f)_\mu = \partial_\mu f$. Covariant derivatives (Levi-Civita connection) are indicated with ∇ $(n = 4)$ or D $(n = 3)$. ∇ applied to scalars reduces to the gradient $\nabla f = \mathrm{d}f$ (components $\nabla_\mu f = (\mathrm{d}f)_\mu = \partial_\mu f$) and it is consistent with the concept of tangent vector $\boldsymbol{v}(f) = v^\mu \nabla_\mu f$. The symbol $:=$ is an assignment, while $\equiv$ an identity. We work in $n = 4$ dimensions if not stated differently. Units: $c = G = 1$.

I welcome constructive feedbacks. Red text is work in progr...

2. Resources

2.1 Books

Specialistic

- M.Alcubierre "Introduction to 3+1 Numerical Relativity", Oxford Science Publications (2008)
- T.W.Baumgarte & S.L. Shapiro "Numerical Relativity", Cambridge University Press (2010)
- L.Rezzolla & O.Zanotti "Relativistic Hydrodynamics" Oxford University Press (2013)
- M.Shibata "Numerical Relativity" World Scientific Publishing (2016)

General

- A.M.Anile "Relativistic Fluids and Magneto-fluids" Cambridge University Press (1990)
- Y.Choquet-Bruhat "General Relativity and the Einstein Equations" Oxford Mathematical Monographs (2009)
- R.Wald "General Relativity" University of Chicago Press (1984)

2.2 Lecture notes

Specialistic

- T.W.Baumgarte & S.L.Shapiro Numerical Relativity and Compact Binaries Phys. Rep.376, 41 (2003)
- E.Gourgoulhon 3+1 Formalism and Bases of Numerical Relativity Lecture Notes in Physics (Springer) (2012)
- E.Gourgoulhon Construction of initial data for 3+1 numerical relativity J. Phys.: Conf. Ser. 91 012001 (2007)
- E.Gourgoulhon An introduction to relativistic hydrodynamics
- E.Gourgoulhon An introduction to the theory of rotating relativistic stars
- E.Arnowitt, S.Deser, C.W.Misner The Dynamics of General Relativity
- D.Hilditch An Introduction to Well-posedness and Free-evolution

General

- M.Blau Lecture Notes on General Relativity
- S.M.Carrol Lecture Notes on General Relativity
- P.T. Chru'sciel Lectures on Energy in General Relativity

2.3 Suggested articles

Original

- Hahn and Lindquist (1964) First supercomputer numerical relativity simulation of colliding black holes
- Smarr et al (1976), Anninos et al (1993), Anninos et al (1994) Head-on collision of black holes
- R.F.Stark and T.Piran (1985) Gravitational-Wave Emission from Rotating Gravitational Collapse
- Nakamura et al (1987) Gravitational collapse and gravitational waves from black holes
- Choptuik (1993), Abrahams and Evans (1993) Critical collapse
- Bernstein (1993), Bona et al (1994) Anninos et al.(1995) 1+log slicing
- Balakrishna et al (1996) Alcubierre et al (2000) (2002) Gamma-drivers
- Anninos et al (1994) Apparent and event horizons
- Wilson & Mathews (1995) and (2000), Oechslin et al (2001) Neutron star mergers with IWM
- Shibata and Nakamura (1995), Baumgarte and Shapiro (1998); H.Beyer and O.Sarbach Gundlach and Martin-Garcia (2004) BSSNOK formulation and hyperbolicity analysis
- Brandt and Bruegmann (1997) Bowen-York puncture initial data
- Gourgoulhon (1998) on Bonazzola et al (1997) Shibata (1998) Teukolsky (1998) Irrotational binary neutron star configurations
- Font et al (1998} and (2002) Several tesbeds for general relativistic hydrodynamics
- Shibata and Uryu (1999) First binary neutron star merger in GR

- Gourgoulhon et al (2000) Initial data for binary neutron stars in quasi-circular orbits
- Granclement et al (2001) CTS initial data for binary black hole in quasi-circular orbits
- Bona et al (2003) Gundlach et al (2005) Z4 formulation and constraint damping
- Bonazzola et al (2003) Garfinkle et al (2007) Brown (2009) Baumgarte et al Background metric and non-Cartesian coordinates
- Bonazzola et al (2003) Constrained scheme for GR (alternative to free evolution schemes)
- Bruegmann et al (2003) First one-orbit binary black hole simulation
- Alcubierre et al (2003), Babiuc et al and Cao&Hilditch Apple with Apple tests (testbeds for NR)
- Lindblom et al (2005) Generalized Harmonic formulation in first order form
- Pretorius (2005), Baker et al (2005), Campanelli et al (2005) Black hole mergers breaktrough
- Hannam et al (2006), Brown (2007), Thierfelder et al (2010) On the meaning of the moving puncture gauge
- Baker et al (2006), Campanelli et al (2007), Campanelli et al (2007), Herrmann et al (2007), Gonzalo et al (2007) Black hole kicks
- Palenzuela+ (2008) Palenzuela (2012) GR resistive magnetohydrodynamics
- Tichy (2011), Binary neutron star initial data with spin
- Le Tiec (2012) Helical Killing vector and Kepler's law
- Thorne (1981), Shibata et al (2011), Cardall et al (2013) GR relativistic radiation hydrodynamics, moment formalism and 3+1 decompositions
- Radice (2017) Shibata&Kiuchi (2017) GR viscous hydrodynamics simulations

Reviews

- Y.Choquet-Bruhat & J.W.York "The Cauchy Problem, in General Relativity and Gravitation, one hundred Years after the Birth of Albert Einstein", Vol. 1, edited by A.Held, Plenum Press, New York (1980)
- R.Bartnik & J.Isenberg The Constraint Equations
- G.B.Cook Initial Data for Numerical Relativity
- J.A.Font Numerical Hydrodynamics and Magnetohydrodynamics in General Relativity
- P.Grandcleent & J.Novak Spectral Methods for Numerical Relativity
- L.Lehner & F.Pretorious Numerical Relativity and Astrophysics
- J.L.Jaramillo & E.Gourgoulhon Mass and Angular Momentum in General Relativity
- J.M.Marti & E.Mueller Numerical Hydrodynamics in Special Relativity
- O.Rinne Numerical and analytical methods for asymptotically flat spacetimes
- U.Sperhake The numerical relativity breakthrough for binary black holes
- W.Tichy The initial value problem as it relates to numerical relativity

2.4 Numerical methods

Books and lectures notes

- J.P.Boyd Chebyshev and Fourier Spectral Methods
- M.W.Choptuik Relativistic Astrophysics and Numerical Relativity, Numerical Analysis for Numerical Relativists
- B.Gustafsson, H.O.Kreiss and J.Oliger, Time-dependent problems and difference methods, John Wiley,New York 1995.
- C.W.Shu Numerical Methods for Hyperbolic Conservation Laws

Papers

- M.J.Berger & J.Oliger Adaptive mesh refinement for hyperbolic partial differential equations
- M.J.Berger & P.Colella Local adaptive mesh refinement for shock hydrodynamics

2.5 Web resources and Software

- AMR AMR is a package of Fortran routines for the numerical solution of hyperbolic conservation laws in 2 and 3 space dimensions
- Cactus and Einstein toolkit a community project for numerical relativity
- Choptuik and Pretorius webpages for lectures, tutorial, and examples
- GRChombo open-source code for numerical general relativity simulations based on Chombo
- GRwiki yes, a wikipage!
- GRHypS 1+1 GR code for evolutions with puncture gauge
- GR1D 1+1 GR and neutrino transport code for supernova expolosion
- nuLib Basic standard set of neutrino matter interaction routines that can be readily incorporated in radiation-hydrodynamics codes
- PARAMESH A parallel adaptive mesh refinement community toolkit. See also this paper

- PETSc a suite of data structures and routines for the scalable (parallel) solution of scientific applications modeled by PDEs.
- PySpinSph Spin Weighted Spherical Harmonics for Python/NumPy
- SageMath and SageManifold. See also these lecture notes and this paper. Online notebooks of interest (Thanks to E.Gourgoulhon):
  - Kruskal diagram ipynb (cell 44)
  - Kruskal diagram ipynb (cell 95)
  - Kruskal diagram ipynb (cell 19)
  - 3+1 split
  - 3+1 split ipynb
- xAct and contributed examples and these lectures

3. Introduction

Numerical relativity (NR) is the art of solving Einstein Field Equations (EFEs) with computers. This introductory lecture defines the scope of numerical relativity (NR), summarizes basic facts on EFE as PDE system and introduces the concept of *globally hyperbolic spacetime*. Most of these concepts are typically covered in advanced GR courses, a complete discussion can be found in the

Suggested readings. *Chap. 8,9,10 of Wald's book; Chap. 1 of Alcubierre's book.*

3.1 The numerical relativity problem

The development of NR is motivated by the following physics problems:

- Gravitational collapse and black hole (BH) formation
- BH and neutron star (NS) collisions
- Dynamical stability of stationary solutions (from rotating stars and discs to black strings)

Common features of the physics problems above:

1. Strong gravity
2. No symmetries or reduced symmetries
3. Nonstationary ("dynamical", "time-dependent") solutions of GR

The last two points imply that no Killing vectors, or a minimal number of them, are present. Killing vectors are often the key element to simplify EFE, introduce preferred coordinates, and compute analytical solutions; the alternative is the numerical approach. The NR problem:

Solve EFE

$$G_{ab} = 8\pi T_{ab} \ , \tag{3.1}$$

on a computer to find GR solutions of theoretical and astrophysical relevance.

Breakdown the problem:

(i) Formulate EFE as PDE system (hypothesis on the spacetime/manifold needed)
(ii) Formulate well-posed PDE schemes (if possible) and specify coordinates
(iii) Develop numerical algorithms
(iv) Extract meaningful information (e.g. gravitational waves at null-infinty, global mass-energy)

Item (iii) can be further broken into:

(a) Solution of nonlinear PDE of elliptic/hyperbolic/mixed/unknown type
(b) Space(time) discretization (problem dependent)
(c) Treat singularities and horizons (formation, movement, etc)
(d) High-performance-computing (HPC) techniques

3.2 EFE as PDE system

The EFE can be written as a 2nd order PDE system of 10 equations by introducing a coordinate system. For example in vacuum one obtains

$$0 = R_{\mu\nu} = -\frac{1}{2} g^{\alpha\beta}\partial_\alpha\partial_\beta g_{\mu\nu} + g^{\alpha\beta}\partial_\alpha\partial_{(\mu}g_{\nu)\beta} - \frac{1}{2} g^{\alpha\beta}\partial_\mu\partial_\nu g_{\alpha\beta} + Q_{\mu\nu}[\partial g, g] \tag{3.2a}$$

$$= -\frac{1}{2} g^{\alpha\beta}\partial_\alpha\partial_\beta g_{\mu\nu} - g_{\alpha(\mu}\partial_{\nu)}H^\alpha + \tilde{Q}_{\mu\nu}[\partial g, g] \tag{3.2b}$$

where $Q_{\mu\nu}$ (and $\tilde{Q}_{\mu\nu}$) represent the *non-principal part* (lower derivatives of $g_{\mu\nu}$), and the second line is re-written introducing the quantity

$$H^\alpha = \partial_\mu g^{\alpha\mu} + \frac{1}{2} g^{\alpha\beta} g^{\rho\sigma} \partial_\beta g_{\rho\sigma} \tag{3.3}$$

for later use. The resulting equations are not, however, 10 independent equations for the components $g_{\mu\nu}$ of the metric tensor because the 4 Bianchi identities,

$$\nabla_a G^{ab} = 0 \ , \tag{3.4}$$

are further relations between the metric components.

Questions:

(i) What type of equations are EFE?
(ii) How to formulate initial/boundary values problems?
(iii) Are the latter well-posed?

Proper answers will be given during the course. The following operative definition of well-posedness is sufficient for the time being:

Definition 3.2.1. *A PDE problem is well-posed iff exists a unique solution that depends continuously on the boundary data (at least locally in time for IVP)*

3.2.1 Maxwell field equations

Weak-field (linearized) EFE are analogous to Maxwell equations; we start recalling the Cauchy or initial value problem (IVP) in electromagnetism. Call $F_{\alpha\beta}$ the Maxwell tensor and A^α the vector potential, Maxwell equations on flat spacetime in vacuum read

$$0 = \partial^\alpha F_{\alpha\beta} = \partial^\alpha (\partial_\alpha A_\beta - \partial_\beta A_\alpha) \ . \tag{3.5}$$

While Eq. (3.5) appears as 4 wave-like equations for the 4 components of A_α, the $C = 0$ equation ($\beta = 0$ component) does not contain 2nd time derivatives. Indeed, the $\beta = 0$ component is

$$0 = \partial^\alpha (\partial_\alpha A_0 - \partial_0 A_\alpha) = \Box A_0 - \partial_0 \partial^\alpha A_\alpha = \cancel{-\partial_0^2 A_0} + \underbrace{\partial_i \partial^i A_0}_{\Delta A_0} \cancel{+\partial_0^2 A_0} - \partial_0 \partial^i A_i \tag{3.6a}$$

$$= \partial^i (\partial^i A_0 - \partial_0 A_i) = \partial^i F_{i0} = \partial^i E_i =: C \tag{3.6b}$$

The electric field is defined as

$$E_\alpha = F_{\alpha 0} = F_{\alpha\beta} n^\beta \quad \text{with} \quad n^\beta = (1, \vec{0}) \tag{3.7}$$

introducing the timelike vector n^α (that "selects" the components F_{0i}).

If one tries to take a time derivative of the equation to obtain a dynamical one, one just find zero

$$\partial^0 C = \partial^0 [\partial^\alpha (\partial_\alpha A_0 - \partial_0 A_\alpha)] = \partial^i [\underbrace{[\partial^\alpha (\partial_\alpha A_i - \partial_i A_\alpha)}_{\text{l.h.s. of Maxwell eq. for } \beta = i}] \doteq 0 \ , \tag{3.8}$$

as a result of the identity

$$\partial^\alpha [\partial^\beta F_{\alpha\beta}] = \underbrace{\partial^\alpha \partial^\beta}_{\text{sym}} \underbrace{F_{\alpha\beta}}_{\text{antisym}} \equiv 0 \tag{3.9}$$

that was used in the second passage (The $\doteq$ indicates as usual "on solution"/"on shell"). Hence,

- The equation
$$C = \partial_\alpha E^\alpha = \partial^\alpha (\partial_\alpha A_0 - \partial_0 A_\alpha) = 0 \tag{3.10}$$
is a *constraint*, and
- If initially satisfied, it is "transported along the dynamics" because $\partial_0 C = 0$
- The Maxwell equations are *undetermined* (3 equations for the 4 components A_α)
- As formulated above, they do not admint a well-posed IVP: given a solution with initial data $A_\alpha(t=0), \partial_0 A_\alpha(t=0)$ (on a given spatial surface) the component A_0 can be arbitrarily specified to obtain another solution.

At this point, one exploits the gauge freedom: two solutions

$$A_\alpha \quad \text{and} \quad A_\alpha + \partial_\alpha \phi$$

represent the same electric and magnetic fields [Alt. the physical solution is the equivalence class of all the A_α related to each other by the gauge transformation above]. For example, fix

$$\partial^\alpha A_\alpha = 0 \quad \text{(Lorentz gauge, LG)} \ , \tag{3.11}$$

and obtain from Eq. (3.5)

$$0 = \partial^\alpha F_{\alpha\beta} = \partial^\alpha \partial_\alpha A_\beta - \cancel{\partial_\beta \partial^\alpha A_\alpha} \overset{LG}{=} \partial^\alpha \partial_\alpha A_\beta = \Box A_\beta \ . \tag{3.12}$$

- The 4 equations are now dynamical (contain 2nd derivatives)
- The IVP is well posed (4 wave equations)
- For any choice of $A_\alpha(t=0), \partial_0 A_\alpha(t=0)$ that satisfies the gauge

$$\partial^\alpha A_\alpha(t=0) = 0 \quad \text{and} \quad \partial_0 \partial^\alpha A_\alpha(t=0) = 0 \,, \tag{3.13}$$

  The LG is satisfied for all times because

$$0 \doteq \partial_\beta(\Box A^\beta) = \Box(\partial_\beta A^\beta) \tag{3.14}$$

- The constraint $C=0$ ($\beta=0$ eq. before gauge fixing) is sastified along the dynamics

$$C = \Box A_\alpha - \partial^\alpha \partial_0 A_\alpha = \Box A_\alpha - \partial_0 \partial^\alpha A_\alpha \overset{LG}{\doteq} -\partial_0 \partial^\alpha A_\alpha \overset{LG}{\doteq} 0 \tag{3.15}$$

Summary 3.2.1. *Maxwell equations for A_α (Eq. (3.5)) admit a well-posed IVP if one works in an appropriate gauge (e.g. Eq. (3.11)) and if initial data satisfy the constraint Eq. (3.10).*

3.2.2 EFE: constraints and evolution equations

The structure of EFE (no approximation) is very similar to Maxwell equations. Let us assume the spacetime has a timelike vector field n^a that defines a *foliation* of 3D spatial hypersurfaces [Will discuss below the exact hypothesis and formalism]. In vacuum, the projections of EFE along n^b is

$$0 \doteq G_{ab} n^b =: C_a[\partial_i^2 g, \partial g, g] \tag{3.16}$$

and does not depend on 2nd time derivatives: they are 4 constraints. The Bianchi identities (Eq. (3.4)) play the role of the identity in Eq. (3.9) and guarantee that the constraints are transported along the dynamics.

A direct way to see the above equation are constraints is to pick coordinates such that $C^\mu = G^{0\mu}$. The Bianchi identities imply

$$\nabla_\alpha G^{\alpha\mu} = 0 \quad \Rightarrow \quad \partial_0 G^{0\mu} = \underbrace{-\partial_k G^{k\mu} - \Gamma^\mu_{\alpha\beta} G^{\alpha\beta} - \Gamma^\alpha_{\alpha\rho} G^{\mu\rho}}_{\text{this r.h.s contains at most } \partial_0^2 g} \,, \tag{3.17}$$

because the l.h.s. $\partial_0 G^{0\mu}$ contains at most $\partial_0^2 g$, C^μ contains at most first time derivatives.

To show the "propagation" property of these constraints, take initially $C^\mu(t=0) = G^{0\mu}(t=0) = 0$. The EFE in vacuum $G_{\mu\nu} \doteq 0$ (valid for all times) imply the constraints are zero all times:

$$\partial_0 C^\mu = \partial_0 G^{0\mu} \doteq 0 \,. \tag{3.18}$$

Similarly to Maxwell eqs, one is interested to the EFE solution given by the equivalence class of all the metric $g_{\alpha\beta}$ related to each other by coordinate transformation (diffeomorphism invariance). A way to obtain a well-posed IVP for Eq. (3.2a) is to choose coordinates such that $R_{\mu\nu} \sim \Box g_{\mu\nu}$, i.e.

$$H^\alpha \equiv 0 \quad \text{(Harmonic gauge)} \,, \tag{3.19}$$

and initial data for $g_{\mu\nu}$ that satisfy the constraints.

$$0 = \Box x^\mu = g^{\alpha\beta}\nabla_\alpha\nabla_\beta x^\mu = g^{\alpha\beta}\nabla_\alpha(\partial_\beta x^\mu) = g^{\alpha\beta}[\partial_\alpha(\underbrace{\partial_\beta x^\mu}_{\delta^\mu_\beta}) - \underbrace{\partial_\gamma x^\mu}_{\delta^\mu_\gamma}\Gamma^\gamma_{\alpha\beta}] = 0 - g^{\alpha\beta}\Gamma^\mu_{\alpha\beta} = -H^\mu \,. \tag{3.20}$$

3.3 Causality and globally hyperbolic spacetime

Above, when separating the EFE in constraints and evolution equations, we have implicitly assumed the existance of a global notion of time that determines past and future of each event.

In flat spacetime (special relativity) the causal structure is simple and given by the light cones: an event can be connected by spacelike, timelike, null curves to other events, and that determines in an absolute sense its future and its past. In the language of hyperbolic PDE, the light cone determines the domain of dependence and the domain of influence of the solution of the wave equation, $\Box\phi = 0$.

In GR the *global* causal structure of the spacetime is more complex. As extreme example, one can consider a *closed* set of causally-connected events: it is impossible to say which event of the set happened before or after another one. The situation corresponds to the existance of closed timelike curves; an example is given by the Gödel cosmology that satisfies EFE with the cosmological constant, Fig. 3.1 left panel. Other examples are discussed in e.g. Chap. 2 of Carroll's book.

One considers "physically realistic" a spacetime in which "causality can be clearly established", i.e. it is possible to continuously distunguish between past and future as the event p moves in $\mathcal{M}$. Such manifolds are called *time-orientable*. Examples

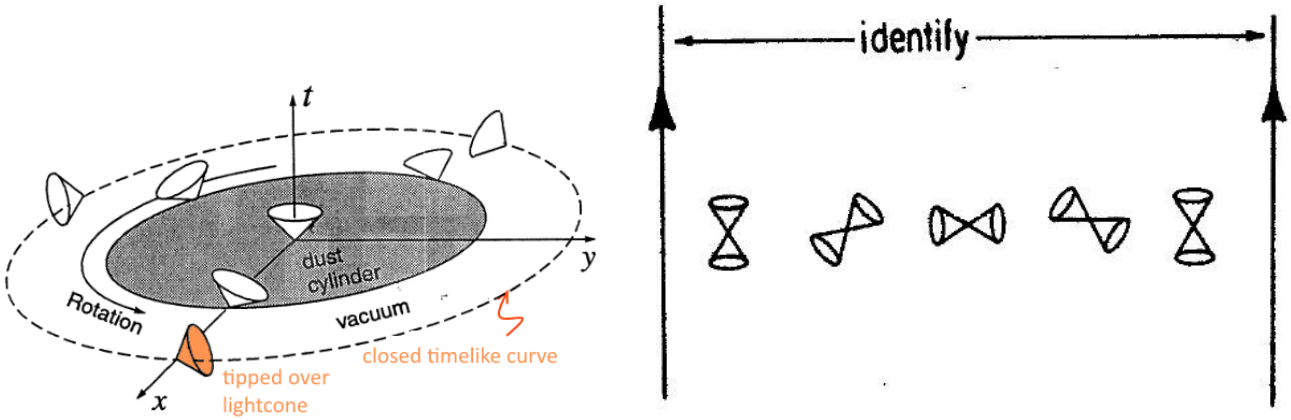

Figure 3.1: Left: closed timelike curves in Gödel Universe. Right: non time-orientable manifold.

- Mikowski and Schwarzschild spacetimes are time-orientable;
- Gödel spacetime is time orientable;
- The right panel of Fig. 3.1 shows a non time-orientable spacetime.

Some definitions in time-orientable manifolds:

- *Achronal set* $S \subset \mathcal{M}$: subset of events that are **not** connected by timelike curves. No event in S is in the future/past of other events in S.
- *Future domain of dependence of* S $D_+(S)$: the set of events such that every causal curve intersect S in the past.
- *Future Cauchy horizon of* S $H_+(S)$: the boundary of $D_+(S)$.
- The two definitions above can be extended "to the past" by substituting $+ \mapsto -$ and "past"$\mapsto$ "future".
- *Domain of dependence* $D(S) = D_+(S) \cup D_-(S)$.
- *Cauchy surface* is a spacelike hypersurface $\Sigma \subset \mathcal{M}$ whose domain of dependence is the entire manifold $D(\Sigma) = \mathcal{M}$ ($H(\Sigma) = 0$). Every causal (timelike or null) curve without end-point intersect Σ only once. In other terms, given Σ one can predict past and future. Note Σ are not unique.

And finally the most important definition:

Definition 3.3.1. $(\mathcal{M}, \boldsymbol{g})$ *is said* globally hyperbolic spacetime *iff admits a Cauchy surface.*

Spacetimes of interest for NR (and in general for most of GR solutions of physical interest) are assumed to be globally hyperbolic. For example, it should be clear that weak-field spacetimes or the spacetime outside a star are of such type. The discussion in the next Section should also convice the reader that Schwarzschild is globally hyperbolic (Recall the singularity $r = 0$ is not part of the manifold).

Remark 3.3.1. *The IVP for the wave equation* $\Box_g \phi = 0$ *is well posed in a globally hyp. spacetime. See e.g. (Baer et al., 2008).*

3.3.1 Trapped surfaces and singularities

The relevance of globally hyperbolic spacetimes for NR can be appreciated in the context of singularity formation. In this discussion we introduce the concept of apparent horizon that will be further developed in Sec. X.

Consider a 3D spatial hypersurface Σ with normal n^a and a closed 2D surface $S \subset \Sigma$ with normal s^a. Construct the null vectors

$$\ell^a_\pm = \frac{1}{\sqrt{2}}(n^a \pm s^a) \tag{3.21}$$

they are tangent to the congruence of outgoing and ingoing null geodesics through S, i.e. they generate light rays leaving or reaching S.

Construct the projection of the derivative of ℓ^a onto S

$$k_{ab} = P^c_a P^d_b \nabla_c \ell^+_d \ . \tag{3.22}$$

This symmetric tensor is the *extrinsic curvature* of the null hypersurface generated by ℓ^a_+ (outgoing light from S) and the explicit form of the projector is [justification will be given later]

$$P^a_b = \delta^a_b + n^a n_b - s^a s_b \ . \tag{3.23}$$

The *expansion* of the congruence of outgoing null geodesics S is the trace

$$\theta = k^a_a \ , \tag{3.24}$$

that measures how the light rays separate as they leave S. The value $\theta < 0$ (> 0) everywhere on S indicates that the volume enclosed by the light rays is smaller (larger) as they leave S, i.e. they are getting closer (apart). In these cases the surface S is said

$$\begin{aligned} \theta < 0 \ &: \ \text{trapped surface} \\ \theta = 0 \ &: \ \text{marginally trapped surface} \end{aligned}$$

Definition 3.3.2. *The outermost marginally trapped surface is called* apparent horizon.

Remark 3.3.2. *In flat spacetime there are no trapped surfaces.*

Example 3.3.1. *In Schwarzschild spacetime all the spheres with $r < 2M$ are trapped surfaces. That is immediately clear considering radial null rays. The apparent horizon coincides with the $r = 2M$ horizon.*

Theorem 3.3.1. *Penrose's theorem (Penrose, 1965; Hawking and Ellis, 2011) states that*

$$\left.\begin{array}{l} \mathcal{M} \text{ is a globally hyperbolic spacetime with} \\ \text{Null energy condition } T_{ab}\ell^a\ell^b \geq 0 \ \forall \ell^a : \ell^a\ell_a = 0 \\ \exists \text{ trapped surface} \end{array}\right\} \Rightarrow \text{a singularity will necessarily form in the future .}$$

Remark 3.3.3. *Under such conditions, a singularity will form during the gravitational collapse.*

Remark 3.3.4. *The theorem does not imply the existance of a horizon (BH). The formation of a naked singularity is possible and it would break the causality. Hence, naked singularity are not compatible with globally hyperbolic spacetimes and singularities should be hidden by an horizon* (Cosmic censorship conjecture) *(Penrose, 1969).*

4. 3+1 Geometry

In this lecture we will discuss
(i) The concepts of 3-metric γ_{ij} and extrinsic curvature K_{ij}
(ii) The 3-metric as the dynamical variable for 3+1 GR
(iii) The "kinematical" 3+1 equation (Eq. (4.30))
Differential geometry concepts:
- Hypersurfaces in manifold
- Spacelike hypersurfaces and projector
- 3+1 foliations of globally hyperbolic spacetime
- Gauss-Codazzi-Ricci equations for the 3+1 geometry

All results are independent on EFE.

Suggested readings. *Chap. 10 of Wald's books; Chap. 2-3 of Gourgoulhon's 3+1 lecture notes.*

4.1 Hypersurfaces

A *hypersurface* $\Sigma = \phi(\hat{\Sigma})$ (dimension $n-1=3$) of a time-orientable manifold (dimension $n=4$) is the image of an *embedding* (1-to-1 map)

$$\phi : \hat{\Sigma} \mapsto \mathcal{M} \ . \tag{4.1}$$

The 1-to-1 character of the embedding map guarantes that Σ does not intersect itself. Introducing a coordinate system x^μ in $\mathcal{M}$, Σ can be locally defined as the level set of a scalar field. Take for example the first coordinate,

$$\forall p \in \mathcal{M},\ p \in \Sigma \ \Leftrightarrow \ x^0(p) = 0 \ . \tag{4.2}$$

The push-forward and pull-back maps are used to identify the tangent and cotangent spaces in $\mathcal{M}$ and $\hat{\Sigma}$

$$\phi_* : T_p(\hat{\Sigma}) \mapsto T_p(\mathcal{M}) \tag{4.3a}$$
$$v^i \mapsto \phi_* v^\mu = (0, v^i)$$
$$\phi^* : T^*_p(\mathcal{M}) \mapsto T^*_p(\hat{\Sigma}) \tag{4.3b}$$
$$\omega_\mu = (\omega_0, \omega_i) \mapsto \phi_* \omega_\mu = \omega_i$$

Obviously, the reverse maps cannot be in general defined [See e.g. Appendix A and D of Carroll's book for the definition of pullback/pushforward], but for spacelike hypersurfaces a projector operator is possible (see below). Conventionally, $\hat{\Sigma}$ and Σ are identified; vectors (and tensors) on $\hat{\Sigma}$ and the push-forward image in $\mathcal{M}$ are also identified.

The pull-back operation allows one to define the *induced metric* (3-metric) on Σ,

$$\boldsymbol{\gamma} := \phi^* \boldsymbol{g} \ , \tag{4.4}$$

whose components are

$$\gamma_{ij} = \frac{\partial x^\alpha}{\partial y^i} \frac{\partial x^\beta}{\partial y^j} g_{\alpha\beta} \ . \tag{4.5}$$

Σ is characterized by the 1-form $\mathbf{d}x^0$ (gradient) associated to the scalar function x^0. The *normal* to Σ is the vector associated to the 1-form,

$$(\nabla t)^a = g^{ab} \nabla_b t = g^{ab} (\mathrm{d}x^0)_b \ , \tag{4.6}$$

and it defines the unique direction perperndicular to Σ.

Characterization:
- Σ spacelike iff γ_{ab} has signature $(+,+,+)$; $(\nabla t)^a$ is timelike
- Σ timelike iff γ_{ab} has signature $(-,+,+)$; $(\nabla t)^a$ is spacelike
- Σ null iff γ_{ab} has signature $(0,+,+)$; $(\nabla t)^a$ is null

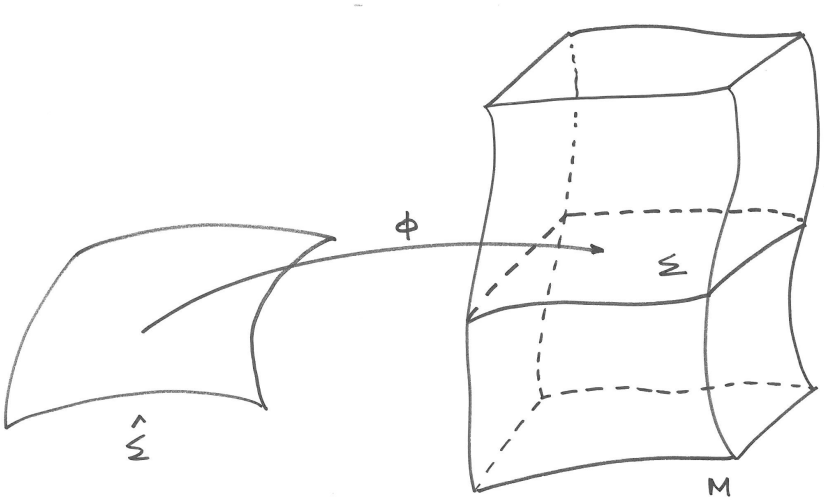

Figure 4.1: Sketch of an embedding.

Note that the normal to a null hypersurface cannot be normalized. In the other cases, the two unit normal vectors are defined via

$$n^a = \pm\alpha(\nabla t)^a \quad \text{with} \quad \alpha := \left(\pm g^{ab}\nabla_a t \nabla_b t\right)^{-1/2} \ . \tag{4.7}$$

If Σ is not null, the metric γ is nondegenerate and it exists a Levi-Civita connection D and a Riemann tensor,

$$(D_i D_j - D_j D_i)v^k = R^k_{lij} v^l \ . \tag{4.8}$$

The Riemann tensor R^k_{lij} describes the curvature of $(\Sigma, \boldsymbol{\gamma})$ exactly as ${}^4R^c_{dab}$ does for the ambient spacetime $(\mathcal{M}, \boldsymbol{g})$. Thus, it is an *intrinsic* curvature measure. It does not tell, however, how Σ is bent in $\mathcal{M}$. State differently one may ask: How does n^a changes when it is transported along Σ ? To measure that, one defines the *extrinsic curvature* of Σ as the symmetric tensor (Note the use of "nonindex notation")

$$\begin{aligned} \boldsymbol{K} &: T_p(\Sigma) \times T_p(\Sigma) \mapsto \mathbb{R} \\ (\boldsymbol{u}, \boldsymbol{v}) &\mapsto \boldsymbol{K}(\boldsymbol{u}, \boldsymbol{v}) = K_{ab} u^a v^b = -u_a v^b \nabla_b n^a \ , \end{aligned} \tag{4.9}$$

The extrisic cuvature measures the projection of the derivative of n^a along a vector in v^a in Σ with another vector u^a in Σ, see Fig. (4.2). The symmetry of $\boldsymbol{K}$ follows from Frobenius theorem [see e.g. Wald's book].

4.2 Spacelike hypersurfaces

Focus now on spacelike hypersurfaces. The tangent space of $\mathcal{M}$ can be decomposed as the sum of the tangent space of Σ and the space generated by the unit vector n^a,

$$\begin{aligned} T_p(\mathcal{M}) &= V_p(n) \oplus T_p(\Sigma) \\ v^a &= v_\perp n^a + v^a_\parallel \ . \end{aligned} \tag{4.10}$$

One can then define the reverse maps of Eq. (4.3) in terms of the *projector*

$$\begin{aligned} P &: T_p(\mathcal{M}) \mapsto T_p(\Sigma) \\ v^a &\mapsto v^a + (v^b n_b) n^a \end{aligned} \tag{4.11}$$

whose explicit form is

$$P^a_b = \delta^a_b + n^a n_b \tag{4.12}$$

since

$$P^a_b v^b = (\delta^a_b + n^a n_b)(v_\perp n^b + v^b_\parallel) = v_\perp n^a + v_\perp n^a \underbrace{n_b n^b}_{=-1} + v^b_\parallel + n^a \underbrace{n_b v^b_\parallel}_{=0} = v^b_\parallel \ . \tag{4.13}$$

For vectors tangent to $T_p(\Sigma)$ ($v_\perp = 0$) P is the identity operator; for normal vectors $P(v^a_\parallel) = 0$.

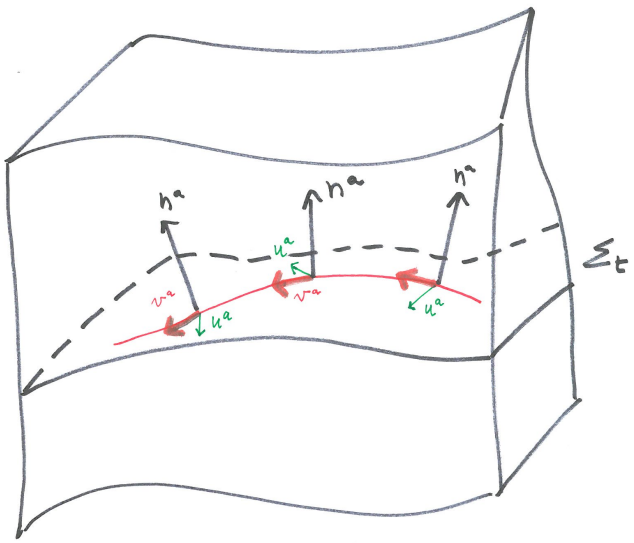

Figure 4.2: Geometrical meaning of extrinsic curvature, see Eq. (4.9).

In particular, a formula for the induced metric on Σ can be obtained as [1]

$$\gamma_{ab} = P^c_a P^d_b g_{cd} = (\delta^c_a + n^c n_a)(\delta^d_b + n^d n_b) g_{cd} \tag{4.14a}$$
$$= \delta^c_a \delta^d_b g_{cd} + \delta^c_a n^d n_b g_{cd} + \delta^d_b n^c n_a g_{cd} + n^c n_a n^d n_b g_{cd} \tag{4.14b}$$
$$= g_{ab} + n^d n_b g_{ad} + n^c n_a g_{cb} + n_a n_b \underbrace{n^d n^c g_{cd}}_{=-1} \tag{4.14c}$$
$$= g_{ab} + n_a n_b \tag{4.14d}$$

From the above formula one notices that the projector is nothing else than the 3-metric γ_{ab} with an index raised with g_{ab}:

$$P^a_b = \delta^a_b + n^a n_b = g^{ac}\gamma_{cb} =: \gamma^a_b \ . \tag{4.15}$$

The projector (from now on we use the notation γ^a_b) can be used to project tensors on Σ. Not surprisingly, the covariant derivative D can be obtained from the ∇ cov. derivative as

$$D_e T^{a_1 \dots a_p}_{b_1 \dots b_q} = \gamma^{a_1}_{c_1} \dots \gamma^{a_p}_{c_p} \gamma^{d_1}_{b_1} \dots \gamma^{d_q}_{b_q} \gamma^f_e \nabla_f T^{c_1 \dots c_p}_{d_1 \dots d_q} \ . \tag{4.16}$$

Although intuitive, this result would need proof (D is a connection, is torsion free, and is compatible with the metric).

In terms of the projector, the extrinsic curvature of Σ is defined as

$$K_{ab} := -\gamma^c_a \gamma^d_a \nabla_{(c} n_{d)} = -\gamma^c_a \gamma^d_a \nabla_c n_d \ , \tag{4.17}$$

which is compatible with the formula/definition introduced above. The curvature of the ambient spacetime $\mathcal{M}$ can be expressed in terms of the intrisinc curvature of Σ and of K_{ab} by using the projector. The resulting geometrical equations are known as Gauss-Codazzi-Ricci and are reported in Sec. 4.4.

4.3 Spacelike foliations & Eulerian observers

Consider now globally hyperbolic spacetimes. The main property of such spacetimes is that they can be foliated by a family of nonintersecting spatial hypersurfaces Σ_t,

$$\mathcal{M} = \cup \Sigma_t \ , \tag{4.18}$$

where $t(p) = x^0(p)$ is the scalar function (its value is also conventionally indicated with the same letter, $t \in \mathbb{R}$). The unit normal is taken with a minus

$$n^a = -\alpha (\nabla t)^a \quad \text{with} \quad \alpha := \left(-g^{ab}\nabla_a t \nabla_b t\right)^{-1/2} > 0 \quad (\textit{lapse} \text{ function}) \tag{4.19}$$

[1] See Gourgoulhon 3+1 lecture notes for the underlining formal aspects of the following three formulas.

in such a way it is future pointing if t is increasing in the future (Recall the contraction with the Lorentzian metric to go from 1-form to vector). The normal vector defines worldlines orthogonal to Σ_t; these observes are called *Eulerian observers*. Physically, Σ_t can be then locally interpreted as the set of events that are simultaneous in the Eulerian frame. The acceleration of Eulerian observers is

$$a_a := n^b \nabla_b n_a \ , \tag{4.20}$$

and as every acceleration it is orthogonal to the velocity, $a_a n^a = 0$. Together with n^a one defines the *normal evolution vector*

$$m^a := \alpha n^a \ , \tag{4.21}$$

with the properties

$$m^a m_a = -\alpha^2 \tag{4.22a}$$

$$\nabla_m t = m^a \nabla_a t = \alpha n^a \nabla_a t = -\frac{\cancel{\alpha}}{\cancel{\alpha}} \underbrace{n^a n_a}_{=-1} = +1 \ ; \tag{4.22b}$$

the latter property can be taken as alternative definition.

With these definitions at hand, one can understand the geometrical properties of spacelike foliations that represent the "kinematics" of 3+1 GR. The main characteristics of the foliation are

(i) The normal evolution vector carries points from Σ_t to points to $\Sigma_{t+\delta t}$;
(ii) The lapse function relates the coordinate time t (used to label each hypersurface) to the *proper* time measured by Eulerian observers;
(iii) Tensors defined on Σ_t can be transported to tensors on $\Sigma_{t+\delta t}$ using the Lie derivative along the normal evolution vector m^a;
(iv) The Lie derivative (evolution) of the 3-metric is given by the extrinsic curvature.

In other words, hypersurfaces Σ_t and $\Sigma_{t+\delta t}$ are identified by the diffeomorphism generated by m^a. The globally hyperbolic spacetime $(\mathcal{M}, g)$ can be interpreted as representing the time development of the 3-dimensional (Σ_0, γ). Hence, the 3-metric is identified as the dynamical variable of GR in globally hyperbolic spacetimes.

Start showing (i). Consider a point $p \in \Sigma_t$ and displace it to $p' = p + \delta t \boldsymbol{m}$ using the vector $\boldsymbol{m}$ (Note the use of the notation without indexes). The value of the scalar function t defining the foliation at p' is simply given by the very definition of gradient of a function:

$$t(p') = t(p + \delta t \boldsymbol{m}) = t(p) + \delta t \underbrace{\nabla_m t}_{=1} = t(p) + \delta t \ , \tag{4.23}$$

which proves the claim. One says that Σ_t *are Lie dragged by* m^a.

Show (ii). Choose the 2 points p and p' in such a way they are on the worldline of a Eulerian observer. The proper time interval measured by the Eulerian observer is given by the length of the displacement vector $\delta t \boldsymbol{m}$

$$\delta\tau = \sqrt{-\boldsymbol{g}(\delta t \boldsymbol{m}, \delta t \boldsymbol{m})} = \sqrt{-\boldsymbol{g}(\boldsymbol{m}, \boldsymbol{m})}\delta t = \sqrt{-m^a m_a}\delta t = \alpha \delta t \tag{4.24}$$

Property (iii) follows instead from (i) and the definition of Lie derivative [2], Fig. (4.3). Given a vector <u>field</u> $\boldsymbol{v}$,

$$\mathcal{L}_m \boldsymbol{v}(t + \delta t) := \lim_{\delta t \to 0} \frac{\boldsymbol{v}(t + \delta t) - \Phi_{\delta t}\boldsymbol{v}(t)}{\delta t} \ , \tag{4.26}$$

where Φ is the diffeomorphism associated to $\boldsymbol{m}$, i.e. transporting the vector $\boldsymbol{v}(t) = \vec{pq}(t)$ along the field lines of $\boldsymbol{m}$. Because of (i), both the transported points $\Phi_{\delta t}(p)$ and $\Phi_{\delta t}(q)$ belong to $\Sigma_{t+\delta t}$, the transported vector belong to Σ_t. The $\mathcal{L}_m \boldsymbol{v}(t + \delta t)$ is a vector in $\Sigma_{t+\delta t}$ because it results from the difference of two vector in $\Sigma_{t+\delta t}$.

To show (iv) one needs the following expression for the extrinsic curvature in terms of the acceleration of Eulerian observers

$$K_{ab} = -\gamma_a^c \gamma_b^d \nabla_c n_d = -\gamma_a^c (\delta_b^d + n^d n_b)\nabla_c n_d = -\gamma_a^c (\nabla_c n_b + n_b \underbrace{n^d \nabla_c n_d}_{=1/2\nabla_c(n^d n_d)=0}) \tag{4.27a}$$

$$= -\gamma_a^c \nabla_c n_b = -(\delta_a^c + n^c n_a)\nabla_c n_b = -\nabla_a n_b - n^c n_a \nabla_c n_b \tag{4.27b}$$

$$= -\nabla_a n_b - n_a a_b \ . \tag{4.27c}$$

[2] The Lie derivative can be used to define *Killing vectors* (KVs):

$$\mathbf{k} \ \text{ is a KV iff } \ \mathcal{L}_k \mathbf{g} = 0 \ , \tag{4.25}$$

i.e. the metric is left invariant if transported along $\mathbf{k}$. KVs implement symmetries of the spacetime: they transform the points (events) on the manifold (spacetime) in such a way the distance between these points remain invariant (KVs are infitesimal generators of isometries). It is possible to show that each KV of a spacetime corresponds to a conserved quantity along geodesics; this quantity is given by $\boldsymbol{g}(\boldsymbol{k}, \boldsymbol{v})$, where $\boldsymbol{v}$ ($\dot{x}^\mu$ in components) is the geodesic's tangent vector.

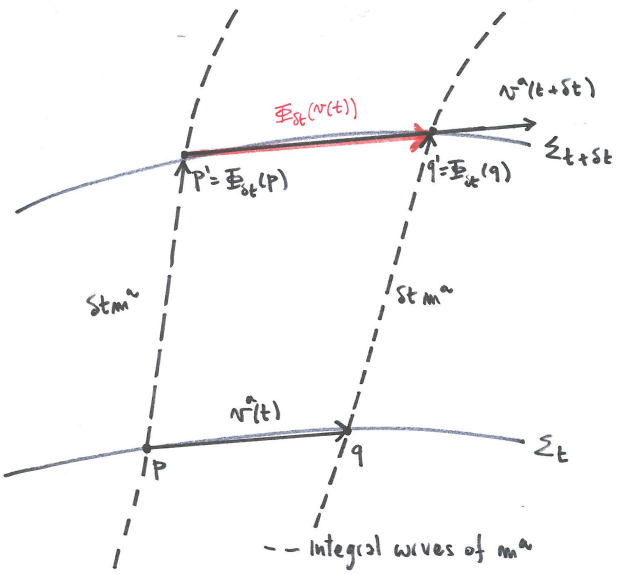

Figure 4.3: Lie derivative of vector field $\boldsymbol{v}$ along the normal evolution vector.

Then use the definition of the Lie derivative for tensors

$$\mathcal{L}_n \gamma_{ab} = \mathcal{L}_n (g_{ab} + n_a n_b) = 2\nabla_{(a} n_{b)} + n_a \mathcal{L}_n n_b + n_b \mathcal{L}_n n_a = 2(\nabla_{(a} n_{b)} + n_{(a} a_{b)}) = -2K_{ab} \ . \tag{4.28}$$

The expression above can be used to define the extrinsic derivative. Now using the property of the Lie derivative,

$$\mathcal{L}_n \gamma_{ab} = \phi^{-1} \mathcal{L}_{\phi n} \gamma_{ab} \quad \forall \phi \text{ scalar} \ , \tag{4.29}$$

that simply follows from the definition of $\mathcal{L}$ and from $\gamma_{ab} n^b = 0$, one obtains:

$$\boxed{\mathcal{L}_m \gamma_{ab} = -2\alpha K_{ab}} \tag{4.30}$$

4.4 Gauss-Codazzi-Ricci equations

The GCR equations are the fundamental equations connecting the 4-dimensional Riemann ${}^4R_{abcd}$ and Ricci tensors to the 3-dimensional ones.

Remark 4.4.1. *Gauss and Codazzi eqs are defined on a single spatial hypersurface Σ and thus they do not require a foliation Σ_t (They do not require the hypothesis of globally hyperbolic spacetime) Ricci eqs contain instead derivative in the direction normal to the hypersurface, i.e. terms $\propto \mathcal{L}_n$.*

4.4.1 Gauss eq.

Spatial projection:

$$\gamma_a^p \gamma_b^q \gamma_c^r \gamma_d^s \ {}^4R_{pqrs} = R_{abcd} + K_{ac} K_{bd} - K_{ad} K_{bc} \tag{4.31a}$$

Contracted equations:

$$\gamma_a^p \gamma_b^q \gamma_c^r \gamma_d^s \ {}^4R^c_{spq} = R^c_{dab} + K^c_a K_{bd} - K_{ad} K^c_b \tag{4.31b}$$

$$\gamma_{ap} n^q \gamma_b^r n^s \ {}^4R^p_{qrs} + \gamma_a^p \gamma_b^q \ {}^4R_{pq} = R_{ab} + K K_{ab} - K_{as} K^s_b \tag{4.31c}$$

$${}^4R + 2 \ {}^4R_{ab} n^a n^b = R + K^2 - K_{ab} K^{ab} \tag{4.31d}$$

4.4.2 Codazzi eq.

Three spatial projection and one n^a contraction:

$$\gamma_b^r \gamma_a^p \gamma_c^q n^s \ {}^4R_{rpqs} = D_a K_{bc} - D_b K_{ac} \tag{4.32a}$$

Contracted equations:

$$\gamma^c_r n^s \gamma^p_a \gamma^q_b \, {}^4R^r_{sqp} = D_b K^c_a - D_a K^c_b \tag{4.32b}$$

$$\gamma^p_a n^q \, {}^4R_{pq} = D_a K - D_r K^r_a \tag{4.32c}$$

4.4.3 Ricci eq.

Two spatial projections and two n^a contractions:

$$\gamma_{ap} n^r \gamma^q_b n^s \, {}^4R^p_{rps} = \alpha^{-1} \mathcal{L}_m K_{ab} + \alpha^{-1} D_a D_b \alpha + K_{as} K^s_b \tag{4.33a}$$

Contracted equations:

$$\gamma^p_a \gamma^q_b \, {}^4R_{qp} = -\alpha^{-1} \mathcal{L}_m K_{ab} - \alpha^{-1} D_a D_b \alpha + R_{ab} + K K_{ab} - 2 K_{ac} K^c_b \tag{4.33b}$$

The above equation is derived by combining the Ricci equation with the term "$\gamma\gamma nn \, {}^4R$" of the contracted Gauss eq.

Note the derivation of the Ricci requires to the following relation between the acceleration of Eulerian observers and the covariant derivative of the lapse:

$$a_a = n^p \nabla_p n_a = -n^p \nabla_p (\alpha \nabla_a t) = -n^p \nabla_p \alpha \underbrace{\nabla_a t}_{=-\alpha^{-1} n_a} - \alpha n^p \underbrace{\nabla_p \nabla_a t}_{\nabla_a(-\alpha^{-1} n_p)} \tag{4.34a}$$

$$= +\alpha^{-1} n_a n^p \nabla_p \alpha + \alpha n^p \nabla_a (-\alpha^{-1} n_p) = +\alpha^{-1} n_a n^p \nabla_p \alpha + \frac{\cancel{\alpha}}{\alpha^{\cancel{2}}} \underbrace{n^p n_p}_{=-1} \nabla_a(\alpha) - \underbrace{n^p \nabla_a n_p}_{=0} \tag{4.34b}$$

$$= +\alpha^{-1} n_a n^p \nabla_p \alpha + \alpha^{-1} \nabla_a \alpha = +\alpha^{-1} \underbrace{(n_a n^q + g^q_a)}_{\gamma^q_a} \nabla_q \alpha = \alpha^{-1} \gamma^q_a \nabla_a \alpha = D_a \ln \alpha \tag{4.34c}$$

5. 3+1 Decomposition of GR

In this lecture the EFE

$$ {}^4G_{ab} = {}^4R_{ab} - \frac{1}{2}\,{}^4R g_{ab} = 8\pi T_{ab} \tag{5.1} $$

are written as equations for the 3-metric and extrisinc curvature in a form that is adapted to the 3+1 foliation of the spacetime. The resulting equations split into

- *constraints*: Hamiltonian (Eq. (5.5)) and Momentum (Eq. (5.9))
- *evolution (or dynamical) equations*: for the extrinsic curvature (Eq. (5.15))

Together with the kinematical equation for the 3-metric (Eq. (4.30)) they form the basic equations for 3+1 GR.

Suggested readings. *Chap. 4 of Gourgoulhon 3+1 lecture notes; Chap. 2 of Baumgarte lecture notes (Book's Chap. 2); Chap. 2 of Alcubierre's book; Chap. 10 of Wald's book.*

5.1 Historical remark

Key steps:
1927 Darmois, Gaussian coordinates ($\alpha = 1$, $\beta^i = 0$)
1939 Lichnerowicz, Zero shift coordinates ($\alpha \neq 1$, $\beta^i = 0$)
1948 - 1956 Choquet-Bruhat, generic coordinates
1962 Arnowitt+Deser+Misner (ADM) Hamiltonian formulation
1979 York, 3+1/ADM form of the equations using $\boldsymbol{K}$ as momentum (Hereafter ADMY equations)

5.2 Constraints

The constraints are the equations $({}^4G_{ab} - 8\pi T_{ab})n^b = 0$.

5.2.1 Hamiltonian

Consider the projection of ${}^4G_{ab}$ orthogonal to Σ_t, i.e. along $n^a n^b$:

$$ {}^4G_{ab}n^a n^b = {}^4R_{ab}n^a n^b - \frac{1}{2}{}^4R g_{ab}n^a n^b = \underbrace{{}^4R_{ab}n^a n^b + \frac{1}{2}{}^4R(+1)}_{1/2\times \text{ l.h.s of contracted Gauss eq.}} = \frac{1}{2}(R + K^2 - K_{ab}K^{ab}) \tag{5.2} $$

where the second lines uses

$$ -g_{ab}n^a n^b = -n^a n^b(\gamma_{ab} - n_a n_b) = 0 + n^a n^b n_a n_b = +(-1)(-1) = +1 \ , \tag{5.3} $$

and the third line substitutes the contracted Gauss Eq. (4.31d).

From the very definition of stress-energy tensor, the projection

$$ E := n^a n^b T_{ab} \quad \text{(Matter energy density)} \tag{5.4} $$

is the energy density measured by the Eulerian observers.

The projection of Eq. (5.1) orthogonal to Σ_t is thus

$$ \boxed{\mathcal{C}_0 := R + K^2 - K_{ab}K^{ab} - 16\pi E = 0 \quad \text{(Hamiltonian constraint)} \ .} \tag{5.5} $$

Note it contains only spatial quantities and spatial derivatives.

5.2.2 Momentum

Consider the mixed projection of ${}^4G_{ab}$ along $\gamma^p_a n^q$:

$$ {}^4G_{pq}\gamma^p_a n^q = {}^4R_{qp}\gamma^p_a n^q - \frac{1}{2}{}^4R g_{pq}\gamma^p_a n^q = \underbrace{{}^4R_{qp}\gamma^p_a n^q}_{\text{l.h.s of contracted Codazzi eq.}} + 0 = D_a K - D_p K^q_a \tag{5.6}$$

where the second line uses

$$ g_{pq}\gamma^p_a n^q = (\gamma_{pq} - n_p n_q)\gamma^p_a n^q = \underbrace{\gamma_{pq}n^q}_{=0}\gamma^p_a - \underbrace{n_p\gamma^p_a}_{=0}\underbrace{n_q n^q}_{=-1} = 0 \ , \tag{5.7}$$

and the third line substitutes the contracted Codazzi Eq. (4.32c).

From the very definition of stress-energy tensor, the projection

$$ P_a := -\gamma^p_a n^q T_{pq} \quad \text{(Matter momentum density)} \tag{5.8}$$

is the momentum density measured by the Eulerian observers.

The projection of Eq. (5.1) along $\gamma^p_a n^q$ is thus

$$ \mathcal{C}_i := D_j K^j_i - D_i K - 8\pi P_i = 0 \quad \text{(Momentum constraint)} \ . \tag{5.9}$$

Note these equations contain only spatial quantities and spatial derivatives. With an abuse of notation we use the spatial indexes $i, j, ...$ instead of $a, b, ...$ for some of the final equations. This anticipates the expressions in adapted coordinates.

5.3 Evolution

Consider the $\gamma^a_q\gamma^b_p$ projection of the trace reverse EFE,

$$ {}^4R_{ab} = 8\pi(T_{ab} - \frac{1}{2}T g_{ab}) \ . \tag{5.10}$$

The l.h.s of Eq. (5.10) is the l.h.s. of the contracted Ricci eq combined with the contracted Gauss eq, Eq. (4.33b).

Project now the stress-energy tensor. From the definition, the projection

$$ S_{ab} := \gamma^p_a\gamma^q_b T_{pq} \quad \text{(Stress tensor)} \tag{5.11}$$

is the stress tensor for the Eulerian observers, a purely spatial tensor on Σ_t. Its trace is

$$ S := g^{ab}S_{ab} = \gamma^{ij}S_{ij} \ . \tag{5.12}$$

Using the above definitions, one can directly verify that the 4-dimensional stress-energy tensor has been decomposed as

$$ T_{ab} = S_{ab} + 2n_{(a}P_{b)} + n_a n_b E \ , \tag{5.13}$$

and its trace is

$$ T = g^{ab}T_{ab} = g^{ab}S_{ab} + \underbrace{g^{ab}n_a P_b}_{(\gamma^{ab}+n^a n^b)n_a P_b = 0} + g^{ab}n_b P_a + \underbrace{n_a n_b g^{ab}}_{=-1}E = S - E \ , \tag{5.14}$$

since for each term involving the momentum $(\gamma^{ab} + n^a n^b)n_a P_b = \gamma^{ab}n_a \times P_b + n^b P_b \times (n^a n_a) = 0 \times P_b + 0 \times (-1)$.

The projection of Eq. (5.10) along $\gamma^a_q\gamma^b_p$ is thus

$$ \mathcal{L}_m K_{ij} = -D_i D_j \alpha + \alpha\{R_{ij} + K K_{ij} - 2K_{ik}K^k_j + 4\pi[(S-E)\gamma_{ij} - 2S_{ij}]\}. \tag{5.15}$$

The above equation complete the 3+1 decomposition in tensor equations.

Summary 5.3.1. *The EFE are equivalent to the system of equations composed by the Hamiltonian (Eq. (5.5), one scalar eq) and Momentum (Eq. (5.9), one rank-1 tensorial equation with 3 components), plus the dynamical equations for the 3-metric (Eq. (4.30)) and the extrinsic curvature (Eq. (5.15)). The latter are rank-2 tensorial equations involving symmetric 3-tensors (6 components). Hence, the 10 EFE equations [4 involving only first "time derivatives" of g_{ab} and 6 involving second time derivatives of g_{ab}] are decomposed in 4 equations involving at most time derivatives of γ_{ij} (K_{ij}) and 6+6 equations involving up to first time derivatives of γ_{ij} and K_{ij}.*

Remark 5.3.1. *General covariance (coordinate gauge freedom) is maintained in the 3+1 equations; in the equations above the lapse and the coordinates on Σ_t are unspecified. The gauge freedom is translated in the freedom for choice of the* slicings *(lapse) + 3 spatial coords.*

In Sec. 5.4 coordinate adapted to the foliation are introduced to reduce the system to PDEs.

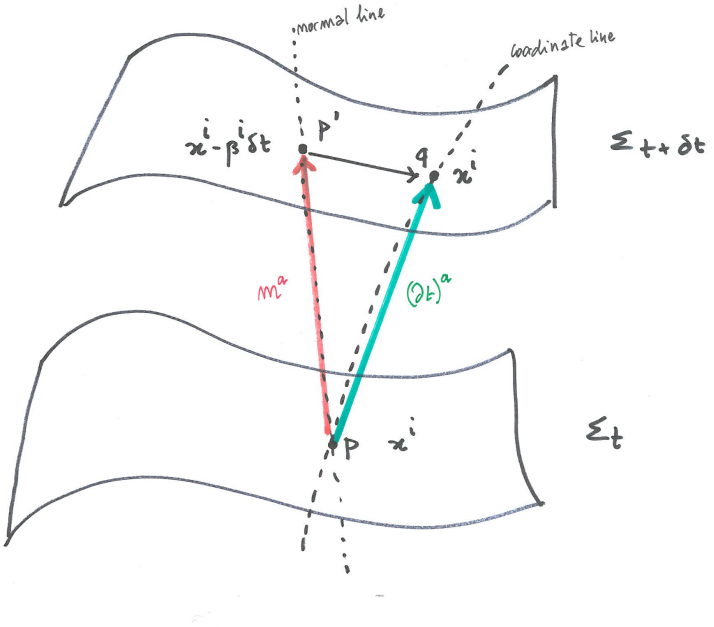

Figure 5.1: Adapted coordinates for 3+1 decomposition.

5.4 Adapted coordinates

The natural coordinates adapted to the 3+1 decomposition of $\mathcal{M}$ are

$$x^\mu = (t, x^i) \ , \tag{5.16}$$

where x^i are coordinates on Σ_t. The *natural basis* for $T_p(\mathcal{M})$ is thus composed by the vectors

$$\boldsymbol{e}_\mu = \boldsymbol{\partial}_\mu = (\boldsymbol{\partial}_t, \boldsymbol{\partial}_i) \ , \tag{5.17}$$

where $\boldsymbol{\partial}_i \in T_p(\Sigma_t)$ and $\boldsymbol{\partial}_t$ is called the *time vector*. The dual basis is composed of the coordinate gradients

$$\boldsymbol{e}^{*\mu} = \mathbf{d}x^\mu \ . \tag{5.18}$$

Properties of the time vector [see Fig. (5.1)]:

(i) $\boldsymbol{\partial}_t$ is tangent to the curves defined by constant values of the spatial coordinates $c(t): \ x^i = (const)^i$;

(ii) $\boldsymbol{\partial}_t$ Lie-drags the hypersurfaces exactly as the normal evolution vector $\boldsymbol{m}$ does. That is because $\mathbf{d}t(\boldsymbol{\partial}_t) = \nabla_a t (\partial_t)^a = 1$ follows from the definition of dual basis $\mathbf{d}x^\mu(\boldsymbol{\partial}_\nu) = \delta^\mu_\nu$;

(iii) $\boldsymbol{\partial}_t$ is **not**, in general, a timelike vector! The direction of $\boldsymbol{\partial}_t$ depends on the spatial coordinates and it is written as

$$(\partial_t)^a := m^a + \beta^a = \alpha n^a + \beta^a \ ; \tag{5.19}$$

where β^a is a spatial *shift vector*, $n_a \beta^a = 0$, defined by the expression [1] In other terms, in general, $\boldsymbol{\partial}_t$ is not parallel to $\boldsymbol{m}$. Taking the time vector norm,

$$||\boldsymbol{\partial}_t||^2 = (\partial_t)_a (\partial_t)^a = -\alpha^2 + \beta_a \beta^a = -\alpha^2 + \beta^2 \ , \tag{5.20}$$

one has

$$(\partial_t)^a \ \text{timelike} \Leftrightarrow \beta^2 < \alpha^2 \tag{5.21a}$$

$$(\partial_t)^a \qquad \text{null} \Leftrightarrow \beta^2 = \alpha^2 \tag{5.21b}$$

$$(\partial_t)^a \ \text{spacelike} \Leftrightarrow \beta^2 > \alpha^2 \tag{5.21c}$$

Remark 5.4.1. *If $\boldsymbol{\partial}_t$ is spacelike, then the shift vector is said* superluminar *and coordinates from one surface to the next "change at a speed faster than light". This is not unphysical since there are no observers associated to the time vector (Eulerian observers are associated to $\boldsymbol{n}$).*

[1] The introduction of the shift vector is due to Choquet-Bruhat in 1956; the names lapse/shift are due to Wheeler (1964).

It is now easy to express the key quantities in adapted coordinates:

$$(\partial_t)^a = (1,0,0,0) \tag{5.22a}$$
$$\beta^a = (0,\beta^i) \tag{5.22b}$$
$$n^a = \alpha^{-1}(\partial_t)^a - \alpha^{-1}\beta^a = \alpha^{-1}[(1,0,0,0) - (0,\beta^i)] = (\alpha^{-1}, -\alpha^{-1}\beta^a) \tag{5.22c}$$
$$n_a = (-\alpha,0,0,0) \tag{5.22d}$$

and the metric

$$g_{00} = \boldsymbol{g}(\boldsymbol{\partial}_t,\boldsymbol{\partial}_t) = -\alpha^2 - \beta^2 \tag{5.22e}$$
$$g_{0i} = \boldsymbol{g}(\boldsymbol{\partial}_t,\boldsymbol{\partial}_i) = (m_a+\beta_a)(\partial_i)^a = \underbrace{m_a(\partial_i)^a}_{=0} + \beta_a(\partial_i)^a = \beta_i \tag{5.22f}$$
$$g_{ij} = \boldsymbol{g}(\boldsymbol{\partial}_i,\boldsymbol{\partial}_j) = \boldsymbol{\gamma}(\boldsymbol{\partial}_i,\boldsymbol{\partial}_j) = \gamma_{ij}\ . \tag{5.22g}$$

The line element is

$$ds^2 = -\alpha^2 \mathrm{d}t^2 + \gamma_{ij}(\mathrm{d}x^i + \beta^i \mathrm{d}t)(\mathrm{d}x^j + \beta^j \mathrm{d}t) \tag{5.23}$$

Example 5.4.1. *The* weak field *metric*

$$ds^2 = -(1+2\phi)\mathrm{d}t^2 + (1-2\phi) f_{ij}\mathrm{d}x^i \mathrm{d}x^j \tag{5.24}$$

where f_{ij} is the flat metric is in the 3+1 with

$$\alpha = \sqrt{1+2\phi} \approx 1+\phi\ ,\quad \beta^i = 0\ ,\quad \gamma_{ij} = (1-2\phi) f_{ij}\ . \tag{5.25}$$

Matrix form and the inverse metric:

$$g_{\mu\nu} = \begin{bmatrix} g_{00} & g_{0i} \\ g_{0i} & g_{ij} \end{bmatrix} = \begin{bmatrix} -\alpha^2+\beta^2 & \beta_i \\ \beta_i & \gamma_{ij} \end{bmatrix}\ ;\quad g^{\mu\nu} = \begin{bmatrix} g^{00} & g^{0i} \\ g^{0i} & g^{ij} \end{bmatrix} = \begin{bmatrix} -\alpha^{-2} & \alpha^{-2}\beta^i \\ \alpha^{-2}\beta^i & \gamma^{ij} - \alpha^{-2}\beta^i\beta^j \end{bmatrix} \tag{5.26a}$$

Note that $g^{ij} \neq \gamma^{ij}$. In 3+1 formalism the determinants are often indicated as

$$g := \det g_{\mu\nu}\ ;\quad \gamma := \det \gamma_{ij}\ . \tag{5.27}$$

By combining the Cramer rule for the matrix inversion with the expression of g^{00} in terms of the lapse,

$$g^{00} = \frac{1}{\det g_{\mu\nu}} \det g_{ij} = \frac{1}{\det g_{\mu\nu}} \det \gamma_{ij} \tag{5.28}$$
$$= -\alpha^{-2}\ , \tag{5.29}$$

one finds the relation

$$\sqrt{-g} = \alpha\sqrt{\gamma}\ . \tag{5.30}$$

Finally, the Lie derivatives becomes true time derivatives:

$$\mathcal{L}_m = \mathcal{L}_{\partial_t} - \mathcal{L}_\beta = \partial_t - \mathcal{L}_\beta \tag{5.31a}$$
$$\mathcal{L}_\beta \gamma_{ij} = \underbrace{\beta^k D_k \gamma_{ij}}_{=0} + 2D_{(i}\beta_{j)} = 2\partial_{(i}\beta_{j)} - 2\Gamma^k_{ij}\beta_k \tag{5.31b}$$
$$\mathcal{L}_\beta K_{ij} = \beta^k D_k K_{ij} + K_{ik}D_j\beta^k + K_{jk}D_i\beta^k = \beta^k\partial_k K_{ij} + K_{ik}\partial_j\beta^k + K_{jk}\partial_i\beta^k \tag{5.31c}$$

One can now specify the tensorial ADMY equations in adapted coordinates and obtain PDEs. It is immediately clear that the Hamiltonian (Eq. (5.5)) and Momentum (Eq. (5.9)) constraints do not contain second (first) time derivatives ∂_t of the 3-metric (extrisinc curvature) but only the extrinsic curvature. It also immediate to note that there are no equations for the lapse and the shift vectors. As already stated above, the latter are gauge but they *must* be specified to close the system. The simplest choice is to choose (locally)

$$\alpha \equiv 1\ ;\quad \beta^i \equiv 0\ \ \text{(Geodesic gauge)} \tag{5.32}$$

that imply the time coordinate $t = \tau$ represents the proper time of Eulerian observes (Gaussian normal coords) and the curves of constant spatial coordinates $c(t)$ are orthogonal to the hypersurfaces Σ_t. Alt. said, the worldlines of the Eulerian observers are geodesics

$$a_a = n^b\nabla_b n_a = D_a \ln\alpha = 0\ . \tag{5.33}$$

ADMY in geodesic gauge:

$$\partial_t \gamma_{ij} = -2K_{ij} \tag{5.34a}$$
$$\partial_t K_{ij} = R_{ij} + KK_{ij} - 2K_{ik}K^k_j + 4\pi[(S-E)\gamma_{ij} - 2S_{ij}] \tag{5.34b}$$
$$\mathcal{C}_0 := R + K^2 - K_{ij}K^{ij} - 16\pi E = 0 \tag{5.34c}$$
$$\mathcal{C}_i := D_j K^j_i - D_i K - 8\pi P_i = 0 \tag{5.34d}$$

The dynamical ADMY equations are a nonlinear PDE system of first-order-in-time and second-order-in-space wave-like equations. Linearization of the equations around flat background gives for the perturbation h_{ij} [cf. Eq. (3.2a)]

$$\partial_t h_{ij} = -2K_{ij} \tag{5.35a}$$
$$\partial_t K_{ij} = R_{ij} \simeq -\frac{1}{2}\partial_k\partial^k h_{ij} \ , \tag{5.35b}$$

that are the tensor generalization of the wave equation in the form

$$\Box\phi = 0 \quad \Rightarrow \quad \begin{cases} \partial_t \phi &= \Pi \\ \partial_t \Pi &= \partial_i \partial^i \phi \ . \end{cases} \tag{5.36a}$$

It also interesting to re-write the ADMY equations as 2nd order system for the 3-metric. Using the notation $\dot\gamma_{ij} := \partial_t \gamma_{ij}$, the *principal part* (indicated by the use of the symbol $\simeq$) reads:

$$-\ddot\gamma_{ij} + \gamma^{kl}\left(\partial_k\partial_l\gamma_{ij} + \partial_i\partial_j\gamma_{kl} - \partial_i\partial_k\gamma_{jl} - \partial_j\partial_k\gamma_{il}\right) \simeq 0 \tag{5.37a}$$
$$\mathcal{C}_0 := \gamma^{ik}\gamma^{jl}\partial_k\partial_l\gamma_{ij} - \gamma^{ij}\gamma^{kl}\partial_k\partial_l\gamma_{ij} \simeq 0 \tag{5.37b}$$
$$\mathcal{C}_i := \gamma^{jk}\partial_j\dot\gamma_{ki} - \gamma^{kl}\partial_i\dot\gamma_{kl} \simeq 0 \ . \tag{5.37c}$$

The above equations are $6+1+3=10$ second-order PDE equations for the 6 components of γ_{ij} (overdetermined). The inverse metric must be interpreted as a function of the 3-metric using the Cramer inversion formula $\gamma^{ij}(\gamma_{kl})$, hence the depedence in γ_{ij} is in the form of rational polynomials. The first equation is the only one involving second time derivatives of γ_{ij}; it is *quasilinear*: linear in the highest derivatives, while the dependence of the nonprincipal terms on the metric derivatives is quadratic. The Hamiltonian constraint equation involves no metric time derivatives but it is of no known type. Similarly for the momentum. In order to obtain a GR solution, initial data to the first equations must satisfy the solution of the constraint equations. Because constraints are only 4 equations, providing an initial slice also requires to specify some free data. Hence, constraints are usually rewritten in different forms such that (i) the elliptic equations can be mathematically analysed and numerically solved; (ii) the choice of free data in the initial data has physical meaning. This *initial data problem* will be discussed in Sec. 8.

5.5 Z4 system & constraint evolution

Before specifying the 3+1 EFE in adapted coordinates we discuss how constraints propagate along the dynamics. The Z4 equations (Bona et al., 2003),

$${}^4G_{ab} + 2\nabla_{(a}Z_{b)} - g_{ab}\nabla_c Z^c \color{blue}{-\kappa(2n_{(a}Z_{b)} + g_{ab}n_c Z^c)} = 8\pi T_{ab} \ , \tag{5.38}$$

are extended (general covariant extension) field equations that reduce to EFE if the new vector field $Z_a \equiv 0$ (or if it is a Killing vector). The terms in blue are *constraint damping terms* and $\kappa \in \mathbb{R}$ is a damping parameter; we temporarily ignore them. For simplicity the following focus on vaccum equations.

The 3+1 split of Eq. (5.38) reads

$$\mathcal{L}_m \gamma_{ij} = -2\alpha K_{ij} \tag{5.39a}$$
$$\mathcal{L}_m K_{ij} = [\text{... As in Eq 5.15 ...}] + \alpha D_{(i}Z_{j)} \tag{5.39b}$$
$$\mathcal{L}_m \theta = \frac{1}{2}\mathcal{C}_0 - \theta K + D_k Z^k - Z^k D_k \ln\alpha \color{blue}{-3\kappa\theta} \tag{5.39c}$$
$$\mathcal{L}_m Z_i = \mathcal{C}_i + D_i\theta - \theta D_i \ln\alpha - 2K^k_i Z_k \color{blue}{-\kappa Z_i} \ , \tag{5.39d}$$

where $\theta := -n_a Z^a$. In the system above all the equations are dynamical thanks to the introduction of Z_a; the constraints "are translated into a r.h.s" for the time derivatives of Z_a.

From the Bianchi identities one immediately obtains an evolution linear wave-like equation for the field Z_a (see Chap. 10),

$$\nabla^b G_{ab} = 0 \ \Rightarrow \ \ 0 = \Box_g Z_a + R_{ab}Z^b \color{blue}{-\kappa\nabla^b(2n_{(a}Z_{b)} + g_{ab}n_c Z^c)} \ , \tag{5.40}$$

that shows that if initially $\mathcal{C}_0 = \mathcal{C}_i = Z_a = 0$, then the Z4 equations reduce to EFE at all times and the constraints are satisfied all times. In general, the Z4 equations propagate constraints violationg according to the wave-like equation above; the role of the additional terms for $\kappa > 0$ is to damp the violation.

Remark 5.5.1. *The Z4 approach used in GR is a specific case of a general strategy to turn a mixed systems of equations composed by evolution equations (hyperbolic PDEs type) and constraints equations (e.g. elliptic PDEs) into a hyperbolic system of equations by adding extra variables. For example, in magnetohydrodynamics the induction equation and the* $\mathrm{div}\vec{B} = 0$ *constraint can be turned into a hyperbolic system as follows (divergence cleaning, (Dedner et al., 2002)):*

$$\begin{cases} \partial_t B^i + \partial_k (B^k v^i - B^i v^k) & = 0 \\ C := \partial_i B^i & = 0 \end{cases} \Rightarrow \begin{cases} \partial_t B^i + \partial_k (B^k v^i - B^i v^k) + \partial^i \psi & = 0 \\ \partial_t \psi + \partial_i B^i + \kappa \psi & = 0 \ . \end{cases} \tag{5.41}$$

The extended system is a set of hyperbolic equations. By taking a time derivative of the second equation of the extended system and then substituting the first one, one obtains that the field ψ *(time derivative of the constraint* C*) obeys a wave equation with damping term,*

$$\partial_t^2 \psi - \partial_i \partial^i \psi + \kappa \partial_t \psi = 0 \ . \tag{5.42}$$

Moreover it is easy to show that the constrain C *itself satisfy the same equation as* ψ *[exercise]. If initially* $C(0) = 0$ *and* $\partial_t C(0) = \psi = 0$*, then* $C(t) \equiv 0$ *at any time* $t > 0$*. This also implies that a numerical constraint violation localized in a compact region propagates away and is damped as time goes.*

5.6 ADM Hamiltonian formulation

The Hamiltonian formulation of GR starts from the 3+1 decomposition of the action (boundary terms are omitted in what follows, see Chap. 7):

$$S_{\rm GR} = \int {}^4R \sqrt{-g} + (\text{boundary terms}) \tag{5.43}$$

$$\simeq \int dt \int_{\Sigma_t} \underbrace{(R + K_{ij}K^{ij} - K^2)}_{:=\mathcal{L}\ \text{Lagrangian density}} \alpha\sqrt{\gamma} \ . \tag{5.44}$$

The *conjugate momenta* of the 3-metric are

$$\pi^{ij} := \frac{\partial \mathcal{L}}{\partial \dot{\gamma}_{ij}} = \sqrt{\gamma}(K\gamma^{ij} - K^{ij}) \ , \tag{5.45}$$

and the Hamiltonian density is defined from the Legendre transform

$$\mathcal{H} := \pi^{ij}\dot{\gamma}_{ij} - \mathcal{L} = ... = \sqrt{\gamma}\left(\alpha\mathcal{C}_0 + 2\beta^i\mathcal{C}_i + 2D_j(K\beta^j - K_i^j\beta^i)\right) \ . \tag{5.46}$$

The derivation of the last equality simply uses the kinematical equation Eq. (4.30) in adapted coordinates to express K_{ij} in terms of $\dot{\gamma}_{ij}$.

The Hamiltonian is

$$H := \int_{\Sigma_t} \mathcal{H} = \int_{\Sigma_t} \sqrt{\gamma}\left(\alpha\mathcal{C}_0 + 2\beta^i\mathcal{C}_i\right) \ , \tag{5.47}$$

where the divergence term $2D_j(...)$ in $\mathcal{H}$ became a boundary term set to zero, and H should be considered a function of

$$H[\gamma_{ij}, \alpha, \beta^i; \pi^{ij}, \pi^\alpha, \pi_i^\beta] \ , \quad \text{with} \ \ \pi^{(\alpha)} := \frac{\partial \mathcal{L}}{\partial \dot{\alpha}} \equiv 0 \ \text{and} \ \pi_i^{(\beta)} := \frac{\partial \mathcal{L}}{\partial \dot{\beta}^i} \equiv 0 \ ,$$

Hamilton equations then read

$$\dot{\gamma}_{ij} = \frac{\partial \mathcal{H}}{\partial \pi^{ij}} = -2\frac{\alpha}{\sqrt{\gamma}}(\pi_{ij} - \frac{1}{2}\pi\gamma_{ij}) + 2D_{(i}\beta_{j)} \tag{5.48}$$

$$\dot{\pi}^{ij} = -\frac{\partial \mathcal{H}}{\partial \gamma_{ij}} = [... \ \sim \ \text{Eq. (5.15)} \ \ + \ \ \mathcal{C}_0 \ ...] \tag{5.49}$$

$$\dot{\pi}^{(\alpha)} = -\frac{\partial \mathcal{H}}{\partial \alpha} = \mathcal{C}_0 = 0 \quad \text{(Hamiltonian constraint)} \tag{5.50}$$

$$\dot{\pi}_i^{(\beta)} = -\frac{\partial \mathcal{H}}{\partial \beta^i} = \mathcal{C}_i = 0 \quad \text{(Momentum constraint)} \tag{5.51}$$

where Eq. (5.49) (not written down) is equivalent to the 3+1 equation $\mathcal{L}_m K_{ij}$ derived above but with a term proportional to the Hamiltonian constraint. The other difference between the ADM and the York formulation is the use of π_{ij} instead of the extrinsic curvature; they are related by

$$K_{ij} = -\frac{1}{\sqrt{\gamma}}(\pi_{ij} - \frac{1}{2}\pi\gamma_{ij}) \ . \tag{5.52}$$

Note finally that in the ADM formulation lapse and shift are Lagrangian multipliers enforcing the constraints.

6. 3+1 Conformal Decomposition of GR

This lecture introduces the conformal decomposition of 3+1 GR, a key formalism for the solution of the initial data and evolution problems. Concepts

- Conformal decomposition of the 3-metric Eq. 6.1 and background metric.
- Tracelss & conformal decomposition of extrinsic curvature
- Conformally decomposed 3+1 EFE
- Isemberg-Wilson-Mathews approximation of GR

Suggested readings. *Appendix D of Wald's book; Chap. 6 of Gourgoulhon 3+1 lecture notes; Sec. 3.1-3.3 and Sec. 10.2 of Baumgarte lecture notes (Book's Chap.3 and 11); Chap. 2 of Alcubierre's book;*

6.1 Historical remark

1944 Lichnerowicz (1944) introduces the conformal decomposition of the 3-metric and extrinsic curvature for the resolution of the constraint equations. The *initial data problem* consist in the specification of the γ_{ij} and K_{ij} (12 components) on Σ_0 using the 4 constraint equations. The problem is overdetermined, and it is necessary to prescribe some quantities and to solve for some others. The conformal decomposition is the tool used to re-write the constraints in a form that is mathematically (more) tractable and that allows one to identify the physical quantities to prescribe. The initial data problem will be discussed in Chap. 8.

1971 York (1971, 1972) shows that the conformal decomposition of the 3-metric is key to isolate the two degrees of freedom of the gravitational field (grav. waves). The latter are carried by the *conformal equivalence classes of 3-metric* related by a conformal transformation. In other terms, all the 3-metric solution of EFE and related to $\boldsymbol{\gamma}$ via a transformation as in Eq. (6.1) have the same gravitational-wave content. In particular, a conformally flat spacetime $\tilde{\boldsymbol{\gamma}} = \boldsymbol{f}$ contains no waves. York obtains these results in the context of Hamiltonian GR and using a symmetric, traceless, transverse (divergence-free) and conformally invariant rank-2 tensor density (Cotton-York tensor).

90s-. A number of authors e.g. (Shibata and Nakamura, 1995; Frittelli and Reula, 1996; Baumgarte and Shapiro, 1999; Frittelli and Reula, 1999; Alcubierre et al., 2000; Gundlach and Martin-Garcia, 2006) use the conformal decomposition of the ADMY equations to introduce hyperbolic formulations of EFE that give a well-posed initial boundary value problem (IBVP). These formulations, associated to specific gauge conditions that handle singularities (expressed also by hyperbolic eqs, Appendix A), developed into the BSSN and Z4c *free-evolution schemes* for EFE. The latter are currently used for state-of-art simulations of supernovae core collapse and black holes and neutron star binaries.

6.2 Conformal decomposition of the metric

Among all the conformal metrics related to the 3-metric $\boldsymbol{\gamma}$ by

$$\boldsymbol{\gamma} = \Psi^4 \tilde{\boldsymbol{\gamma}} \ , \tag{6.1}$$

it is common to choose the representative (of the conformal equivalence class) given by the one with unit determinant, $\tilde{\gamma} = 1$. For any $n \times n$ matrix A and a number c

$$\det(cA) = c^n \det A \quad \Rightarrow \quad \gamma = \Psi^{12} \tilde{\gamma} \ , \tag{6.2}$$

thus, the unideterminant conformal metric corresponds to a specific choice of the *conformal factor*

$$\Psi = \gamma^{1/12} \quad \Rightarrow \quad \tilde{\gamma} = 1 \ , \quad \tilde{\gamma}_{ij} = \Psi^{-4} \gamma_{ij} = \gamma^{-1/3} \gamma_{ij} \ . \tag{6.3}$$

Problem: Using the definition above

- Ψ is not a scalar field because the determinant transform as

$$\gamma' = \left(\det \frac{\partial x^i}{\partial x^{i'}}\right)^2 \gamma = (\det J^i_{i'})^2 \gamma = J^2 \gamma \tag{6.4}$$

  under coordinate transformation $x^i \mapsto x^{i'}$;
- $\tilde{\gamma}_{ij}$ is not a tensor, but a tensor density of weight $-2/3$ [1] and has **no** unique Levi-Civita connection associated.

6.2.1 Background metric

The problem above can be solved introducing a *background metric* $\boldsymbol{f}$ on Σ_t with the following properties

(i) $\boldsymbol{f}$ is with signature Riemannian $(+,+,+)$ with determinant $f := \det \boldsymbol{f}$;
(ii) The components are time independent,

$$\mathcal{L}_{\partial t} f_{ij} = \frac{\partial f_{ij}}{\partial t} = 0 \ , \tag{6.5}$$

i.e. the background metric is Lie-dragged along the time vector;
(iii) Inverse metric is defined by $f^{ik} f_{jk} = \delta^i_j$
(iv) Associated Levi-Civita connection $\mathcal{D}_k f_{ij} = 0$ with

$$\mathcal{D}^i := f^{ij}\mathcal{D}_j \ \text{ and } \ F^k_{ij} := \frac{1}{2} f^{kl}(\partial_i f_{lj} + \partial_j f_{il} - \partial_l f_{ij}) \ . \tag{6.6}$$

The conformal decomposition is then defined w.r.t. the background metric

$$\Psi := \left(\frac{\gamma}{f}\right)^{1/12} \tag{6.7}$$

$$\tilde{\gamma}_{ij} := \Psi^{-4}\gamma_{ij} \ , (\text{Conformal 3-metric}) \ , \ \ \tilde{\gamma} = f \ . \tag{6.8}$$

$$\tilde{\gamma}^{ij} := \Psi^4 \gamma^{ij} \ \ (\text{Inverse conformal 3-metric}) \ . \tag{6.9}$$

The definition guarantees the Ψ is a scalar on Σ_t and $\tilde{\gamma}_{ij}$ a tensor.

Remark 6.2.1. *In Cartesian coordinates the obvious choice of background metric is the flat metric* $\boldsymbol{f} = \mathrm{diag}(1,1,1)$ *($F^i_{jk} = 0$, $f = 1$) and the formulas simplify ($\mathcal{D}_i = \partial_i$). However, in spherical coordinates the natural choice is* $\boldsymbol{f} = \mathrm{diag}(1, r^2, r^2 \sin^2\theta)$ *leading to nontrivial Christoffel symbols and* $f = r^4 \sin^2\theta$.

Example 6.2.1. *The* weak field *metric is in the form of Eq. (6.1) with conformal factor*

$$\Psi = (1-2\phi)^{1/4} \sim 1 - \frac{1}{2}\phi \ , \tag{6.10}$$

and conformal metric = background metric = flat metric, $\tilde{\boldsymbol{\gamma}} = \boldsymbol{f}$.

Example 6.2.2. *The* Schwarzschild *metric in isotropic coordinates,*

$$ds^2 = -\frac{(1-M/2r)^2}{\psi^2}\mathrm{d}t^2 + \psi^4(\mathrm{d}r^2 + r^2 \mathrm{d}\Omega^2) \tag{6.11}$$

with the function $\psi(r) := (1 + M/2r)$, *is in the form of Eq. 6.1 with conformal factor*

$$\Psi = \psi = 1 + \frac{M}{2r} \tag{6.12}$$

if one takes the background metric $f_{ij} = \mathrm{diag}(1, r^2, r^2\sin^2\theta)$. *The conformal metric coincides with the background metric,* $\tilde{\gamma}_{ij} = f_{ij}$. *Comparing with the conformal factor of the weak field metric one immediately verifies that* $\phi \simeq -M/r$ *that indicates the conformal factor is directly related to the gravitational potential.*

[1] A (p,q) tensor density τ of weight w transforms as $\tau^{a_1\ldots a_p}_{b_1\ldots b_q} \mapsto J^w \, J^{c_1}_{a_1}\ldots J^{b_q}_{d_q} \tau^{a_1\ldots a_p}_{b_1\ldots b_q}$.

6.3 Conformal connection & Ricci tensor

It is now possible to associate a Levi-Civita connection $\tilde{D}\tilde{\gamma}=0$ with Christoffel symbols given by the usual formula applied to $\tilde{\gamma}_{ij}$. The relation between the physical and conformal covariant derivative is given by the formula:

$$D_k T^{i_1\dots i_p}_{j_1\dots j_q} = \tilde{D}_k T^{i_1\dots i_p}_{j_1\dots j_q} + \sum_{r=1}^{p} C^{i_r}_{kl} T^{i_1\dots l\dots i_p}_{j_1\dots j_q} - \sum_{r=1}^{p} C^{l}_{kj_r} T^{i_1\dots i_p}_{j_1\dots l\dots j_q} \tag{6.13}$$

$$C^k_{ij} := \Gamma^k_{ij} - \tilde{\Gamma}^k_{ij} = \frac{1}{2}\gamma^{kl}(\tilde{D}_i\gamma_{lj} + \tilde{D}_j\gamma_{il} - \tilde{D}_l\gamma_{ij}) = 2\left(\delta^k_i\tilde{D}_i\ln\Psi^4 + \delta^k_j\tilde{D}_j\ln\Psi^4 - \tilde{D}^k\ln\Psi\tilde{\gamma}_{ij}\right) \tag{6.14}$$

where the second line defines the tensor C^k_{ij} in terms of the physical and conformal metric. The formula above can be proven by direct calculation but should not be unfamiliar: it is the general relation between two connections [See e.g. Wald's book]. Note the contraction

$$C^k_{ki} = 6\tilde{D}_i\ln\Psi\ . \tag{6.15}$$

The physical and conformal Ricci tensor are related by the general formula relating the Ricci tensors of two connections,

$$R_{ij} = \tilde{R}_{ij} + \tilde{D}_k C^k_{ij} - \tilde{D}_i C^k_{kj} + C^k_{ij}C^l_{lk} - C^k_{ij}C^l_{kj} \tag{6.16a}$$

$$= \tilde{R}_{ij} \underbrace{-2\tilde{D}_i\tilde{D}_j\ln\Psi - 2\tilde{D}_k\tilde{D}^k\ln\Psi\tilde{\gamma}_{ij} + 4\tilde{D}_i\ln\Psi\tilde{D}_j\ln\Psi - 4\tilde{D}_k\ln\Psi\tilde{D}^k\ln\Psi}_{=:R^{\Psi}_{ij}} \tag{6.16b}$$

$$= \tilde{R}_{ij} + R^{\Psi}_{ij} \tag{6.16c}$$

where the second line specifies the expression to the conformal metric case.

Finally, the conformal Ricci scalar $\tilde{R} := \tilde{\gamma}^{ij}\tilde{R}_{ij}$ is related to the physical one by

$$R = \gamma^{ij}R_{ij} = \Psi^{-4}\tilde{\gamma}_{ij}R_{ij} = \dots = \Psi^{-4}\tilde{R} - 8\Psi^{-5}\tilde{D}_i\tilde{D}^i\Psi\ . \tag{6.17}$$

The geometrical formulas above are necessary to conformally decomposed the 3+1 EFE.

6.4 Traceless & conformal decomposition of extrinsic curvature

The conformal decomposition of the extrinsic curvature is performed by first decomposing it in its trace K and traceless part A_{ij}, and then decomposing the "up-up" contraction of the latter, $A^{ij} := \gamma^{ik}\gamma^{jl}A_{kl}$:

Conformal decomposition of the extrinsic curvature:

$$K_{ij} := A_{ij} + \frac{1}{3}K\gamma_{ij}\ , \tag{6.18a}$$

$$A^{ij} := \Psi^p\tilde{A}^{ij}\ . \tag{6.18b}$$

There are two natural choices for the *conformal rescaling*

- $p=-4$, based on the evolution equation $\mathcal{L}_m\gamma_{ij} = -2\alpha K_{ij}$ [Nakamura (1994)]
- $p=-10$, based on the momentum constraint [Lichnerowicz (1944)].

6.4.1 Kinematical equation rescaling

Consider the kinematical eq in conformal variables, and multiply by Ψ^{-4}

$$\mathcal{L}_m(\Psi^4\tilde{\gamma}_{ij}) = -2\alpha A_{ij} - \frac{2}{3}\alpha K(\Psi^4\tilde{\gamma}_{ij}) \quad\Rightarrow\quad \mathcal{L}_m(\tilde{\gamma}_{ij}) = -4\tilde{\gamma}_{ij}\underbrace{\Psi^{-4}\Psi^3\mathcal{L}_m\Psi}_{\mathcal{L}_m\ln\Psi} - 2\alpha\Psi^{-4}A_{ij} - \frac{2}{3}\alpha K\tilde{\gamma}_{ij}\ ; \tag{6.19}$$

Take the trace of the l.h.s. and derive two equations: one for the trace r.h.s. and one using the matrix identity $\mathrm{Tr}(M^{-1}\delta M) = \delta(\ln\det M)$ valid for any matrix M and differential operator δ:

$$\tilde{\gamma}^{ij}\mathcal{L}_m\tilde{\gamma}_{ij} = -4\underbrace{\tilde{\gamma}^{ij}\tilde{\gamma}_{ij}}_{=3}\mathcal{L}_m\ln\Psi - 2\alpha\Psi^{-4}\underbrace{\tilde{\gamma}^{ij}A_{ij}}_{=0} - \frac{2}{3}\alpha K\underbrace{\tilde{\gamma}^{ij}\tilde{\gamma}_{ij}}_{=3} = -12\mathcal{L}_m\ln\Psi - 2\alpha K \tag{6.20a}$$

$$\tilde{\gamma}^{ij}\mathcal{L}_m\tilde{\gamma}_{ij} = \mathcal{L}_m\ln\tilde{\gamma} = (\partial_t - \mathcal{L}_\beta)\ln f = -\mathcal{L}_\beta f = \tag{6.20b}$$

$$= -\tilde{\gamma}^{ij}\mathcal{L}_\beta\tilde{\gamma}_{ij} = -\tilde{\gamma}^{ij}(\beta^k\underbrace{\tilde{D}_k\tilde{\gamma}_{ij}}_{=0} + \tilde{\gamma}_{kj}\tilde{D}_i\beta^k + \tilde{\gamma}_{ik}\tilde{D}_j\beta^k) = -\delta^i_k\tilde{D}_i\beta^k - \delta^i_k\tilde{D}_j\beta^k = -2\tilde{D}_i\beta^i\ . \tag{6.20c}$$

The two expressions implies that

$$6\mathcal{L}_m\Psi + \alpha K = \tilde{D}_i\beta^i \ , \tag{6.21}$$

$$\mathcal{L}_m \ln\Psi = \frac{1}{6}(\tilde{D}_i\beta^i - \alpha K) \ \text{(Evolution equation for conformal factor)} \tag{6.22}$$

$$\mathcal{L}_m\tilde{\gamma}_{ij} = -2\alpha \underbrace{\Psi^{-4}A_{ij}}_{:=\tilde{A}_{ij}} - \frac{2}{3}\tilde{D}_k\beta^k\tilde{\gamma}_{ij} \ \text{(Evolution equation for conformal metric)} \ . \tag{6.23}$$

which suggests the $p=-4$ scaling since:

$$\tilde{A}^{ij} = \tilde{\gamma}^{ik}\tilde{\gamma}^{lj}\tilde{A}_{kl} = \underbrace{\tilde{\gamma}^{ik}}_{\Psi^4\gamma^{ik}}\underbrace{\tilde{\gamma}^{lj}\Psi^4}_{\gamma^{lj}}A_{kl} = \Psi^4 A^{ij} \ . \tag{6.24}$$

6.4.2 Momentum constraint rescaling

The momentum equation contains the divergence of the extrinsic curvature, $D_jK^{ij} = D_jA^{ij} + \frac{1}{3}D^iK$. The direct calculation

$$D_jA^{ij} = \tilde{D}A^{ij} + C^i_{jk}A^{kj} + C^j_{jk}A^{ik} = ... = \tilde{D}A^{ij} + 10A^{ij}\tilde{D}\ln\Psi - 2\tilde{D}^i\ln\Psi \underbrace{\tilde{\gamma}_{jk}A^{jk}}_{=\Psi^{-4}\gamma_{jk}A^{jk}=0} = \Psi^{-10}\tilde{D}_j(\underbrace{\Psi^{10}A^{ij}}_{=:\hat{A}^{ij}}) \tag{6.25}$$

suggests the $p=-10$ conformal scaling (now denoted with a hat):

$$\hat{A}^{ij} := \Psi^{10}A^{ij} \ \text{ and } \ \hat{A}_{ij} = \Psi^2 A^{ij} \ . \tag{6.26}$$

$$\mathcal{C}^i := \tilde{D}_j\hat{A}^{ij} - \frac{2}{3}\Psi^6\tilde{D}^iK - 8\pi\Psi^{10}P^i \ \text{(Momentum constraint)} \ . \tag{6.27}$$

The relation between the two conformal rescalings is:

$$\hat{A}^{ij} = \Psi^6\tilde{A}^{ij} \quad \hat{A}_{ij} = \Psi^6\tilde{A}_{ij} \ . \tag{6.28}$$

6.5 Conformal 3+1 EFE

Conformal EFE equations are composed by

(i) Evolution equations for the conformal factor (Eq. (6.22)) and the conformal metric (Eq. (6.23)) derived from the kinematical eq;
(ii) Evolution equations for the trace K (Eq. (6.40a)) and the conformal extrinsci curvature $\tilde{A}_{ij}$ with scaling $p=-4$ (Eq. (6.40c));
(iii) Lichnerowicz equation for the conformal factor as Hamiltonian constraint (Eq. (6.31)) or, alternatively, a similar equation for the $\tilde{A}^{ij}$ with scaling $p=-4$;
(iv) Momentum constraint for the conformal extrinsic curvature $\hat{A}^{ij}$ with scaling $p=-10$ (Eq. (6.27)) or, alternatively, a similar equation for the $\tilde{A}^{ij}$ with scaling $p=-4$.

Below the missing equations are derived or presented.

6.5.1 Hamiltonian constraint: Lichnerowicz equation

Using the conformal decomposition of the Ricci scalar, Eq. (6.17), and

$$K_{ij}K^{ij} = (A_{ij} + \frac{1}{3}K\gamma_{ij})(A^{ij} + \frac{1}{3}K\gamma^{ij}) = A_{ij}A^{ij} + 2\frac{1}{3}K\underbrace{\gamma_{ij}A^{ij}}_{=0} + \frac{1}{3}\frac{1}{3}K^2\underbrace{\gamma^{ij}\gamma_{ij}}_{=3} = \tilde{A}_{ij}\tilde{A}^{ij} + \frac{1}{3}K^2 \ , \tag{6.29}$$

the expression $\mathcal{C}_0 = R + K^2 - K_{ij}K^{ij} - 16\pi E$ translates into

$$\mathcal{C}_0 := \tilde{D}_i\tilde{D}^i\Psi - \frac{1}{8}\tilde{R}\Psi + \left(\frac{1}{8}\tilde{A}_{ij}\tilde{A}^{ij} - \frac{1}{12}K^2 + 2\pi E\right)\Psi^5 = 0 \ . \tag{6.30}$$

Alternatively, the equation for the $p=-10$ scaling is simply obtained using Eq. (6.28):

$$\mathcal{C}_0 := \tilde{D}_i\tilde{D}^i\Psi - \frac{1}{8}\tilde{R}\Psi + \frac{1}{8}\hat{A}_{ij}\hat{A}^{ij}\Psi^{-7} + \left(-\frac{1}{12}K^2 + 2\pi E\right)\Psi^5 = 0 \quad \text{(Lichnerowicz eq.)} \tag{6.31}$$

The Lichnerowicz eq is usually interpreted as a nonlinear ellitic equation for the conformal factor. Note that it simplifies if one takes $K=0$ (*Maximal slicing*, see below). Well-posedness and uniqueness of the BVP for the Lichnerowicz eq under the *constant mean curvature (CMC)* condition $K=const$ (maximal slicing is a subcase) have been studied in some detail. In summary, for CMC slices:

- asymptotically flat (see Chap. 7) with $K=0=E$, the problem is solvable iff $\tilde{\gamma}$ belong to the positive yamabe class (conformal to a metric with zero scalar curvature) (Cantor, 1977).
- closed manifolds, the problem is solvable except the cases in which the free data (see Chap. 7) are choosen such that for $\Psi>0$ the r.h.s of the Lichnerowicz eq written as $\Delta\Psi = (r.h.s.)$ is positive or negative definite (Maximum principle of elliptic eqs) (Isenberg, 1995).
- asymptotically hyperbolic, the problem is always solvable.

For details refer to (Choquet-Bruhat and York, 1980, 1996; Bartnik and Isenberg, 2002). In the following we discuss only uniqueness and show, in particular, the different sign of the Ψ exponent in the "$A_{ij}A^{ij}$" term in the two equations (-7 or $+5$) play an important role.

Remark 6.5.1. *Consider the uniqueness of the Dirichlet problem associated to the elliptic equation (f is some function in this example):*

$$\Delta u = +f^2 u^p \quad x\in\Omega\ . \tag{6.32}$$

The equation has at a least a solution for $1<p<5$ (in 3 dimensions) (Evans, 1998). Results:
(i) linear case ($p=1$), with boundary data $u\equiv 0$ in $x\in\partial\Omega$: $u\equiv 0$ is the unique solution;
(ii) nonlinear case: exists a unique solution iff $p>0$ (p had the same sign as the coefficient of u^p).

Show the linear case ($p=1$). Indirect proof using the maximum principle: if the solution $u\neq 0$, then u has a maximum, say positive: $u_* := \max u > 0$. But a positive maximum implies $\Delta u|_{u_*} < 0$, that is in contraddition with $f^2 u_* > 0$. A similar argument hold for $u_* < 0$, impling that the only option left is $u\equiv 0$.

Show the nonlinear case. Suppose $u_0>0$ is a solution and look for a second one $u_\epsilon(x) = u_0(x)+\epsilon(x)$ for $x\in\Omega$ ($u_0 = u_\epsilon$ for $x\in\partial\Omega$; same boundary values/BVP). Linearizing in ϵ one obtains

$$0 = \Delta(u_0+\epsilon) - \underbrace{f^2(u_0+\epsilon)^p}_{H(\epsilon)} = \Delta u_0 + \Delta\epsilon - \underbrace{H(u_0)}_{=f^2u_0^p} - \frac{\partial H}{\partial\epsilon}|_{u_0}\epsilon + ... = 0 + \Delta\epsilon - \underbrace{pf^2u_0^{p-1}}_{:=w}\epsilon + \mathcal{O}(\epsilon^2) \tag{6.33}$$

and from the linear case the solution is unique if $w = pf^2u_0^{p-1} > 0$.

Study uniqueness of the Lichnerowicz eq. in the case $K=0$. Linearizing Eq. (6.31) around a solution Ψ_0 one obtains $\tilde{D}_i\tilde{D}^i\epsilon = w\epsilon$ with

$$w = \frac{1}{8}\tilde{R} + \frac{7}{8}\hat{A}_{ij}\hat{A}^{ij}\Psi_0^{-8} - 10\pi E\Psi_0^4\ . \tag{6.34}$$

Note that $K=0 \Rightarrow R>0$ and $\tilde{R}>0$.

Problem: Using the linear analysis sketched above, well-posedness would require $w>0$ but the above equation has a negative term! Is it possible to rewrite the equation in such a way it leads to a well-posed problem? Yes, the trick is *rescaling* of the energy with a power of the conformal factor :

$$\tilde{E} := \Psi^s E \quad \Rightarrow \quad -5\cdot 2\pi E\Psi_0^4 \ \mapsto\ +(s-5)\cdot 2\pi\tilde{E}\Psi_0^{4-s}\ . \tag{6.35}$$

Any choice $s>5$ does the job. Note this is not only a formal step: the solution of nonlinear elliptic equations requires iterative methods that iterate on successive linearized approximation of the equation. The prescription of Eq. (6.35) clearly indicates how the linearized equations should be iterated.

6.5.2 Conformal rescaling of energy and momentum

What choice to make for s? A good choice is $s=8$.

The momentum constraint Eq. (6.27) suggests a natural choice for the conformally rescaled momentum. If one additionally take the $s=8$ conformal rescaling for the energy,

$$\tilde{E} := \Psi^8 E \ \text{ and } \ \tilde{P}^i := \Psi^{10}P^i\ , \tag{6.36}$$

then one can express the *dominant energy condition* directly in conformally rescaled variables

$$\tilde{E}^2 \geq \tilde{P}^i\tilde{P}_i = \tilde{\gamma}_{ij}\tilde{P}^i\tilde{P}^j \quad \Rightarrow \quad E^2 \geq P^iP_i = \gamma_{ij}P^iP^j\ . \tag{6.37}$$

That holds because

$$\tilde{E}^2 \geq \tilde{P}^i \tilde{P}_i \tag{6.38}$$

$$\Psi^{2s} E^2 \geq \Psi^{-4}\Psi^{10}\Psi^{10} P^i P_i \ . \tag{6.39}$$

6.5.3 Dynamical equation

Eq. (5.15) split into

$$\mathcal{L}_m K = -D_i D^i \alpha + \alpha[4\pi(E+S) + K_{ij}K^{ij}] \tag{6.40a}$$

$$= -\Psi^{-4}(\tilde{D}_i\tilde{D}^i\alpha + 2\tilde{D}_i \ln\Psi \tilde{D}^i\alpha) + \alpha[4\pi(E+S) + \tilde{A}_{ij}\tilde{A}^{ij} + \frac{1}{3}K^2] \tag{6.40b}$$

$$\mathcal{L}_m \tilde{A}_{ij} = -\frac{2}{3}\tilde{D}_k\beta^k\tilde{A}_{ij} + \alpha[K\tilde{A}_{ij} - 2\tilde{\gamma}^{kl}\tilde{A}_{ik}\tilde{A}_{lj} - 8\pi(\Psi^{-4}S_{ij} - \frac{1}{3}S\tilde{\gamma}_{ij})] \tag{6.40c}$$

$$+ \Psi^{-4}\{-\tilde{D}_i\tilde{D}_j\alpha + 2\tilde{D}_i\ln\Psi\tilde{D}_j\alpha + 2\tilde{D}_j\ln\Psi\tilde{D}_i\alpha + \frac{1}{3}[\tilde{D}_k\tilde{D}^k\alpha - 4\tilde{D}_k\ln\Psi\tilde{D}^k\alpha]\tilde{\gamma}_{ij}$$

$$+ \alpha[\tilde{R}_{ij} - \frac{1}{3}\tilde{R}\tilde{\gamma}_{ij} - 2\tilde{D}_i\tilde{D}_j\ln\Psi + 4\tilde{D}_i\ln\Psi\tilde{D}_j\ln\Psi + \frac{2}{3}(\tilde{D}_k\tilde{D}^k\ln\Psi - 2\tilde{D}_k\ln\Psi\tilde{D}^k\ln\Psi)\tilde{\gamma}_{ij}]\}$$

Note the last line of Eq. (6.40c) is the trace-free $\alpha[\tilde{R}_{ij} + R^\Psi_{ij} - \frac{1}{2}(\tilde{R}+R^\Psi)\tilde{\gamma}_{ij}] = \alpha[\tilde{R}_{ij} + R^\Psi_{ij}]^{\rm TF}$; and the whole r.h.s. is trace-free (last terms in the last two lines are the traces of the respective terms at the beginning of the lines).

Show the derivation of the first equation, Eq. (6.40a). The first line of Eq. (6.40a) follows from the combination of the trace of $\mathcal{L}_m K_{ij}$ with Eq. (5.15). The trace reads

$$\gamma^{ij}[\ \mathcal{L}_m K_{ij}\ ] = \gamma^{ij}[\ \mathcal{L}_m(A_{ij} + \frac{1}{3}K\gamma_{ij})\ ] = \gamma^{ij}[\ \mathcal{L}_m A_{ij} + \frac{1}{3}\mathcal{L}_m K\gamma_{ij} + \frac{1}{3}K\ \underbrace{\mathcal{L}_m\gamma_{ij}}_{=-2\alpha K_{ij}}\ ] \tag{6.41}$$

$$= \gamma^{ij}\mathcal{L}_m A_{ij} + \frac{1}{3}\mathcal{L}_m K\underbrace{\gamma^{ij}\gamma_{ij}}_{=3} - \frac{2}{3}\alpha K\underbrace{\gamma^{ij}K_{ij}}_{=K} \tag{6.42}$$

$$= \underbrace{\mathcal{L}_m(\gamma^{ij}A_{ij})}_{=0} - A_{ij}\underbrace{\mathcal{L}_m\gamma_{ij}}_{2\alpha K^{ij}} + \mathcal{L}_m K - \frac{2}{3}\alpha K^2 \tag{6.43}$$

$$= -2\alpha K^{ij}\underbrace{(A_{ij} + \frac{1}{3}K\gamma_{ij} - K_{ij})}_{=0} - 2\alpha K^{ij}K_{ij} + \mathcal{L}_m K \ , \tag{6.44}$$

where in the last line one adds $\pm 2\alpha K^{ij}K_{ij}$. For the second line of Eq. (6.40a) uses the following relation

$$D_i v^i = \Psi^{-6}\tilde{D}_i(\Psi^6 v^i) \tag{6.45}$$

for the divergence of a vector (that can be shown in Cartesian coordinates using $D_i v^i = \gamma^{-1/2}\partial_i(\gamma^{1/2}v^i)$), to show that

$$D_i D^i\alpha = \Psi^{-6}\tilde{D}_i(\Psi^6 D^i\alpha) = \Psi^{-6}\tilde{D}_i[\Psi^{-6}\ \underbrace{\gamma^{ij}}_{=\Psi^{-4}\tilde{\gamma}^{ij}}\ D_j\alpha)] = \Psi^{-6}\tilde{D}_i(\Psi^2\tilde{D}^i\alpha) = \Psi^{-4}\tilde{D}_i\tilde{D}^i\alpha + 2\Psi^{-5}\tilde{D}_i\Psi\tilde{D}^i\alpha \tag{6.46}$$

$$= \Psi^{-4}(\tilde{D}_i\tilde{D}^i\alpha + 2\tilde{D}_i\ln\Psi\tilde{D}^i\alpha) \ . \tag{6.47}$$

The rest of the calculation is trivial.

To clarify the role of Eq. (6.40a), take the Newtonian limit:

$$\alpha \simeq 1+\phi \ , \quad \beta^i = 0 \ , \quad \gamma_{ij} = (1+2\phi)f_{ij} \ , \quad K_{ij} = 0 \ , E+S \simeq \rho \ , \quad D_i \mapsto \mathcal{D}_i \ , \tag{6.48}$$

$$0 = -\mathcal{D}_i\mathcal{D}^i\phi + 4\pi\rho \quad \text{(Weak-field limit of Eq. (6.40a))} \ . \tag{6.49}$$

6.6 Maximal slicing: geometric meaning

The condition that the trace of the extrinsic curvature vanishes,

$$K = 0 \quad \text{(Maximal slicing)} \ , \tag{6.50}$$

is a gauge choice for the foliation that implies that Σ_t have maximal volume.

To show this fact, notice that the trace of the curvature is related to the determinant of the 3-metric by

$$K = \gamma^{ab}K_{ab} = -\frac{1}{2\alpha}\gamma^{ij}\mathcal{L}_m\gamma_{ij} = -\frac{1}{2\alpha}\mathcal{L}_m \ln\gamma = -\frac{1}{\alpha}\mathcal{L}_m \ln\sqrt{\gamma} \ . \tag{6.51}$$

Hence, K relates to the coordinate volume element $\sqrt{\gamma}\mathrm{d}^3x$ on Σ_t; the volume of the hypersurface (or a part of it) is given by the integral

$$V = \int \sqrt{\gamma}\mathrm{d}^3x \ . \tag{6.52}$$

Consider now a close surface $S \subset \Sigma_t$ and a variation of the volume contained in S around Σ_t. Formally, one can define a displacement vector of δt along $\boldsymbol{\partial}_t$ inside S,

$$v^a = \delta t(\alpha n^a + \beta^a) \quad \text{and} \quad v^a|_S = 0 \quad \Leftrightarrow \quad \alpha|_S = 0 \text{ and } \beta^a|_S = 0 \ , \tag{6.53}$$

and consider the volume variation δV given by the displacement vectors:

$$\frac{dV}{dt} = \int_{\delta V} \partial_t\sqrt{\gamma}\mathrm{d}^3x = \int_{\delta V}(-\alpha K + D_i\beta^i)\sqrt{\gamma}\mathrm{d}^3x = -\int_{\delta V}\alpha K\sqrt{\gamma}\mathrm{d}^3x + \underbrace{\int_S \beta^i s_i\sqrt{q}\mathrm{d}^2y}_{=0} = -\int_{\delta V}\alpha K\sqrt{\gamma}\mathrm{d}^3x \ . \tag{6.54}$$

The surface integral is zero because the displacemente vector (variation) is zero at S, and the above expression proves that $K = 0$ *extremizes* the volume enclosed into S.

Remark 6.6.1. *The above problem corresponds to the problem of minimizing the surface of a soap film given a fixed ring "holding" the soap ball, i.e. minimizing the surface tension, in 2D Euclidean geometry. In case of 3+1 GR, it can be proven that the $K = 0$ extremization is actually a maximum because one works with Lorentzian manifold (cf. geodesics are curves of maximal lenght between two points).*

The properties and implication of this gauge choice for singularity formation and evolution will be discussed in Sec. 9.

6.7 Isemberg-Wilson-Mathews approximation to GR

The IWM equations are an approximation to GR under the hypothesis
(i) $\tilde{\gamma}_{ij} = f_{ij}$: *Conformally flat spacetime*
(ii) $K = 0$: Maximal slicing condition.
Implications
(a) (i) $\Rightarrow$ the covariant derivatives $\tilde{D}_i \mapsto \mathcal{D}_i$, and $\tilde{D}_i\tilde{D}^i = \mathcal{D}_i\mathcal{D}^i = \Delta$ (Laplacian operator on flat space)
(b) (i) $\Rightarrow \tilde{R} = 0$
(c) (i) $\Rightarrow \mathcal{L}_m\tilde{\gamma}_{ij} = \partial_t f_{ij} - \mathcal{L}_\beta f_{ij} = -\mathcal{L}_\beta f_{ij}$
(d) (ii) $\Rightarrow$ Lichnerowicz eq simplifies
(e) (ii) $\Rightarrow \mathcal{L}_m K = 0 \Rightarrow$ elliptic eq for the lapse
(f) (ii) $\Rightarrow$ hypersurfaces have maximum volume [see above]
The conformal 3+1 equations simplify to

$$\Delta\Psi + \frac{1}{8}\hat{A}_{ij}\hat{A}^{ij}\Psi^{-7} + 2\pi\tilde{E}\Psi^{-3} = 0 \tag{6.55a}$$

$$\Delta\beta^i + \frac{1}{3}\mathcal{D}^j\mathcal{D}_j\beta^i + 2\tilde{A}^{ij}(6\alpha\mathcal{D}_j \ln\Psi - \mathcal{D}_j\alpha) = 16\pi\alpha\Psi^4 P^i \tag{6.55b}$$

$$\Delta\alpha + 2\mathcal{D}_i \ln\Psi\mathcal{D}^i\alpha = \alpha[4\pi(E+S) + \tilde{A}_{ij}\tilde{A}^{ij}]\Psi^4 \tag{6.55c}$$

The above system are 3 elliptic eqs for α, β^i, Ψ. The conformal traceless extrinsic curvature $\tilde{A}_{ij}$ must be considered a function of lapse and shift via the kinematical equation $\mathcal{L}_m\tilde{\gamma}_{ij} = ...$:

$$2\alpha\tilde{A}_{ij} = f_{ik}\mathcal{D}_j\beta^k + f_{kj}\mathcal{D}_i\beta^k - \frac{2}{3}\mathcal{D}_k\beta^k f_{ij} \tag{6.56}$$

usually written as

$$\tilde{A}^{ij} = (2\alpha)^{-1}(L\beta)^{ij} \tag{6.57}$$

$$(L\beta)^{ij} := \mathcal{D}^i\beta^j + \mathcal{D}^j\beta^i - \frac{2}{3}\mathcal{D}_k\beta^k f^{ij} \quad \text{(Conformal Killing operator)} \ . \tag{6.58}$$

The last line defines the operator L called the *conformal Killing operator* associated to the metric f_{ij} and applied to the vector β^i. $(L\beta)^{ij}$ is traceless w.r.t its associated metric and plays an important role in the context of the initial data problem and vector Laplacian [See Chap. 8; Appendix B of Gourgoulhon 3+1 notes and Chap. 3 of Baumgarte notes] Given the above expression for $\tilde{A}_{ij}$ the other equations are found by

- Inserting the expression for $\tilde{A}_{ij}$ into momentum constraint $\Rightarrow$ Eq. (6.55b)
- Simplifying Lichnerowicz eq with (i) and (ii) $\Rightarrow$ Eq. (6.55a)
- $\mathcal{L}_m K \equiv 0$ and simplifying with (i) and (ii) $\Rightarrow$ Eq. (6.55c).

Properties of IWM spacetime

(i) No gravitational-wave content in the spacetime
(ii) Exact for spherically symmetric spacetime (Schwarzschild)
(iii) Exact to 1-post-Newtonian order.

Remark 6.7.1. *The IWM approximation has been used for neutron star oscillation and core-collapse simulations coupled to general relativistic hydrodynamics, e.g. (Dimmelmeier et al., 2002). Some of the results are in very good agreement with those of general relativity also in the cases in which rotation is present. Gravitational-waves are not simulated but eventually calculated using a quadrupole formula from the mass distribution. The IWM was developed by Isemberg as a* waveless *approximation of GR and by Wilson-Mathews for binary neutron star mergers simulations, e.g. (Wilson et al., 1996; Oechslin et al., 2002). In the latter case the radiation reaction driving the dynamics must be approximated by a quadrupole formula. The IWM formalism is also used for constructing quasiequilibrium configuration of compact binaries in circular orbit, see Chap. 8.*

7. Asymptotic flatness & global quantities

This lecture gives a brief overview of the main concepts of energy in GR. Global concepts of energy exist for asymptotically flat spacetimes (ADM mass and momenta) or in presence of Killing vectors (Komar charges). In both cases the energy can be defined as surface integrals on the hypersurface Σ_t. Those quantities are used in numerical relativity as a meaningful way to characterize the numerically computed spacetimes.

Suggested readings. *Chap. 4 of Gourgoulhon 3+1 lecture notes; Review of Jaramillo & Gourhoulhon; Appendix A of Alcubierre's book; Chap. 11 of Wald's book; Chrusciel lecture notes.*

7.1 Asymptotically flat spacetime

A globally hyperbolic spacetime is *asymptotically flat* (AF) iff [1]

$$\forall \Sigma_t \quad \exists f_{ij} \text{ (background metric)} \ :$$

(i) f_{ij} is flat, Riemann tensor $\equiv 0$ (except on a compact domain, "strong field" region)

(ii) There exists a Cartesian-type coordinate system x^i such that for $r = \sqrt{x^i x_i} \to \infty$ the metric components are $f_{ij} = \mathrm{diag}(1,1,1)$

(iii) In the asymptotic region $r \to \infty$, the 3-metric and extrinsic curvature components satisfy the following decay conditions:

$$\gamma_{ij} = f_{ij} + \mathcal{O}(r^{-1}) \tag{7.1a}$$
$$\partial_k \gamma_{ij} = \mathcal{O}(r^{-2}) \tag{7.1b}$$
$$K_{ij} = \mathcal{O}(r^{-2}) \tag{7.1c}$$
$$\partial_k K_{ij} = \mathcal{O}(r^{-3}) \tag{7.1d}$$

The asymptotic region defined by $r \to \infty$ is called *spatial infinity*, i_0.

Properties:

- AF spacetimes are an idealization,
  - They describe the spacetime of an *isolated body*
  - They do not describe cosmological spacetimes
- AF spacetimes cannot contain gravitational waves (GW) at spatial infinity. A GW solution would violate the asymptotic conditions for the metric derivatives:

$$\gamma_{ij} = f_{ij} + \frac{h_{ij}(t-r)}{r} + \mathcal{O}(r^{-2}) \quad \Rightarrow \quad \partial_k \gamma_{ij} = -\frac{h'_{ij}(t-r)}{r}\frac{x^k}{r} - \frac{h_{ij}(t-r)}{r^2}\frac{x^k}{r} + \mathcal{O}(r^{-2}) \ . \tag{7.2}$$

  GWs are anyway considered in AF spacetime with the only restriction/assumption that they start at finite time in the past; hence, they can reach scri but do not (or have not yet) reached i_0 .
- The definition of AF depends on the foliation Σ_t and on the spatial coordinates x^i. The coordinate transformation that preserve the AF properties are of the type

$$x'^{\mu} = \Lambda^{\mu}_{\alpha} x^{\alpha} + c^{\mu}_{r}(\theta,\phi) + \mathcal{O}(r^{-1}) \ , \tag{7.3}$$

  where Λ^{μ}_{α} is a Lorentz matrix and the c^{μ}_{r} functions are simply the transformation from spherical angles to Cartesian coordinates at given radius r. The transformation above contain rotations and traslation on Σ_t

[1] See [Wald's book] for a geometrical definition (coordinate independent) based on the addition to the manifold of "points at infinity".

($c^\mu = const$), and supertranslations on Σ_t ($c^\mu \neq const$ and $\Lambda^\mu_\alpha = \delta^\mu_\alpha$), as well as boost that change the slicing Σ_t ($c^\mu = const$). The transformation group is called the *Spi group* (spatial infinity) (Ashtekar and Hansen, 1978)

7.2 ADM mass

In AF spacetimes a global, conserved energy contained in Σ_t can be defined (Arnowitt et al., 1959, 1960).

The GR action can be written

$$S_{\rm GR} = \int_{\mathcal{V}} {}^4R\sqrt{-g}\mathrm{d}^4x + \oint_{\partial\mathcal{V}} (Y - Y_0)\sqrt{h}\mathrm{d}^3y \tag{7.4}$$

where a *boundary term* is introduced in order to obtain the (2nd order) EFE from the variation of the action w.r.t. the metric $\delta S/\delta g^{ab}$ by keeping fixed the metric at the boundary (and not its derivatives) [Regge&Teitelboim 1974]. The boundary term is defined on a timelike hypersurface $\partial\mathcal{V}$ representing the boundary of the manifold $\mathcal{V}$. The embedding of $\partial\mathcal{V}$ into $(\mathcal{M}, g)$ induces the metric $\boldsymbol{h}$ with extrinsic curvature $\boldsymbol{Y}$ (in the equation, Y is the trace). Similarly, $\boldsymbol{Y}_0$ is the extrinsic curvature of $(\partial\mathcal{V}, \boldsymbol{h})$ embedded in $(\mathcal{M}, \boldsymbol{\eta})$, where $\boldsymbol{\eta}$ is a flat Lorentzian metric in the region of $\partial\mathcal{V}$.

The Hamiltonian reads

$$H = -\int_{\Sigma_t} \sqrt{\gamma}\left(\alpha\mathcal{C}_0 + 2\beta^i\mathcal{C}_i\right) - 2\oint_{\partial\Sigma_t} \sqrt{q}[\alpha(\kappa - \kappa_0) + \beta^i s^j(K_{ij} - K\gamma_{ij})] \ , \tag{7.5}$$

where $\partial\Sigma_t = \partial\mathcal{V}\bigcap\Sigma_t$ with normal vector s^j and the first integral is understood only in the interior of Σ_t. In the equation above $\boldsymbol{q}$ and $\boldsymbol{\kappa}$ are the induced metrics and extrinsic curvatures of $\partial\Sigma_t$ embedded in $(\Sigma, \boldsymbol{\gamma})$; and $\boldsymbol{\kappa}_0$ is the extrinsic curvature in $(\Sigma, \boldsymbol{f})$. The κ, κ_0 appearing in the equation are again the traces.

On a solution of GR the constraints are satisfied and the first term in Eq. (7.5) is zero. The *ADM mass* is defined by setting $\alpha = 1$ and $\beta^i = 0$ at i_0 for the boundary term,

$$M_{\rm ADM} := -\frac{1}{8\pi}\lim_{r\to\infty}\oint_{\partial\Sigma_t}\sqrt{q}(\kappa - \kappa_0) \quad \text{(ADM Mass)} \tag{7.6a}$$

$$= +\frac{1}{16\pi}\lim_{r\to\infty}\oint_{\partial\Sigma_t}\sqrt{q}s^i[\mathcal{D}^j\gamma_{ij} - \mathcal{D}_i(f^{kl}\gamma_{kl})] \tag{7.6b}$$

$$= +\frac{1}{16\pi}\lim_{r\to\infty}\oint_{\partial\Sigma_t}\sqrt{q}s^i(\partial_j\gamma_{ij} - \partial_i\gamma^k_k) \tag{7.6c}$$

$$= -\frac{1}{2\pi}\lim_{r\to\infty}\oint_{\partial\Sigma_t}\sqrt{q}s^i(\mathcal{D}_i\Psi - \frac{1}{8}\mathcal{D}^j\tilde{\gamma}_{ij}) \tag{7.6d}$$

The second line expresses the extrinsic curvatures on the boundary in terms of the background metric; the third line specifies to Cartesian coordinates, $\mathcal{D} \mapsto \partial$ and $f^{kl} = \delta^{kl}$. The last line is the expression in terms of the conformal variables, the result is proven in Sec. 7.2.2 below.

Remark 7.2.1. *AF conditions (asymptotic decays) guarantee the existance of the integral, M_{ADM} is finite.*

Example 7.2.1. *In the* weak field *limit and using Cartesian coordinates*

$$\tilde{\gamma}_{ij} = f_{ij} \ , \quad \mathcal{D}^i\tilde{\gamma}_{ij} = 0 \ , \quad \Psi = 1 - \phi/2 \ , \quad \mathcal{D}_i\Psi = -\mathcal{D}_i\phi/2 \ , \tag{7.7}$$

which gives immediately:

$$M_{ADM} = +\frac{1}{2\cdot 2\pi}\lim_{r\to\infty}\oint_{\partial\Sigma_t}\sqrt{q}s^i\mathcal{D}_i\phi\mathrm{d}^2y = \frac{1}{4\pi}\lim_{r\to\infty}\int_{\Sigma_t}\sqrt{f}\mathcal{D}^i\mathcal{D}_i\phi\mathrm{d}^3x = \int_{\Sigma_t}\sqrt{f}\rho\mathrm{d}^3x \ . \tag{7.8}$$

Example 7.2.2. *For* Schwarzschild *spacetime (in isotropic coordinates) one takes $\partial\Sigma_t$ as the sphere of radius r and one needs necessarily to use the formula with $\mathcal{D}$ because the background is not in Cartesian coordinates:*

$$\Psi = 1 + \frac{M}{2r} \ , \quad \tilde{\gamma}_{ij} = f_{ij} = \mathrm{diag}(1, r^2, r^2\sin\theta) \ , \quad s^i\sqrt{q}\mathrm{d}^2y = (\boldsymbol{\partial})^i\, r^2\sin\theta\mathrm{d}\theta\mathrm{d}\phi \quad \textit{at } \mathrm{i}_0 \ , \quad s^i\mathcal{D}_i = \frac{\partial}{\partial r} \ , \tag{7.9}$$

leading to

$$M_{ADM} = -\frac{1}{2\pi}\lim_{r\to\infty}\int_{r=const}\underbrace{\frac{\partial\Psi}{\partial r}}_{-M/(2r^2)} r^2\sin\theta\mathrm{d}\theta\mathrm{d}\phi = +\frac{1}{2\pi}\frac{M}{2}4\pi = M \tag{7.10}$$

Theorem 7.2.1. *(Schoen and Yau, 1979; Schon and Yau, 1981; Witten, 1981) If the matter obeys the* dominant energy condition $E^2 \geq P_i P^i$, *then*

$$M_{ADM} \geq 0 \tag{7.11}$$

and

$$M_{ADM} = 0 \quad \Leftrightarrow \quad \Sigma_t \text{ is hypersurface of Minkowski} \tag{7.12}$$

Moreover, since the Hamltonian does not depend explicitely on time the mass is conserved:

$$\frac{\mathrm{d}M_{ADM}}{\mathrm{d}t} = 0 \ . \tag{7.13}$$

Remark 7.2.2. *In simulations, the ADM mass is approximated by integrals computed on spheres at finite coordinate radii (largest values of r in the computational domain). These integrals are* ***not*** *conserved in general. For example, a gravitational wave traveling to null infinity can cross the spheres and alter the value of the integral at successive times; approximate conservation is obtained by correcting the value of the integral by the radiated energy.*

7.2.1 Euristic derivation

An euristic derivation of the ADM mass can be given by starting from the Newtonian definition of mass:

$$M = \int_V \rho = \int_V \frac{1}{4\pi} \partial_i \partial^i \phi = \oint_{\partial V} s^i \partial_i \phi \ , \tag{7.14}$$

where in the second step we substitute Poisson equation for the gravitational potential and in the last the volume integral is converted to a surface integral using Stokes theorem. The last formula suggests that the mass can be expressed as a surface integral where the flux is given by the metric's first derivative (recall in the weak field limit $\phi \sim h_{00}$). Consider then the Hamiltonian constraint in the weak field limit,

$$R + K^2 - K_{ij}K^{ij} = 16\pi E \ \text{ with} \tag{7.15}$$

$$\gamma_{ij} = f_{ij} + h_{ij} \ , \quad R \simeq \partial_i(\partial_j h_{ij} + \partial_i h^k_k) \ , \quad K^2 \simeq K_{ij}K^{ij} \simeq 0 \ , \quad E \simeq \rho \ . \tag{7.16}$$

Use the Hamiltonian constraint to postulate that the "flux" is given by integrating R and obtain the ADM formula (in other notation):

$$M = \int_V \rho \simeq \int_V R \simeq \oint_{\partial V} s^i(\partial_j h_{ij} + \partial_i h^k_k) \ . \tag{7.17}$$

7.2.2 Derivation of ADM mass expression for conformal variables

For the conformal decomposition one assumes that the background metric is the same as the background metric appearing the AF definition. The asymptotic decays translate then into

$$\Psi = 1 + \mathcal{O}(r^{-1}) \ , \quad \partial_k \Psi = \mathcal{O}(r^{-2}) \ , \quad \tilde{\gamma}_{ij} = f_{ij} + \mathcal{O}(r^{-1}) \ , \quad \partial_k \tilde{\gamma}_{ij} = \mathcal{O}(r^{-2}) \ . \tag{7.18}$$

$$\mathcal{D}^j \underbrace{\gamma_{ij}}_{\Psi^4\tilde{\gamma}_{ij}} - \mathcal{D}_i(f^{kl}\gamma_{kl}) = 4\underbrace{\Psi^3}_{\sim 1}\mathcal{D}^j\Psi\underbrace{\tilde{\gamma}_{ij}}_{\sim f_{ij}} + \underbrace{\Psi^4}_{\sim 1}\mathcal{D}^j\tilde{\gamma}_{ij} - 4\underbrace{\Psi^3}_{\sim 1}\mathcal{D}_i\Psi\underbrace{f^{kl}\tilde{\gamma}_{kl}}_{\sim 3} - \underbrace{\Psi^4}_{\sim 1}\mathcal{D}_i(f^{kl}\tilde{\gamma}_{kl}) \tag{7.19a}$$

$$= 4\mathcal{D}^j\Psi f_{ij} + \mathcal{D}^j\tilde{\gamma}_{ij} - 4\cdot 3\mathcal{D}_i\Psi - \mathcal{D}_i(f^{kl}\tilde{\gamma}_{kl}) = -8\underbrace{\mathcal{D}_i\Psi}_{\mathcal{O}(r^{-2})} + \underbrace{\mathcal{D}^j\tilde{\gamma}_{ij}}_{\mathcal{O}(r^{-2})} - \underbrace{\mathcal{D}_i(f^{kl}\tilde{\gamma}_{kl})}_{?} \tag{7.19b}$$

The first two terms contribute to the integral and give the expression in Eq. (7.6d)above. The last term is $\mathcal{O}(r^{-3})$ and can be discarded. To show that write

$$\tilde{\gamma}_{ij} = f_{ij} + \epsilon_{ij} \ \text{ with } \ \epsilon_{ij} = \mathcal{O}(r^{-1}) \ , \quad \partial_k \epsilon_{ij} = \mathcal{O}(r^{-2}) \tag{7.20}$$

and compute:

$$f^{ij}\tilde{\gamma}_{ij} = 3 + \epsilon_{xx} + \epsilon_{yy} + \epsilon_{zz} \tag{7.21a}$$

$$\mathcal{D}_k(f^{ij}\tilde{\gamma}_{ij}) = \partial_k(\epsilon_{xx} + \epsilon_{yy} + \epsilon_{zz}) \sim \partial_k(\epsilon^2 + \epsilon^3) \sim \epsilon\partial\epsilon \sim \mathcal{O}(r^{-3}) \tag{7.21b}$$

where the second step is a consequence of requiring $\tilde{\gamma} = 1$ since

$$\tilde{\gamma} = \det\begin{bmatrix} 1+\epsilon_{xx} & \epsilon_{xy} & \epsilon_{xz} \\ \epsilon_{yx} & 1+\epsilon_{yy} & \epsilon_{yz} \\ \epsilon_{zx} & \epsilon_{zy} & 1+\epsilon_{zz} \end{bmatrix} = 1 + \epsilon_{xx} + \epsilon_{yy} + \epsilon_{zz} + \mathcal{O}(\epsilon^2) + \mathcal{O}(\epsilon^3) \tag{7.22a}$$

$$\Rightarrow \ \epsilon_{xx} + \epsilon_{yy} + \epsilon_{zz} = \mathcal{O}(\epsilon^2) + \mathcal{O}(\epsilon^3) \ . \tag{7.22b}$$

7.3 ADM momentum

Consider again the Hamiltonian in Eq. (7.5). Spatial translations at i_0 are identified by the 3 possible directions $\boldsymbol{\partial}_k$. The ADM momentum is defined by setting $\alpha = 0$ and $\beta^i = (\boldsymbol{\partial}_k)^i$ at i_0 in the boundary term,

$$P_k^{\rm ADM} := \frac{1}{8\pi} \lim_{r\to\infty} \oint_{\partial\Sigma_t} \sqrt{q} (\boldsymbol{\partial}_k)^i s^j (K_{ij} - K\gamma_{ij}) \quad \text{(ADM Momentum)} \tag{7.23}$$

Remark 7.3.1. *AF conditions (asymptotic decays) guarantee the existance of the integrals.*

Properties

(i) The 3 quantities $P_k^{\rm ADM}$ transform as the components of a 1-form under a change of Cartesian coordinates corresponding to rotation and/or a translation at i_0;

(ii) Similarly, $P_\alpha^{\rm ADM} = (-M_{\rm ADM}, P_k^{\rm ADM})$ behaves like a 1-form under coordinates transformation that preserve AF: $P'^{\rm ADM}_\alpha = (\Lambda^{-1})^\mu_\alpha P^{\rm ADM}_\mu$.

7.4 ADM angular momentum

Rotations at i_0 about the 3 axis of a Cartesian frame are identified by the 3 Killing vectors of f_{ij}:

$$\boldsymbol{\phi}_x = -z\boldsymbol{\partial}_y + y\boldsymbol{\partial}_z \tag{7.24a}$$
$$\boldsymbol{\phi}_y = -x\boldsymbol{\partial}_z + z\boldsymbol{\partial}_x \tag{7.24b}$$
$$\boldsymbol{\phi}_z = -y\boldsymbol{\partial}_x + x\boldsymbol{\partial}_y \ . \tag{7.24c}$$

Note that $\boldsymbol{\phi}_k \sim \mathcal{O}(r)$.

The ADM angular momentum is defined by setting $\alpha = 0$ and $\beta^i = (\boldsymbol{\phi}_k)^i$ at i_0 in the boundary term,

$$J_k^{\rm ADM} := \frac{1}{8\pi} \lim_{r\to\infty} \oint_{\partial\Sigma_t} \sqrt{q} (\boldsymbol{\phi}_k)^i s^j (K_{ij} - K\gamma_{ij}) \quad \text{(ADM Momentum)} \tag{7.25}$$

Properties

(i) AF conditions (asymptotic decays) **do not** guarantee in general the existance of the integrals because

$$(K_{ij} - K\gamma_{ij})(\phi_k)^j = \mathcal{O}(r^{-1}) \ . \tag{7.26}$$

(ii) However, J_k can be finite because of the contraction with s^i. For example, $\gamma_{kj} s^k (\boldsymbol{\phi}_i)^j = 0$ because $\boldsymbol{s} = x^i/r\boldsymbol{\partial}_i$ $[s^j(\boldsymbol{\phi}_a)_j = f_{jk} s^j (\boldsymbol{\phi}_a)^k = (x/r, y/r, z/r)\cdot(0, -z, y)^T = -zy/r + yz/r = 0$, etc.] The contraction $K_{kj} s^k (\boldsymbol{\phi}_i)^j = 0$ can be verified to be true for standard BH solutions.

(iii) J_k **do not** transform as 1-form components at infty. J_k can be asymptotically a vector if one considers a restricted class of asymptotic transformation instead of Eq. (7.3). In particular, one should substitute the AF conditions with the stronger conditions:

$$\partial_k \tilde{\gamma}_{ij} = \mathcal{O}(r^{-3}) \quad \text{(Quasi-isotropic gauge)} \tag{7.27a}$$
$$K = \mathcal{O}(r^{-3}) \quad \text{(Asymptotically maximal gauge)} \tag{7.27b}$$

Example 7.4.1. *Isotropic coordinates for Schwarzschild are quasi-isotropic, standard Schwarzschild coordinates are not.*

7.5 Komar currents

Conserved quantities in GR naturally arise in presence of Killing vector (symmetries). The Komar method (1959) consists in taking flux integrals of the derivative of the Killing vector over closed 2-surfaces surrounding the matter sources.

7.5.1 General argument

Consider a Killing vector K^a,

$$\mathcal{L}_K g_{ab} = 2\nabla_{(a}K_{b)} = 0 \ . \tag{7.28}$$

For any symmetric and divergence-free tensor T_{ab}, there exists a conserved current $J^a := T^{ab}K_b$:

$$\nabla_a(T^{ab}K_b) = \underbrace{\nabla_a T^{ab}}_{=0} K_b + T^{ab}\nabla_a K_b = \frac{1}{2}(T^{ab}\nabla_a K_b + T^{ab}\nabla_a K_b) \tag{7.29a}$$

$$= \frac{1}{2}(T^{ab}\nabla_a K_b + \underbrace{T^{ba}}_{=T^{ab}}\nabla_b K_a) = \frac{1}{2}T^{ab}\underbrace{(\nabla_a K_b + \nabla_b K_a)}_{\text{Killing eq.}} = 0 \ . \tag{7.29b}$$

Take now the Einstein tensor as symmetric and divergence-free tensor. The current

$$J^a_{(1)} := G^{ab}K_b = {}^4R^{ab}K_b - \frac{1}{2}{}^4RK^a \tag{7.30}$$

is conserved. More in general, the conservation of

$$J^a_{(c)} := G^{ab}K_b = {}^4R^{ab}K_b - c\frac{1}{2}{}^4RK^a \ , \quad c \in \mathbb{R} \tag{7.31}$$

follows from the properties of Killing vectors and their contractions with the Ricci tensor [2]

$$\nabla_a J^a_{(c)} = \nabla_a({}^4R^{ab}K_b) - \frac{c}{2}\nabla_a({}^4RK^a) = \nabla_a({}^4R^{ab}K_b) - \frac{c}{2}{}^4R\underbrace{\nabla_a(K^a)}_{=0 \text{ antisym}} - \frac{c}{2}\underbrace{K^a\nabla_a{}^4R}_{=0 \ R \text{ invariant along } K^a} \tag{7.32a}$$

$$= \nabla_a({}^4R^{ab}K_b) = \nabla_c\nabla^c\underbrace{\nabla_a K^a}_{=0} = 0 \tag{7.32b}$$

Among all the possible choices of c, the case $c = 0$ is "special" since the conserved current can be written in terms of the antisymmetric tensor $A^{ab} := \nabla^a K^b$:

$$J^a_{(0)} := {}^4R^{ab}K_b = \nabla_b(\nabla^a K^b) = -\nabla_b(\underbrace{\nabla^b K^a}_{:=A^{ba}=A^{[ba]}}) \ . \tag{7.33}$$

Specifying Stokes theorem to the hypersurfaces Σ_t (or any subset of it) one sees immediately that conserved quantities associated to the current $J^a_{(o)}$ can be expressed as integrals of $\nabla^a K^b$ on closed 2-surface on hypersurfaces of the 3+1 foliation:

$$\int_{\mathcal{M}} \mathbf{d}\boldsymbol{\omega} = \oint_{\partial\mathcal{M}} \boldsymbol{\omega} \quad \Rightarrow \quad \int_{\Sigma_t} \mathrm{d}s_a \nabla_b A^{ab} = \oint_{\partial\Sigma_t} \mathrm{d}s_{ab}A^{ab} =: Q_K \ , \tag{7.34a}$$

where

$$\mathrm{d}s_a = \mathrm{d}^3x\sqrt{\gamma}n_a \ \text{ volume element on } \Sigma_t \tag{7.34b}$$

$$\mathrm{d}s_{ab} = \mathrm{d}^2y\sqrt{q}(s_a n_b - n_a s_b) \ \text{ surface element on } \partial\Sigma_t \text{ with normal } s^a \ . \tag{7.34c}$$

Remark 7.5.1. *The flux integrals Q_K are conserved and correspond to volume integrals of the matter distribution via EFE ($R_{ab} = 8\pi(T_{ab} - \frac{1}{2}Tg_{ab})$). They do not depend upon the choice of the integration 2-surface as long as the latter stays outside the matter.*

A simple way to show the above result is the following. Due to symmetry/antisymmetry $\nabla_a\nabla_b A^{ab} = 0$. Take $\Omega \subset \mathcal{M}$ with boundary $\partial\Omega = \Sigma_{t_1} \cup \sigma \cup \Sigma_{t_2}$, i.e. composed of two spatial hypersurfaces and timelike cylindrical world-tube. Then using Stokes theorem [Appendix B of Wald's book]

$$0 = \int_\Omega \nabla_a\nabla_b A^{ab} = \oint_{\partial\Omega} n_a\nabla_b A^{ab} = \int_{\Sigma_{t_1}} ... + \int_\sigma ... - \int_{\Sigma_{t_2}} ... \tag{7.35}$$

Since $\nabla_b A^{ab} = {}^4R^{ab}K_b = 8\pi(T^{ab} - \frac{1}{2}Tg^{ab})n_b$, if the timelike hypersurface σ is outside the matter distribution, then $\int_\sigma = 0$ and $\int_{\Sigma_{t_1}} = \int_{\Sigma_{t_2}}$ (This proves conservation). Applying Stokes one more time leads to Eq. (7.34a).

[2] From antisymmetry/Killing eq: $\nabla_a K^a = 0$. From invariance of curvature along the Killing vector: $K^a\nabla_a{}^4R = 0$. From definition of Riemann and antisymmetry/Killing eq ${}^4R^{ab}K_b = \nabla_c\nabla^c K^a$ and $\nabla_a({}^4R^{ab}K_b) = \nabla_a\nabla_c\nabla^c K^a = 0$.

7.5.2 Komar mass

A stationary spacetime has Killing vector $\boldsymbol{K}=\boldsymbol{\partial}_t$ or $K^a=(\partial_t)^a=\alpha n^a+\beta^a$. Hence

$$\nabla^a K^b \mathrm{d}s_{ab} = \nabla_a K_b (s^a n^b - n^a s^b)\sqrt{q}\mathrm{d}^2y = (\nabla_a K_b s^a n^b - \underbrace{\nabla_a K_b}_{-\nabla_b K_a} n^a s^b)\sqrt{q}\mathrm{d}^2y \tag{7.36a}$$

$$= 2\nabla_a K_b s^a n^b \sqrt{q}\mathrm{d}^2y = 2(\nabla_a \alpha n_b + \alpha \nabla_a n_b + \nabla_a \beta_b) s^a n^b \sqrt{q}\mathrm{d}^2y \tag{7.36b}$$

$$= 2(\nabla_a \alpha s^a \underbrace{n_b n^b}_{=-1} + \alpha s^a \underbrace{n^b \nabla_a n_b}_{=0} + s^a \underbrace{n^b \nabla_a \beta_b}_{=\beta_b \nabla_a n^b})\sqrt{q}\mathrm{d}^2y \tag{7.36c}$$

$$= -2(s^i D_i \alpha - K_{ij} s^i \beta^j)\sqrt{q}\mathrm{d}^2y \tag{7.36d}$$

The *Komar mass* is defined as

$$M_K := -\frac{1}{8\pi}\oint_{\partial\Sigma_t} \mathrm{d}s_{ab}\nabla^a K^b = \frac{1}{4\pi}\oint_{\partial\Sigma_t}(s^i D_i\alpha - K_{ij}s^i\beta^j)\sqrt{q}\mathrm{d}^2y \quad \text{(Komar mass)}\ . \tag{7.37}$$

Example 7.5.1. *The* weak field *metric has $\alpha = 1+\phi$, $K_{ij}=0$, and $D_i=\mathcal{D}_i$. The Komar mass integrals correctly gives*

$$M_K = \frac{1}{4\pi}\oint_{\partial\Sigma_t} s^i D_i\alpha = \frac{1}{4\pi}\oint_{\partial\Sigma_t} s^i \mathcal{D}_i\phi = \frac{1}{4\pi}\int_{\Sigma_t}\mathcal{D}^i\mathcal{D}_i\phi = \int_{\Sigma_t}\rho\ . \tag{7.38}$$

Example 7.5.2. *The* Schwarzschild *metric in standard coordinates has*

$$\alpha^2 = 1-\frac{2M}{r}\ ,\quad K_{ij}=0\ ,\quad y^\mu=(\theta,\phi)\ ,\quad \sqrt{q}=r^2\sin\theta\ ,\quad s^i=(1,0,0)\ , \tag{7.39}$$

where the surface $\partial\Sigma_t$ is taken as the sphere at radius r. One obtains

$$M_K = \frac{1}{4\pi}\int_{r=const}\left(1-\frac{2M}{r}\right)^{1/2}\frac{\partial}{\partial r}\left(1-\frac{2M}{r}\right)^{1/2} r^2\sin\theta\mathrm{d}\theta\mathrm{d}\phi = \frac{1}{4\pi}\int(...)^{1/2}(...)^{-1/2}\frac{1}{2}\frac{2M}{r^2}r^2\sin\theta\mathrm{d}\theta\mathrm{d}\phi = M \tag{7.40}$$

independently on the choice of the sphere.

Remark 7.5.2. *The equivalence of ADM and Komar mass is a general result for any foliattion Σ_t with timelike unit vector = timelike Killing vector at spatial infinity,*

$$M_K = M_{ADM} \quad\Leftrightarrow\quad n^a = K^a \text{ at } \mathrm{i}_0\ . \tag{7.41}$$

7.5.3 Komar angular momentum

An axisymmetric spacetime has Killing vector $\boldsymbol{K}=\boldsymbol{\phi}$ implementing the rotational symmetry. Choosing a foliation such that $\phi^a n_a = 0$, one has

$$\nabla^a K^b \mathrm{d}s_{ab} = \nabla_a\phi_b(s^a n^b - n^a s^b)\sqrt{q}\mathrm{d}^2y = 2\nabla_a\phi_b s^a n^b\sqrt{q}\mathrm{d}^2y = 2[\nabla_a(\underbrace{\phi_b n^b}_{=0}s^a) - \phi_b\nabla_a(s^a n^b)]\sqrt{q}\mathrm{d}^2y \tag{7.42a}$$

$$= -2\phi_b s^a\nabla_a n^b\sqrt{q}\mathrm{d}^2y = 2K_{ij}s^i\phi^j\sqrt{q}\mathrm{d}^2y \tag{7.42b}$$

The *Komar angular momentum* is defined as

$$J_K := \frac{1}{16\pi}\oint_{\partial\Sigma_t}\mathrm{d}s_{ab}\nabla^a\phi^b = \frac{1}{8\pi}\oint_{\partial\Sigma_t} K_{ij}s^i\phi^j\sqrt{q}\mathrm{d}^2y \quad \text{(Komar angular momentum)}\ . \tag{7.43}$$

8. Initial data problem

This lecture discusses the initial data problem in 3+1 GR, i.e. the solution of the constraints. The CTT and CTS formalisms are presented together with basic black-hole solutions. The latter include Misner data at a moment of time symmetry, as those used in the early-times head-on collision simulations, and the generalized Brill-Lindquist data as those used for binary black hole simulations in the puncture moving framework.

Suggested readings. *Chap. 8 of Gourgoulhon's lecture notes; Chap. 3 of Baumgarte's lecture notes (Book's Chap. 3, 12, 15, App. I); Chap. 3 of Alcubierre's book;*

8.1 Problem's setup

Given the 4 constraint eqs

$$\mathcal{C}_0 := R + K^2 - K_{ij}K^{ij} - 16\pi E = 0 \tag{8.1a}$$

$$\mathcal{C}_i := D_j K^j_i - D_i K - 8\pi P_i = 0 \ , \tag{8.1b}$$

want to determine γ_{ij} and K_{ij} (12 components in total) on Σ_0 such that

(i) Constraints equations are satisfied:

(ii) The solution is physically meaningful, e.g. represents black hole and neutron stars of interest for GR or astrophysics.

The discussion here assumes the matter fields are given.

The constraint eqs are 4 eqs; independently on the particular strategy one decides to follow, one has to prescribe 8 fields/quantities and solve for the remaining 4. The initial data problem thus split into determining

- FREE DATA
- CONSTRAINED DATA

The choice of free/constrained data is based on

(i) Astrophysical/physical expectations for the solution

(ii) Physical meaning (and intuition) of the various metric fields

(iii) Mathematical necessity (linear eqs, decoupled eqs, well-posed eqs).

Two main approaches both based on conformal decomposition of 3+1 eqs following Lichnerowicz (1944) seminal work:

- Conformal transverse traceless (CTT) (York, 1973)
- Conformal thin-sandwich (CTS) (York, 1999)

8.2 Conformal transverse traceless

The CTT approach relies on the decomposition of the conformal traceless extrisic curvature $\hat{A}^{ij}$ ($p = -10$ conformal rescaling) into a *longitudinal* (L) and *transverse* (TT) part:

$$\hat{A}^{ij} := \hat{A}^{ij}_{\rm L} + \hat{A}^{ij}_{\rm TT} = (\tilde{L}X)^{ij} + \hat{A}^{ij}_{\rm TT} \ , \tag{8.2}$$

where the TT part is by definition traceless and divergence free

$$\tilde{\gamma}_{ij}\hat{A}^{ij}_{\rm TT} = 0 \ , \quad \tilde{D}_j \hat{A}^{ij}_{\rm TT} = 0 \ ; \tag{8.3}$$

and the L part is expressed in terms of the *conformal Killing operator*

$$(\tilde{L}X)^{ij} := \tilde{D}^i X^j + \tilde{D}^j X^i - \frac{2}{3}\tilde{D}_k X^k \tilde{\gamma}^{ij} \ , \tag{8.4}$$

associated to the conformal metric and operating on the vector field X^i. The L part is also traceless and symmetric.

Given $\hat{A}^{ij}$, the L/TT decomposition is determined by taking the divergence and solving for the vector X^i the equation

$$\tilde{D}_j \hat{A}^{ij} = \tilde{D}_j (\tilde{L}X)^{ij} = \tilde{D}_j \tilde{D}^j X^i + \frac{1}{3}\tilde{D}^i \tilde{D}_j X^j + \tilde{R}^i_j X^j =: \tilde{\Delta}_{\rm L} X^i \tag{8.5}$$

involving the *conformal vector Laplacian* operator. In other terms:

$$\exists!\ \text{L+TT decomposition} \quad \Leftrightarrow \quad \exists!\ \text{solution of the conformal Laplacian eq.}$$

Theorem 8.2.1. *Cantor (1979)*

$$\left.\begin{array}{l} \mathcal{M} \text{ is asymptotically flat} \\ \partial_k \partial_l \tilde{\gamma}_{ij} = \mathcal{O}(r^{-3}) \end{array}\right\} \Rightarrow \textit{existance and uniqueness is guaranteed .}$$

The constraints equations in the CCT approach are

$$\tilde{D}_i \tilde{D}^i \Psi - \frac{1}{8}\tilde{R}\Psi + \frac{1}{8}\hat{A}_{ij}\hat{A}^{ij}\Psi^{-7} - \frac{1}{12}K^2\Psi^5 + 2\pi\tilde{E}\Psi^{-3} = 0 \tag{8.6a}$$

$$\tilde{\Delta}_{\rm L} X^i - \frac{2}{3}\tilde{D}^i K \Psi^6 - 8\pi \tilde{P}^i = 0 \tag{8.6b}$$

with
- FREE DATA: $\tilde{\gamma}_{ij}, \hat{A}^{ij}_{\rm TT}, K, E, P^i$
- CONSTRAINED DATA: Ψ, X^i

The Lichnerowicz eq is considered an equation for the conformal factor (elliptic, quasilinear); the momentum constraint is an elliptic linear equation for the X^i. The equations are coupled but under the assumption $K = const$ (hypersurfaces have *constant mean curvature*, CMC) the system partially decouple: one can solve first the momentum constraint and then plug the solution X^i into the Lichnerowicz eq and solve for Ψ.

8.2.1 Conformally and asymptotically flat & time-symmetric BH data

The simplest choice of free data is

$$\tilde{\gamma}_{ij} = f_{ij} \quad \text{(Conformally flat)} \tag{8.7a}$$

$$\hat{A}^{ij} \equiv 0 \tag{8.7b}$$

$$K \equiv 0 \quad \text{(Maximal slicing)} \tag{8.7c}$$

$$\tilde{E} = \tilde{P}^i \equiv 0 \quad \text{(Vacuum)} \tag{8.7d}$$

The above choice implies that

$$\tilde{D}_i = \mathcal{D}_i\ , \quad \tilde{D}_i \tilde{D}^i = \mathcal{D}_i \mathcal{D}^i = \Delta\ , \quad \tilde{R} \equiv 0\ , \quad \tilde{L} = L\ . \tag{8.8}$$

and the constraints become

$$\Delta\Psi + \frac{1}{8}(LX)_{ij}(LX)^{ij}\Psi^{-7} = 0 \tag{8.9a}$$

$$\Delta_{\rm L} X^i = \Delta X^i + \frac{1}{3}\mathcal{D}^i \mathcal{D}_j X^j = 0 \tag{8.9b}$$

To set up the BVP with these elliptic equations one needs boundary data. We focus on the following choice:
- Asymptotically flatness
$$\Psi = 1\ , \quad X^i = 0\ , \quad \text{at } \mathrm{i}_0\ (r \to \infty) \tag{8.10}$$
- Inner (strong field) boundary conditions as determined by fixing the topology of the solution. Two cases are considered below.

$\Sigma_0 = \mathbb{R}^3$, No inner boundary conditions. The solution of the momentum constraint is $X^i \equiv 0$, which implies the BVP for the Lichnerowicz eq is

$$\Delta\Psi = 0 \text{ on } \Sigma_0 \quad \text{with} \quad \Psi = 1 \text{ at } \mathrm{i}_0\ . \tag{8.11}$$

The solution is clearly $\Psi \equiv 1$; the solution of the initial value problem is flat spacetime.

$\Sigma_0 = \mathbb{R}^3 \setminus B$**, Boundary conditions on a inner ball.** The simplest choice for the boundary conditions at the inner sphere S is

$$X^i|_S = 0 \quad \text{and} \quad \Psi|_S = 1 \ , \tag{8.12}$$

and leads again to flat spacetime.

Another interesting choice of boundary conditions is

$$X^i|_S = 0 \quad \text{and} \quad S \text{ is a closed minimal surface} \ . \tag{8.13}$$

The second requirement translates to a boundary condition of mixed Newmann/Dirichlet type for Ψ, as we show in what follows. Let s^i the normal vector to S, the minimal condition is (Cf. maximal slicing)

$$0 = D_i s^i|_S = \Psi^{-6}\tilde{D}_i(\Psi^6 s^i) = \Psi^{-6}\mathcal{D}_i(\Psi^6 s^i) = \Psi^{-6}\mathcal{D}_i(\Psi^4 \tilde{s}^i) = \Psi^{-6}\frac{1}{\sqrt{f}}\partial_i(\sqrt{f}\Psi^4\tilde{s}^i) \ ; \tag{8.14}$$

where $\tilde{s}^i := \Psi^{+2}s^i$ is the unit normal w.r.t. the conformal metric, since

$$\tilde{\boldsymbol{\gamma}}(\tilde{\boldsymbol{s}}, \tilde{\boldsymbol{s}}) = \Psi^{-4}\boldsymbol{\gamma}(\tilde{\boldsymbol{s}}, \tilde{\boldsymbol{s}}) = \boldsymbol{\gamma}(\boldsymbol{s}, \boldsymbol{s}) = 1 \ . \tag{8.15}$$

Take now a sphere of radius $r = a$, spherical coordinates $x^i = (r, \theta, \phi)$, normal $\hat{s}^i = (1, 0, 0)$, and $f_{ij} = \mathrm{diag}(1, r^2, r^2 \sin\theta)$. The minimal condition becomes the following Newmann/Dirichlet inner boundary condition:

$$\frac{1}{r^2}\partial_r(r^2\Psi^4)|_{r=a} = 0 \quad \Leftrightarrow \quad \left(\partial_r\Psi + \frac{\Psi}{2r}\right)|_{r=a} = 0 \ . \tag{8.16}$$

The solution of the BVP can be expressed up to the constant a as

$$\Psi = 1 + \frac{a}{r} \ , \tag{8.17}$$

the constant can be identified by computing the ADM mass:

$$M_{\mathrm{ADM}} = -\frac{1}{2\pi}\lim_{r\to\infty}\int \frac{\partial\Psi}{\partial r} r^2 \sin\theta \mathrm{d}\theta\mathrm{d}\phi = -\frac{1}{2\pi}\lim_{r\to\infty} 4\pi r^2 \partial_r(1 + \frac{1}{r}) = 2a \ . \tag{8.18}$$

Hence, the solution is Schwarzschild in isotropic coordinates. Note that a solution with topology $S^2 \times \mathbb{R}$ can be constructed by gluing a copy of Σ_0 at S. The transformation

$$r \mapsto r' := \frac{M^2}{4r} \ , \quad [\frac{M}{2}, \infty) \mapsto [\frac{M}{2}, 0) \tag{8.19}$$

is an *isometry*, and the metric "on the other side" of the Rosen-Einstein bridge (S, $r = M/2$) has exactly the same form. One obtains this way a slice of Schwazrschild connecting region I and III, where the region $r \to 0$ correspond to the other AF end of the wormhole.

Remark 8.2.1. *The solutions discussed above are characterized by*

$$\hat{A}^{ij} \equiv 0 \text{ and } X^i \equiv 0 \ \Rightarrow \ K_{ij} \equiv 0 \ \Rightarrow \ \mathcal{L}_m\gamma_{ij} = 0 \text{ at } t = 0 \ . \tag{8.20}$$

That means the slice Σ_0 is momentarily static (nothing guarantees it will remain static for $t > 0$) and implies that the line element is invariant under $t \mapsto -t$ and $\beta^i = 0$. These initial data are called time symmetric *or a* moment of time symmetry *slice. Time-symmetric black hole solutions have neither linear momentum nor spin.*

Multiple BH: Brill-Lindiquist and Misner data. Since the equation for Ψ is linear, one can superpose solution. Multiple black hole solutions with a moment of time symmetry can be constructed with the following conformal factor

$$\Psi = 1 + \sum_{h=1}^{N} \frac{M_h}{|x^i - c_h^i|} =: 1 + \Psi_{\mathrm{BL}} \ , \tag{8.21}$$

where the point $O_h = (c_h^i) \in \mathbb{R}^3$ is the position of the h-th hole (throats). *Brill-Lindiquist* data are precisely made by the superposition of N holes in such a way there are $N + 1$ AF ends (or "universes"); the points $x^i = c_h^i$ are not part of the Manifold which is then $\Sigma_0 = \mathbb{R}^3 \setminus \{O_h\}$. It is also possible to construct solutions in which the N wormholes connect just two AF ends (two isometric universes.) These data are called *Misner* data and $\Sigma_0 = \mathbb{R}^3 \setminus \{B_h\}$, i.e. where N balls are removed. Their construction is nontrivial. Embedding diagrams for $N = 2$ are shown in Fig. (8.1).

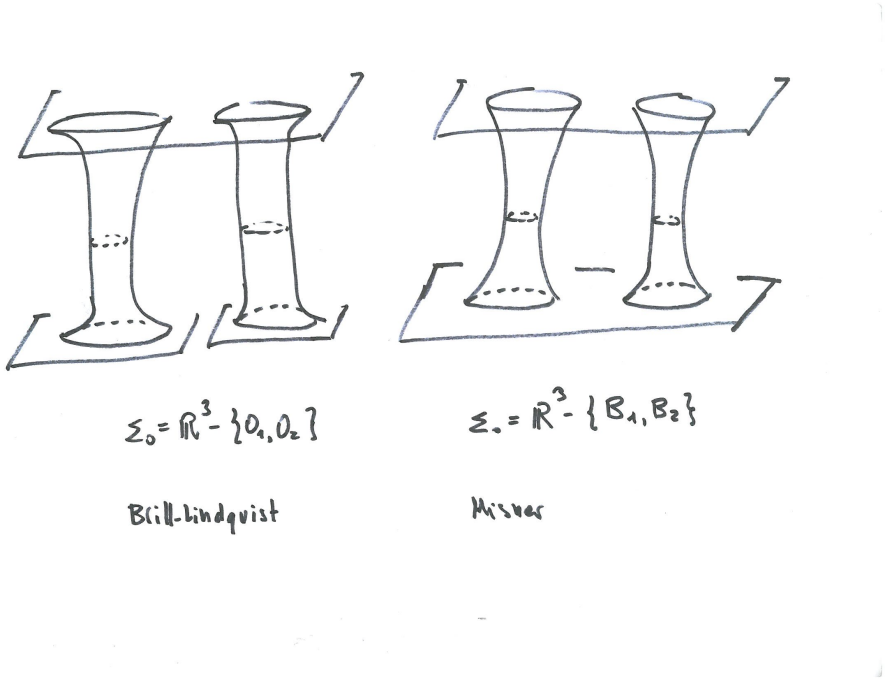

Figure 8.1: Embedding diagrams for two black hole initial data Brill-Lindquist (left) and Misner (right).

8.2.2 Conformally and asymptotically flat & Bowen-York BH data

Continue considering the solution of constraints under the hypothesis Eq. (8.7) and choose, similarly to above, a slice in which one point is removed, $\Sigma_0 = \mathbb{R}^3 \setminus O$. The removed point is called *puncture* and the slice the topology is again $S^2 \times \mathbb{R}$. Instead of the trivial solution of the momentum eq $x^i \equiv 0$, Bowen and York (1980) proposed the following parameteric and generalized solution:

$$X^i = -\frac{1}{4r}\left(7f^{ij}P_j + \frac{1}{r^2}P_j x^j x^i\right) - \frac{1}{r^3}\epsilon^{ij}_k S_j x^k \ , \tag{8.22}$$

where x^i are Cartesian coordinates and P_i, S_i are six free parameters. Note that $P_i = S_i \equiv 0$ reduces to the trivial solution. The corresponding traceless extrinsic curvature is

$$\hat{A}^{ij} = (LX)^{ij} = \underbrace{\frac{3}{2r^3}\left[x^i P^j + x^j P^i + \left(f^{ij} - \frac{x^i x^j}{r^2}\right)P^k x_k\right]}_{\mathcal{O}(r^{-2})} + \underbrace{\frac{3}{r^5}\left(\epsilon^{ik}_l S_k x^l x^j + \epsilon^{jk}_l S_k x^l x^i\right)}_{\mathcal{O}(r^{-3})} \ . \tag{8.23}$$

Meaning of the parameters. The quantities P_i and S_i correspond to the the ADM momentum and angular momentum. Show only the ADM momentum, the calculation for the angular momentum is similar. Since $K = 0$ and $\Psi = 1$,

$$P_i^{\rm ADM} = \frac{1}{8\pi}\lim_{r\to\infty}\int \hat{A}_{ik}x^k r\sin\theta \mathrm{d}\theta\mathrm{d}\phi \tag{8.24a}$$

$$= \frac{1}{8\pi}\lim_{r\to\infty}\int \frac{3}{2r^2}[x_i P_k x^k + \underbrace{x_k x^k}_{=r^2}P^i - \underbrace{(\underbrace{f_{ik}x^k}_{=x_i} - \frac{x^i \overbrace{x^k x_k}^{=r^2}}{r^2})}_{=0}P^j x_j]\sin\theta\mathrm{d}\theta\mathrm{d}\phi + \mathcal{O}(r^{-3}) \tag{8.24b}$$

$$= \frac{1}{8\pi}\lim_{r\to\infty}\int \frac{3}{2}\frac{x_i x^k}{r^2}P_k \sin\theta\mathrm{d}\theta\mathrm{d}\phi + \frac{1}{8\pi}\lim_{r\to\infty}\int\frac{3}{2}P_i\sin\theta\mathrm{d}\theta\mathrm{d}\phi \tag{8.24c}$$

$$= \frac{3}{16\pi}P_k\lim_{r\to\infty}\int\frac{x_i x^k}{r^2}\sin\theta\mathrm{d}\theta\mathrm{d}\phi + 4\pi\frac{3}{16\pi}P_i = \frac{3}{16\pi}(\frac{4\pi}{3}+4\pi)P_i = P_i \ , \tag{8.24d}$$

where the last line uses

$$\int\frac{x^i x^k}{r^2}\mathrm{d}\Omega = \delta^{ik}\int\frac{(x^k)^2}{r^2}\mathrm{d}\Omega = \frac{1}{3}\delta^{ik}\int\frac{r^2}{r^2}\mathrm{d}\Omega = \frac{4\pi}{3}\delta^{ik} \ . \tag{8.25}$$

Note the coordinates employed in the Bowen-York solution belong to the quasi-isotropic gauge since the metric is conformally flat.

Remark 8.2.2. *The* Schwarzschild *solution in isotropic coordinates is recovered for $P_i = S_i \equiv 0$ ($X^i \equiv 0$). However, choosing $P_i \equiv 0$ and $S_i \neq 0$ does* ***not*** *lead to the Kerr solution ! A simple way to grasp this is to observe that Kerr is not conformally flat. Garat and Price (2000) showed that there exists no Kerr foliation that (i) is axisymmetric and conformally flat and (ii) reduces to slices of $t = const$ in the nonrotating limit. The rotating black-holes given by the Bowen-York solution are* ***nonstationary*** *and the evolution of such spacetimes is nontrivial.*

Solution of the Hamiltonian constraint: puncture data. Since $\hat{A}^{ij} \neq 0$ the Lichnerowicz eq must be solved numerically. Possible approaches:

- Generalized Misner data (Cook, 1991; Cook et al., 1993). Solve using the Newmann-Dirichlet condition at the throat, but including the nonvaninshing curvature term.
- Generalized Brill-Lindquist or *puncture* data (Brandt and Brügmann, 1997). Solve on $\mathbb{R}^3$ by analytically separating the singular behaviour at the puncture.

The second approach has become one of the standard methods for black hole simulations, including circular binary mergers. The starting ansatz is

$$\Psi = \Psi_{\rm BL} + u = \sum_{h=1}^{N} \frac{M_h}{|x^i - c_h^i|} + u \ ; \tag{8.26}$$

since the $\Psi_{\rm BL}$ term satisfies $\Delta\Psi_{\rm BL} = 0$ on $\mathbb{R}^3 \setminus \{O_h\}$, the Lichnerowicz eq reduces to an equation for u

$$\Delta u + \frac{\hat{A}_{ij}\hat{A}^{ij}}{8\Psi_{\rm BL}^7}\left(1 + \frac{u}{\Psi_{\rm BL}}\right)^{-7} = 0 \ , \tag{8.27}$$

with outer boundary conditions given y the AF requirement

$$u = 1 + \mathcal{O}(r^{-1}) \quad \text{or} \quad \partial_r u = \frac{1-u}{r} \quad \text{at i}_0 \ (r \to \infty) \ . \tag{8.28}$$

The key observation is that no inner boundary condition is needed at the puncture and the equation can be solved on $\mathbb{R}^3$. Indeed, at the puncture $x^i \approx c_h^i$

$$u \approx |x^i - c_h^i| \tag{8.29a}$$

$$\hat{A}_{ij}\hat{A}^{ij} \approx |x^i - c_h^i|^p \ \text{ with } p = -6 \ (S_i \neq 0) \text{ or } p = -4 \ (S_i = 0) \tag{8.29b}$$

$$\frac{\hat{A}_{ij}\hat{A}^{ij}}{8\Psi_{\rm BL}^7} \approx |x^i - c_h^i|^q \ \text{ with } p = +1 \ (S_i \neq 0) \text{ or } p = +3 \ (S_i = 0) \ , \tag{8.29c}$$

which implies $\Delta u = 0$ at $x^i = c_h^i$. As in the Brill-Lindquist data, the spacetime of puncture data has an AF region for each puncture.

8.3 Conformal thin-sandwich

The CTS approach relies on a different decomposition of the conformal traceless extrinsic curvature than the CTT. The decomposition is suggested by the kinematical eq

$$\mathcal{L}_m \tilde{\gamma}_{ij} = \partial_t \tilde{\gamma}_{ij} - \mathcal{L}_\beta \tilde{\gamma}_{ij} = \partial_t \tilde{\gamma}_{ij} + (\tilde{L}\beta)^{ij} + \frac{2}{3}\tilde{D}_k \beta^k \tilde{\gamma}^{ij} \tag{8.30a}$$

$$= 2\alpha \tilde{A}_{ij} + \frac{2}{3}\tilde{D}_k \beta^k \tilde{\gamma}^{ij} \ , \tag{8.30b}$$

from which one combines the two lines to obtain the decomposition

$$\tilde{A}_{ij} = (2\alpha)^{-1}\left[\partial_t \tilde{\gamma}_{ij} + (\tilde{L}\beta)^{ij}\right] \ . \tag{8.31}$$

Similarly, $\tilde{A}_{ij} = \Psi^{-6}\hat{A}_{ij}$ gives

$$\hat{A}_{ij} = (2\tilde{\alpha})^{-1}\left[\dot{\tilde{\gamma}}_{ij} + (\tilde{L}\beta)^{ij}\right] \quad \text{with} \quad \tilde{\alpha} := \Psi^{-6}\alpha \ , \ \ \dot{\tilde{\gamma}}_{ij} := \partial_t \tilde{\gamma}_{ij} \ . \tag{8.32}$$

Substituting the decomposition into the momentum constraint one finds an alternative equation to Eq. (8.6b).

The constraints equations in the CTS approach are

$$\tilde{D}_i \tilde{D}^i \Psi - \frac{1}{8}\tilde{R}\Psi + \frac{1}{8}\hat{A}_{ij}\hat{A}^{ij}\Psi^{-7} - \frac{1}{12}K^2\Psi^5 + 2\pi\tilde{E}\Psi^{-3} = 0 \tag{8.33a}$$

$$\tilde{D}_j\left(\tilde{\alpha}^{-1}(\tilde{L}\beta)^{ij}\right) + \tilde{D}_j\left(\tilde{\alpha}^{-1}\dot{\tilde{\gamma}}^{ij}\right) - \frac{4}{3}\Psi^6 \tilde{D}^i K - 16\pi\tilde{P}^i = 0 \tag{8.33b}$$

with
- FREE DATA: $\tilde{\gamma}_{ij}, \dot{\tilde{\gamma}}_{ij}, K, E, P^i$
- CONSTRAINED DATA: Ψ, β^i

The Lichnerowicz eq is again considered an equation for the conformal factor (elliptic, quasilinear). The momentum constraint is an elliptic linear equation for the β^i that decouple from the Hamiltonian constraint if $K = 0$ (maximal slicing). Comparing with CTT, the presence of $\dot{\tilde{\gamma}}_{ij}$ brings some intuition for the prescription of the free data w.r.t. $\hat{A}^{ij}_{\rm TT}$, and indeed it is an important element for setting up binary initial data (see below). On the other hand, the conformal lapse $\tilde{\alpha}$ has a more difficult physical interpretation.

Pfeiffer and York (2003) proposed an *extended CTS (XCTS)* approach in which one equation and $\tilde{\alpha}$ is added to the system Eq. (8.33). The additional equation can be found by combining the dynamical eq for K with an identity and the Hamiltonian constraint:

$$\mathcal{L}_m K = \partial_t K - \mathcal{L}_\beta K = \partial_t K - \beta^i \tilde{D}_i K \tag{8.34a}$$

$$= -\Psi^{-4} \underbrace{(\tilde{D}_i \tilde{D}^i \alpha + 2\tilde{D}_i \ln \Psi \tilde{D}^i \alpha)}_{\text{subst. w/ identity in Eq. (8.34c)}} + \alpha[4\pi(E+S) + \hat{A}_{ij}\hat{A}^{ij} + \frac{K^2}{3}] \tag{8.34b}$$

$$\tilde{D}_i \tilde{D}^i \alpha + 2\tilde{D}_i \ln \Psi \tilde{D}^i \alpha = \Psi^{-1}[\tilde{D}_i \tilde{D}^i(\alpha\Psi) + \alpha \underbrace{\tilde{D}_i \tilde{D}^i \Psi}_{\text{subst. w/ Ham. constr.}}] \,, \tag{8.34c}$$

and reads

$$\tilde{D}_i \tilde{D}^i(\tilde{\alpha}\Psi^7) - (\tilde{\alpha}\Psi^7)[\frac{\tilde{R}}{8} + \frac{5}{12}K^2\Psi^4 + \frac{7}{8}\hat{A}_{ij}\hat{A}^{ij}\Psi^{-8} + 2\pi(\tilde{E} + 2S\Psi^8)\Psi^{-4}] + (\dot{K} - \beta^i \tilde{D}_i K)\Psi^5 = 0 \,, \tag{8.35}$$

with $\dot{K} := \partial_t K$

The equations in the XCTS approach are

$$\tilde{D}_i \tilde{D}^i \Psi - \frac{1}{8}\tilde{R}\Psi + \frac{1}{8}\hat{A}_{ij}\hat{A}^{ij}\Psi^{-7} - \frac{1}{12}K^2\Psi^5 + 2\pi\tilde{E}\Psi^{-3} = 0 \tag{8.36a}$$

$$\tilde{D}_j\left(\tilde{\alpha}^{-1}(\tilde{L}\beta)^{ij}\right) + \tilde{D}_j\left(\tilde{\alpha}^{-1}\dot{\tilde{\gamma}}^{ij}\right) - \frac{4}{3}\Psi^6 \tilde{D}^i K - 16\pi\tilde{P}^i = 0 \tag{8.36b}$$

$$\tilde{D}_i \tilde{D}^i(\tilde{\alpha}\Psi^7) - (\tilde{\alpha}\Psi^7)[\frac{\tilde{R}}{8} + \frac{5}{12}K^2\Psi^4 + \frac{7}{8}\hat{A}_{ij}\hat{A}^{ij}\Psi^{-8} + 2\pi(\tilde{E} + 2S\Psi^8)\Psi^{-4}] + (\dot{K} - \beta^i \tilde{D}_i K)\Psi^5 = 0 \tag{8.36c}$$

with
- FREE DATA: $\tilde{\gamma}_{ij}, \dot{\tilde{\gamma}}_{ij}, K, \dot{K}, E, P^i$
- CONSTRAINED DATA: $\Psi, \tilde{\alpha}, \beta^i$

The equations in the XCTS do **not** decouple for $K = 0$. There exists examples of non-unique solutions for certain class of initial data (Pfeiffer and York, 2005; Baumgarte et al., 2007) (See also (Giulini, 1999).) Despite these difficulties, the XCTS can give better control on the time development of the initial data than CTT and CTS. For example, the conditions

$$\dot{\gamma}_{ij} = 0 = \dot{K} \tag{8.37}$$

are necessary conditions for $\boldsymbol{\partial}_t$ to be a Killing vector.

8.3.1 Conformally and asymptotically flat & zero derivatives BH data

The simplest choice of free data is

$$\tilde{\gamma}_{ij} = f_{ij} \quad \text{(Conformally flat)} \tag{8.38a}$$

$$\dot{\tilde{\gamma}}_{ij} = \dot{K} \equiv 0 \tag{8.38b}$$

$$K \equiv 0 \quad \text{(Maximal slicing)} \tag{8.38c}$$

$$\tilde{E} = \tilde{P}^i \equiv 0 \quad \text{(Vacuum)} \tag{8.38d}$$

and the XCTS becomes

$$\Delta\Psi + \frac{1}{8}\hat{A}_{ij}\hat{A}^{ij}\Psi^{-7} = 0 \tag{8.39a}$$

$$\mathcal{D}_j[\tilde{\alpha}^{-1}(L\beta)^{ij}] = 0 \tag{8.39b}$$

$$\Delta(\tilde{\alpha}\Psi^7) - \frac{7}{8}\hat{A}_{ij}\hat{A}^{ij}\tilde{\alpha}\Psi^{-7} = 0 \tag{8.39c}$$

with the usual AF boundary values for the fields; additionally to those described in the previous section on has $\beta^i|_{i_0} = 0$.

Consider a punctured slice $\Sigma_0 = \mathbb{R}^3 \setminus O$. The choice $\beta^i \equiv 0$ is a solution, which implies that the conformal traceless extrisinc curvature is zero,

$$\beta^i \equiv 0 \ , \quad \dot{\tilde{\gamma}}_{ij} = 0 \quad \Rightarrow \quad \hat{A}^{ij} = 0 \ . \tag{8.40}$$

The remaning two eqs further simplify to

$$\Delta\Psi = 0 \quad \Rightarrow \quad \Psi = 1 + \frac{M}{2r} \tag{8.41a}$$

$$\Delta(\tilde{\alpha}\Psi^7) = 0 \quad \Rightarrow \quad \tilde{\alpha}\Psi^7 = 1 + \frac{a}{r} \ . \tag{8.41b}$$

The solution of Eq. (8.41a) with AF data is regular on the *punctured* Σ_0, as seen in the CTT approach. The solution of Eq. (8.41b) with AF data depends on a constant a. Combining the two solution the lapse reads

$$\alpha = \Psi^6\tilde{\alpha} = (\tilde{\alpha}\Psi^7)\Psi^{-1} = \left(1 + \frac{a}{r}\right)\Psi^{-1} = \left(1 + \frac{a}{r}\right)\left(1 + \frac{M}{2r}\right)^{-1} = \frac{r + a}{r + M/2} \ , \tag{8.42}$$

and the value of a can be choosen by selecting the limiting value of the lapse *at* the puncture, $\alpha_0 := \alpha(r = 0) = 2a/M$.

Problem: What to choose for the lapse?, i.e.

$$\alpha_0 = \lim_{r\to 0} \alpha(r) = ? \tag{8.43}$$

There are at least two simple choices resulting to different slices of Schwarzschild:

$$\alpha_0 = +1 \quad \Rightarrow \quad a = +\frac{M}{2} \quad \Rightarrow \quad \alpha \equiv 1 \quad \text{(Geodesic slicing)} \tag{8.44}$$

$$\alpha_0 = -1 \quad \Rightarrow \quad a = -\frac{M}{2} \quad \Rightarrow \quad \alpha = \left(1 - \frac{M}{2r}\right)\left(1 + \frac{M}{2r}\right)^{-1} \quad \text{(Isotropic coords)} \ . \tag{8.45}$$

Consequences:

(i) Both choices lead to a momentarily static initial slice of Schwarzschild, but ...
(ii) ... their time development is different!
(iii) $\alpha_0 = 1$ will result in a nontrivial evolution,
(iv) $\alpha_0 = -1$ will result in trivial evolution since $\boldsymbol{\partial}_t$ is a Killing vector.

Remark 8.3.1. *The choice $\alpha_0 = -1$ implies that the assumption $\alpha > 0$ on Σ_0 is violated, since the lapse takes negative values in some regions. While $\boldsymbol{n}$ remains futre pointing, allowing a negative lapse means that the coordinate time runs "backward" near the AF end $r \to 0$.*

8.3.2 Binary systems and quasi-circular orbits

Initial data for binary simulations must be prepared at finite separatation. Gravitational waves emission leads to fast orbit circularization; standard formation scenarios and channels predict that in the final stages of the coalescence process the compat binary have circularized. Hence, simulations of circular initial data are particularly relevant and are believed to be the most common astrophysical scenario.

Problem: What symmetry should one impose to construct a circular binary spacetime?

Stationary spacetimes have $\boldsymbol{\partial}_t$ as Killing vector; spacetimes with a rotational symmetry generated by $\boldsymbol{\partial}_\phi$. Spacetimes for exactly circular binaries have none of these two symmetries but an observer comoving with an orbit of frequency Ω rotates of angle $\delta\phi$ in a time δt related by

$$\delta\phi = \Omega\delta t \ . \tag{8.46}$$

That suggests the spacetime is invariant for those comoving observers, Fig. (8.2).

Circular orbits can be implemented by imposing the spacetime has a *helical Killing vector* (Gourgoulhon et al., 2002)

$$\mathcal{L}_\xi g = 0 \quad \text{where asymptotically} \quad \xi^a := (\boldsymbol{\partial}_t)^a + \Omega(\boldsymbol{\partial}_\phi)^a \ . \tag{8.47}$$

If one chooses a frame comoving with the orbit, then $\boldsymbol{\partial}_t = \boldsymbol{\xi}$ and the helical symmetry can be simply imposed by requiring that

$$\dot{\tilde{\gamma}}_{ij} = 0 = \dot{K} \ . \tag{8.48}$$

The XCTS formalism is well suited for implementing these conditions; binary black hole and neutron star circular initial data are often generated with this method.

An excellent introduction on the helical Killing vector (and its connection to the Kepler law) can be found in Le Tiec (2012).

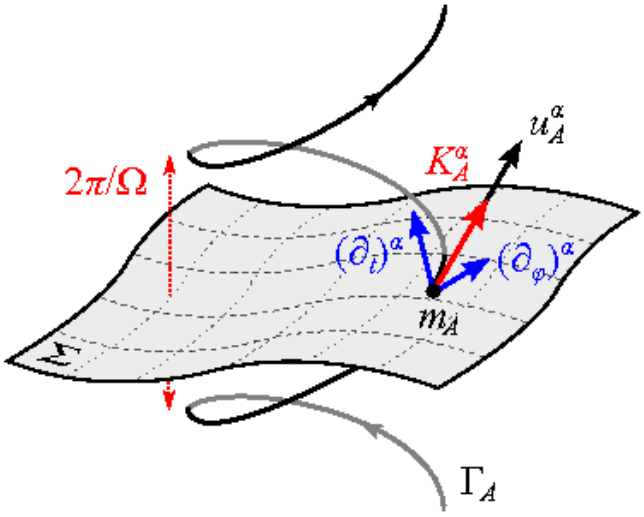

Figure 8.2: Helical Killing vector for binary initial data. Figure taken from (Le Tiec, 2012)

Remark 8.3.2. *The XCTS equations + helical Killing vector + conformally flat metric reduces to the IWM eqs.*

Remark 8.3.3. *For puncture-type initial data it is not possible to find a solution of XCTS+helical Killing vector with regular lapse (Hannam et al., 2003). Circular binary black hole initial data within the Bowen-York CTT approach are not implemented using the helical Killing vector. In that approach the puncture parameters are tuned in order to minimize some experimental measure of the eccentricity, e.g. (Husa et al., 2008). Using a conformally-flat metric, puncture parameters are usually inferred from post-Newtonian results.*

9. Gauge conditions

This lecture discusses some of the most common gauge choices for simulations of black holes (BHs) and neutron stars (NSs). The choice of the foliation/slicing (prescription or equation for the lapse) and of the spatial coordinates (prescription or equation for the shift) is crucial for long-term NR simulations of gravitational collapse, BH formation, and to handle the movement of BHs and NSs. Singularity avoiding coordinates prevent the foliation to fall into the singularity and minimize the spatial distortion. Ideally, good gauge conditions for numerical applications possess some (vaguely defined) "symmetry seeking" property that drives the coordinates to those adapted to the spacetime's Killing vectors (either pre-existing or forming during the simulation.)

Suggested readings. *Chap. 9 of Gourgoulhon 3+1 lecture notes; Chap. 4 of Alcubierre's book; Chap. 5 of Baumgarte's lecture notes (Book's Chap. 4, 8.1, 13.1.3);*

9.1 Slicing

9.1.1 Geodesic slicing

Setting

$$\alpha \equiv 1 \ , \quad \beta^i \equiv 0 \ \ \text{(Geodesic slicing and zero shift).} \tag{9.1}$$

coorresponds to choose Gaussian normal coordinates for the evolution. In these coordinates the acceleration of Eulerian observers is zero (free-falling) and their coordinate time corresponds to proper time,

$$n^a = (\partial_t)^a \ , \quad a_a = D_a \ln\alpha = 0 \ , \quad \mathrm{d}\tau = \mathrm{d}t \ . \tag{9.2}$$

Example 9.1.1. *The geodesic slicing of Schwarzschild corresponds to use Novikov coordinates. These are the coordinates comoving with radially free-falling test particles and measuring proper time. A simulation that uses these coordinates and a grid covering the Schwarzschild radii $2M < r < r_{max}$ in Σ_t would crash at about $t \sim \pi M$, i.e. as soon as the innermost grid point reaches the $r = 0$ singularity (See e.g. Brügmann (1996))*

As suggested by the Schwarzschild example, geodesic coordinates are not suitable for simulations of gravitational collapse. The qualitative behaviour of the simulation can be understood from the evolution equations for the trace of the extrinsic curvature and the determinant of the 3-metric specified to the geodesic case,

$$\partial_t K = K_{ij}K^{ij} + 4\pi(E - S) \geq 0 \tag{9.3a}$$

$$\partial_t \ln\sqrt{\gamma} = -K \ , \tag{9.3b}$$

where the second equation follows from

$$K = \gamma^{ab}K_{ab} = -\frac{1}{2\alpha}\gamma^{ab}\mathcal{L}_m\gamma_{ab} = -\frac{1}{2\alpha}\mathcal{L}_m \ln\gamma = -\frac{1}{\alpha\sqrt{\gamma}}\mathcal{L}_m\sqrt{\gamma} = -\frac{1}{\alpha}\mathcal{L}_m \ln\sqrt{\gamma} \ , \tag{9.4}$$

and relates K to the coordinate volume element $\sqrt{\gamma}$. Under the hypotesis of "ordinary matter" ($E - S \geq 0$), Eq. (9.3) indicates that while the matter collapses and becomes more compact, the mean curvature $K > 0$ increases. At the same time the volume element goes to zero and the free-falling Eulerian observers get closer to each others, coordinates focus and singularities, either physical or coordinate, forms.

9.1.2 Maximal slicing

To improve on the focusing geodesics coordinates, one can consider that the *expansion* of Euler observers is simply given by the trace of the extrinsic curvature (from the definition),

$$K = -\nabla_a n^a \ . \tag{9.5}$$

Geometrically K measures how n^a bends if transported along Σ_t, and hence it tells how much the worldlines of Eulerian observers converge or diverge, Fig. (4.2). The condition

$$K = -\nabla_a n^a = 0 \quad \Rightarrow \quad D_i D^i \alpha - \alpha[4\pi(E+S) + K_{ij}K^{ij}] = 0 \ \ \text{(Maximal slicing)} \tag{9.6}$$

corresponds then to a slicing in which the Eulerian observers do not converge towards the central singularity (if the latter forms.) The Eulerian acceleration $a_a \neq 0$ balances the focusing effect of gravity. Slicings with this property are called *singularity avoding slicings.*

Remark 9.1.1. *The equation above is the same equation describing an* incompressible fluid, $\nabla_a u^a = 0$, *where u^a is the fluid 4-velocity.*

Example 9.1.2. *In the* Schwarzschild spacetime, *the slices $t = const$ (Schwarzschild time coordinate) are spatial hypersurfaces for $R > 2M$ (R is the Schwarzschild radius to distinguish it from the isotropic r). The foliation is a maximal slicing since $K_{ab} \equiv 0$ implies $K = 0$, that is not horizon penetrating: the $R = 2M$ is reached asymptotically at $t \to +\infty$. The foliation can be extended from region I to region III of the Kruskal-Szekere diagram without penetrating the horizon ($R = 2M$). The lapse function in isotropic coordinates is*

$$\alpha = \left(1 - \frac{M}{2r}\right)\left(1 + \frac{M}{2r}\right)^{-1} \ , \tag{9.7}$$

and it is antisymmetric w.r.t. the throat $r = M/2$. Note the lapse is negative for $r < M/2$.

In the region $R < 2M$, the hypersurfaces $R = const$ are spacelike (R is a timelike coordinate). A maximal slice can be easily found by considering the line element in Schwarzschild coordinates, reading off

$$\alpha = \left(\frac{2M}{R} - 1\right)^{-1/2} \ , \quad \gamma = R^4 \sin^2\theta \left(\frac{2M}{R} - 1\right) \ , \tag{9.8}$$

and using Eq. (9.4) in the form $d/dR \ln\gamma = 2\alpha K$ to obtain:

$$K = \frac{3M - 2R}{R^2(2M/R - 1)^{1/2}} \ . \tag{9.9}$$

Hence, $R = 3M/2$ is a maximal slice and it can be proven that it is the only hypersurface $R = const$ which is spacelike and maximal. The $R = 3M/2$ slice is a limiting slice of a maximal foliation of Schwarzschild covering region I,II and III of the Kruskal-Szekere diagram. This maximal foliation has a lapse symmetric about $r = M/2$ and never encounters the singularity. The embedding diagram of this soution is different from the wormhole one: there is one AF end the other end an infinitely long cylinder (hence the name trumpet*.)*

Example 9.1.3. *The* general construction of maximal foliations of Schwarzschild *goes as follows. Take standard coordinates in which the metric is written in term of the function $A(R) = 1 - 2M/R$, and consider the transformatin of the standard time coordinate t to*

$$\tilde{t} = t + h(R) \ , \tag{9.10}$$

where $h(R)$ is the height function *that enters in the expression of the new metric components. The height function can be determined by the maximal slicing condition up to a constant of integration C,*

$$0 = K = -\nabla_a n^a = -(-g)^{-1/2}\partial_a((-g)^{1/2}n^a) \ , \ \ \Rightarrow \ h'(R) = \frac{C^2}{A^2(R)(A(R)R^4 + C^2)} \ . \tag{9.11}$$

The resulting metric has components

$$\alpha^2 = f(R) \ , \quad \beta^r = C\sqrt{f(R)}R^{-2} \ , \quad \gamma_{ij}\mathrm{d}x^i\mathrm{d}x^j = f(R)^{-1}\mathrm{d}R^2 + R^2\mathrm{d}\Omega \ , \quad \textit{with} \ \ f(R) := 1 + \frac{2M}{R} + \frac{C^2}{R^4} \ . \tag{9.12}$$

The constant C parameterizes the family of foliations, e.g. $C = 0$ is the $t = const$ foliation of standard Schwarzschild time. The particular symmetric/antisymmetric foliations discussed in the previous example are included in the foliation family parametrized by C. They also correspond to solutions of the elliptic equation for the lapse, Eq. (9.6). Both cases have $\alpha \to 1$ at i_0 as outer boundary conditions but they differ for the choice of the inner boundary (in a way analogue to what discussed in Chap. 8). The antisymmetric foliation corresponds to $C = 0$ and the Dirichlet condition at the throat $\alpha(R = 2M) = 0$; the symmetric foliation corresponds to $C = 3\sqrt{3}M^2/4$ and the Newmann condition $\partial_R\alpha(R = 3M/2) = 0$ at the asymptotic slice $R = 3M/2$. See [Alcubierre & Baumgarte books for details/discussions].

The Schwarzschild maximal foliations discussed above highlight the singularity-avoidance property of maximal slicing. In practice, the elliptic equation Eq. (9.6) for the lapse guarantees that $\alpha \to 0$ in regions where the curvature increases so that the proper time (of Eulerian observers) between two neighbouring hypersurfaces "freezes" and they do not evolve. For Schwarzschild (Smarr and York, 1978a; Beig and O'Murchadha, 1998) have shown that the lapse at the throat collapse to zero exponentially in a characteristic timescale $\sim 2\sqrt{3}/4M \approx 1.82M$ as the slice approaches $R = 3M/2$ [1]. This effect is called *collapse of the lapse* and it is a generic feature of singularity avoiding slicings (See also below and the middle panel of Fig. (9.1)).

9.1.3 Harmonic slicing

The $\mu = 0$ component of the harmonic gauge $\Box x^\mu = 0$ is a slicing condition that can be expressed as an evolution equation for the lapse.

$$0 = \Box t = (-g)^{-1/2}\partial_\mu[(-g)^{1/2}g^{\mu\nu}\underbrace{\partial_\nu t}_{=\delta^0_\nu}] = (-g)^{-1/2}\partial_\mu[(-g)^{1/2}g^{\mu 0}] \quad \Rightarrow \tag{9.13a}$$

$$0 = \partial_t(\alpha\sqrt{\gamma}g^{00}) + \partial_i(\alpha\sqrt{\gamma}g^{0i}) = -\partial_t(\sqrt{\gamma}\alpha^{-1}) + \partial_i(\sqrt{\gamma}\alpha^{-1}\beta^i) \quad \Rightarrow \tag{9.13b}$$

$$0 = \partial_t\alpha - \beta^i\partial_i\alpha - \alpha\underbrace{[\gamma^{-1/2}\partial_t\sqrt{\gamma} - \underbrace{\gamma^{-1/2}\partial_i(\sqrt{\gamma}\beta^i)}_{=D_i\beta^i}]}_{=-\alpha K} \tag{9.13c}$$

where in the third line the metric component in adapted coordinates have been used together with some of the 3+1 equations previously derived. From the definition of the Lie derivative $\mathcal{L}_m$ one obtains

$$\mathcal{L}_m\alpha = -\alpha^2 K \quad \text{(Harmonic slicing)} \tag{9.14}$$

Example 9.1.4. Schwarzschild *in standard coordinates has*

$$\partial_t\alpha = 0 \ , \quad \beta^i = 0 \ , \quad K = 0 \ , \tag{9.15}$$

implying that t = const slices are hamornic slices. These slices do not penetrate the horizon and are singular at $R = 2M$.

Example 9.1.5. *Horizon penetrating harmonic slicing of Schwarzschild (and Kerr-Newmann) spacetime have been found by Bona and Masso (1988); Cook and Scheel (1997). The foliation can be found by the following transformation of the standard time coordinate t to*

$$\tilde{t} = t + 2M\ln|1 - \frac{2M}{R}| \ , \tag{9.16}$$

and extends to the singularity $R = 0$ at asymptotic times $\tilde{t} \to \infty$.

The above example suggests that the harmonic slicing has singularity avoiding properties similar to the maximal slicing, e.g. (Geyer and Herold, 1995). With zero shift $\beta^i \equiv 0$, Eq. 9.14 can be integrated to obtain the lapse up to an arbitrary function of the spatial coordinates,

$$\alpha = c(x^i)\sqrt{\gamma} \quad \text{(Harmonic slicing and zero shift)} \ . \tag{9.17}$$

Calculating instead the harmonic gauge for the spatial components $\mu = i$ leads to a hyperbolic evolution equation for the shift vector:

$$\mathcal{L}_m\beta^i = -\alpha^2(\gamma^{ij}\partial_j\ln\alpha + \gamma^{ij}\Gamma^i_{jk}) \quad \text{(Harmonic shift)} \ . \tag{9.18}$$

9.1.4 Bona-Masso & 1+log slicings

A general evolution equation for the lapse was proposed by Bona et al. (1996)

$$\mathcal{L}_m\alpha = -\alpha^2 f(\alpha)K \quad \text{(Bona-Masso slicing)} \tag{9.19}$$

[1] At the horizon the lapse is asymptotically $\alpha = 3\sqrt{3}/16 \approx 0.32$ (Reimann and Bruegmann, 2004)

where $f(\alpha)$ is an arbitrary function. Possible choices are:

$$f(\alpha) := 0 \ , \quad \text{Geodesic slicing} \tag{9.20a}$$

$$f(\alpha) := 1 \ , \quad \text{Harmonic slicing} \tag{9.20b}$$

$$f(\alpha) := \frac{2}{\alpha} \ , \quad \text{1+log} \tag{9.20c}$$

The 1+log formula has been proposed by Bernstein and Anninos et al. (1995). For zero shift it can be integrated:

$$(\partial_t - \mathcal{L}_\beta)\alpha = -2\alpha K = \partial_t \ln\gamma - 2D_i\beta^i \ ; \ \ \beta^i \equiv 0 \ \ \Rightarrow \ \ \partial_t\alpha = \partial_t \ln\gamma \tag{9.21a}$$

$$\alpha = 1 + \ln\gamma \ \ \text{(1+log slicing and zero shift)} \tag{9.21b}$$

Example 9.1.6. *Stationary 1+log foliations of* Schwarzschild *have been studied by Hannam et al. (2007); Brown (2008); Hannam et al. (2008) both numerically and analytically with a method similar to the one presented above for maximal foliations. One of the results is an implicit expression for the lapse very similar to the one for maximal slicing:*

$$\alpha^2 = 1 - \frac{2M}{R} + \frac{C^2}{R^4}\mathrm{e}^{\alpha} \quad \textit{(1+log slicing)} \ , \tag{9.22}$$

$$\textit{compare to} \quad \alpha^2 = 1 - \frac{2M}{R} + \frac{C^2}{R^4} \quad \textit{(Maximal slicing)} \tag{9.23}$$

In the case of 1+log slicing the constant C can be determined by demanding the regularity of the derivative $\alpha'(R)$; one finds $C = \sqrt{2}(\sqrt{10}+3)^{3/2}\mathrm{e}^{(3-\sqrt{10})/2}M^2/16 \approx 1.2467M^2$. The solution is similar to the maximal slice trumpet, and has the throat (root of $\alpha^2(R) = 0$) located at $R \approx 1.31241M$ and the horizon at $\alpha \approx 0.3761$.

The 1+log slicing has singularity avoiding properties and it is the slicing choice adopted in the BSSN scheme for the evolution of Bowen-York punctures as well as for the neutron star and gravitational collapse simulations (see Sec. 9.3 below).

9.2 Spatial gauge

Consider a gravitational collapse simulation with a singularity avoiding slicing and zero shift. Along the evolution, the slices can become very distorted due to the lapse collapse in strong field regions and the fields on Σ_t can develop large spatial gradients. As the collapse proceed, more grid points would be needed to resolve such gradients. In black hole simulations with $\beta^i \equiv 0$ one also observers that the coordinate area of the apparent horizon grows. These observations suggest the necessity of a spatial gauge that "minimizes spatial distortion". Minimal spatial distortions can be achieved by deriving appropriate elliptic eqs for shift vector. For computational efficiency and to work with free-evolution schemes, various "drivers" replacing the elliptic with parabolic or hyperbolic equations have been developed, e.g. (Balakrishna et al., 1996).

Current binary black-hole simulations employ the hyperbolic gamma-driver shift as a key element for moving the Bowen-York punctures (with 1+log slicing). The gamma-driver shift is also crucial to handle singularity formation during gravitational collapse (see Sec. 9.3).

9.2.1 Minimal distortion

Define the *distortion tensor* as the symmetric, traceless tensor Σ_{ij} given by

$$Q_{ij} := \partial_t\gamma_{ij} = -2\alpha K_{ij} + \mathcal{L}_\beta\gamma_{ij} \tag{9.24a}$$

$$\Sigma_{ij} := Q_{ij} - \frac{1}{3}Q\gamma_{ij} = -2\alpha A_{ij} + (L\beta)_{ij} = \Psi^4\partial_t\tilde{\gamma}_{ij} \ . \tag{9.24b}$$

An equation for the shift can be found by minimizing the functional

$$I[\beta^i] := \int_{\Sigma_t}\Sigma_{ij}\Sigma^{ij}\sqrt{\gamma}\mathrm{d}^3x = \int_{\Sigma_t}[4\alpha^2 A_{ij}A^{ij} - 4\alpha A_{ij}(L\beta)^{ij} + (L\beta)_{ij}(L\beta)^{ij}]\sqrt{\gamma}\mathrm{d}^3x \tag{9.25}$$

w.r.t to β^i while holding all the other fields fixed.

$$\delta I[\beta^i] = 2\int_{\Sigma_t}\Sigma_{ij}\delta(L\beta)^{ij}\sqrt{\gamma}\mathrm{d}^3x = 2\int_{\Sigma_t}\Sigma_{ij}(D^i\delta\beta^j + D^j\delta\beta^i - \underbrace{\frac{2}{3}D_k\delta\beta^k\gamma^{ij}}_{=0 \ \Leftarrow \ \Sigma_{ij}\gamma^{ij}=0})\sqrt{\gamma}\mathrm{d}^3x = \tag{9.26a}$$

$$= 2\int_{\Sigma_t}\Sigma_{ij}(D^i\delta\beta^j + D^j\delta\beta^i)\sqrt{\gamma}\mathrm{d}^3x = 4\int_{\Sigma_t}\Sigma_{ij}D^i\delta\beta^j\sqrt{\gamma}\mathrm{d}^3x = \quad (\Sigma_{ij} \text{ symmetric}) \tag{9.26b}$$

$$= 4\int_{\Sigma_t}D^i(\Sigma_{ij}\delta\beta^j)\sqrt{\gamma}\mathrm{d}^3x - 4\int_{\Sigma_t}D^i\Sigma_{ij}\delta\beta^j\sqrt{\gamma}\mathrm{d}^3x = \underbrace{4\int_{\partial\Sigma_t}\Sigma_{ij}s^j\delta\beta^i\sqrt{q}\mathrm{d}^2y}_{=0 \ \Leftarrow \ \delta\beta^i|_{\partial\Sigma_t}=0} - 4\int_{\Sigma_t}D^i\Sigma_{ij}\delta\beta^j\sqrt{\gamma}\mathrm{d}^3x \tag{9.26c}$$

Hence, setting $\delta I[\beta^i] = 0$ implies

$$D^i\Sigma_{ij} = 0 \quad \Leftrightarrow \quad \Delta_L\beta^i = 2D_j(\alpha A^{ij}) = 16\pi\alpha P^i + \frac{4}{3}\alpha D^i K + 2A^{ij}D_j\alpha \quad \text{(Minimal distortion shift)}. \tag{9.27}$$

The minimal distortion condition reduces to an elliptic eq for the shift vector in terms of the conformal vector Laplacian associated to the 3-metric. Properties:

- The distortion tensor is identically zero if $\boldsymbol{\partial}_t$ is a Killing vector. The minimal distortion gauge is thus satisfied by stationary spacetimes in adapted coordinates.
- In the weak-field limit the minimal distortion gauge includes the TT gauge of linearized gravity (Smarr and York, 1978b).

Remark 9.2.1. *An alternative derivation of the minimal distortion gauge starts from the decomposition of Σ_{ij} into a transverse-traceless (TT) and a logitudinal (L) part, similarly for what done for the CTT eqs. Then since the TT part is divergence free, $D^i\Sigma_{ij} = D^i\Sigma^{TT}_{ij} + D^i\Sigma^{L}_{ij} = D^i\Sigma^{L}_{ij}$, and one obtains Eq. (9.27) by demanding that the divergence of the L part vanishes.*

An approximate form of the minimal distortion gauge is

$$0 = D^i\Sigma_{ij} = D^i(\Psi^4\partial_t\tilde\gamma_{ij}) = \tilde D^i(\Psi^6\partial_t\tilde\gamma_{ij}) \approx \tilde D^i(\partial_t\tilde\gamma_{ij}), \tag{9.28}$$

The equation reduces to an elliptic equation for the shift in terms of the conformal vector Laplacian associated to the conformal metric. Shibata (1999) proposed to further simplify the shift equation by substituing the conformal vector Laplacian relative to the flat metric f_{ij}. The gauge condition was used in the first binary neutron star merger in general relativity (Shibata and Uryu, 2000).

9.2.2 Gamma freezing & drivers

The *gamma-freezing condition* is a minimal-distortion condition in the form (Alcubierre and Brügmann, 2001)

$$0 = \mathcal{D}_j\dot{\tilde\gamma}^{ij} = \partial_t\mathcal{D}_j(\tilde\gamma^{ij}) \tag{9.29a}$$

$$= \partial_t(\partial_j\tilde\gamma^{ij} + F^i_{jk}\tilde\gamma^{jk} + \underbrace{F^j_{jk}}_{=\frac{1}{2}\partial_k\ln f=\frac{1}{2}\partial_k\ln\tilde\gamma}\tilde\gamma^{ik}) = \partial_t(\partial_j\tilde\gamma^{ij} + \tilde\Gamma^i_{kj}\tilde\gamma^{jk} + (F^i_{jk} - \tilde\Gamma^i_{jk})\tilde\gamma^{jk} + \underbrace{\frac{1}{2}\partial_k\ln\tilde\gamma}_{=\tilde\Gamma^j_{jk}}\tilde\gamma^{ik}) \tag{9.29b}$$

$$= \partial_t(\underbrace{\partial_j\tilde\gamma^{ij} + \tilde\Gamma^i_{kj}\tilde\gamma^{jk} + \tilde\Gamma^j_{jk}\tilde\gamma^{ik}}_{=\tilde D_j\tilde\gamma^{ij}=0} + (F^i_{jk} - \tilde\Gamma^i_{jk})\tilde\gamma^{jk}) = -\partial_t\tilde\Gamma^i\ , \tag{9.29c}$$

where

$$\tilde\Gamma^i := -\mathcal{D}_j\tilde\gamma^{ij} = (\tilde\Gamma^i_{jk} - F^i_{jk})\tilde\gamma^{jk}\ . \tag{9.30}$$

Note that the $\mathcal{D}_j$ and ∂_t derivatives commute since the background metric $\boldsymbol{f}$ is time independent. Taking the flat divergence of the evolution equation for $\dot{\tilde\gamma}^{ij}$ and combining it the momentum constraint, the gamma-freezing reduces to an elliptic equation for the shift:

$$\partial_t\tilde\Gamma^i = 0 \quad \text{(Gamma-freeezing shift)} \quad \Rightarrow \tag{9.31a}$$

$$\tilde\gamma^{jk}\mathcal{D}_j\mathcal{D}_k\beta^i + \frac{1}{3}\tilde\gamma^{ji}\mathcal{D}_j\mathcal{D}_k\beta^k + \frac{2}{3}\tilde\Gamma^i\mathcal{D}_k\beta^k - \tilde\Gamma^k\mathcal{D}_k\beta^i + \beta^k\mathcal{D}_k\tilde\Gamma^i \tag{9.31b}$$

$$= 2\alpha[8\pi\Psi^4P^i - \tilde A^{jk}(\tilde\Gamma^i_{jk} - F^i_{jk}) - 6\tilde A^{ij}\mathcal{D}_j\ln\Psi + \frac{2}{3}\tilde\gamma^{ij}\mathcal{D}_jK] + 2\tilde A^{ij}\mathcal{D}_j\alpha$$

Gamma-driver conditions have been proposed to replace the above elliptic equation with parabolic or hyperbolic equations (Alcubierre et al., 2003):

$$\partial_t\beta^i = k\partial_t\tilde\Gamma^i \quad \text{(Parabolic gamma-driver)} \tag{9.32a}$$

where $k > 0$ is an arbitrary function. Since $\partial_t \tilde{\Gamma}^i \sim \tilde{\gamma}^{jk}\partial_j\partial_k\beta^i + ...$, the equation is parabolic; its "relaxed" ($t \to \infty$) solution approximate the gamma-freezing shift. Alternatively, the gamma-freezing gauge can be replaced by a hyperbolic equation

$$\partial_{tt}\beta^i = k\partial_t\tilde{\Gamma}^i - (\eta - \partial_t \ln k)\partial_t\beta^i \quad \text{(Hyperbolic gamma-driver)} \tag{9.33a}$$

where $\eta > 0$ is an arbitrary function entering a damping term. An equivalent first-order system of the hyperbolic gamma-driver (for k time-independent) is

$$\begin{cases} \partial_t\beta^i &= kB^i \\ \partial_t B^i &= \partial_t\tilde{\Gamma}^i - \eta B^i \ . \end{cases} \tag{9.34}$$

Integrating the last equation leads to a simplified first-order equation van Meter et al. (2006); Gundlach and Martin-Garcia (2006)

$$\partial_t\beta^i = \mu_S\tilde{\Gamma}^i - \eta\beta^i + \beta^j\partial_j\beta^i \ , \tag{9.35}$$

with μ_s is a function setting the characteristic speed.

The hyperbolic gamma-driver shift is a standard choice to handle puncture spacetimes in combination with the 1+log slicing and the BSSN or Z4c schemes. For binary black holes simulations in the puncture framework it is the key ingredient for the "moving puncture" technique Baker et al. (2006); Campanelli et al. (2006). Moreover, it is used in binary neutron star mergers and supernova core-collapse to handle black hole formation.

Remark 9.2.2. *The functions k and η are often set as constants in simulations after numerical experiments. Compact binaries and gravitational collapse simulations often employ $k \sim 0.75 - 1$ and $\eta \sim 1/M$ where M is the ADM mass of the system.*

9.2.3 Dirac gauge

The Dirac (1959) gauge (See also (Smarr and York, 1978a; Bonazzola et al., 2004))

$$0 = \tilde{\Gamma}^i = \mathcal{D}_j(\tilde{\gamma}^{ij}) \quad \text{(Dirac gauge)} \ , \tag{9.36}$$

implies gamma-freezing gauge if enforced at all times. It translates into an elliptic equation for the shift, which is precisely Eq. (9.31a) with $\tilde{\Gamma}^i = 0$. It is used in a *fully constraint* schemes for 3+1 GR in which the number of elliptic equations are maximized, leaving only with two hyperbolic equations corresponding to the gravitational-wave degrees of freedom (Bonazzola et al., 2004).

Remark 9.2.3. *Differently from the spatial gauge conditions discussed above the Dirac gauge completely fix the spatial coordinates x^i on the slice. The other spatial gauges discussed so far leave the freedom of choosing x^i and constrain the way these coordinate propagates from one slice to the next.*

9.3 Role of 1+log and Gamma drivers in simulations

9.3.1 Single black hole

Consider Bowen-York puncture initial data for a single black hole (nonspinning, unboosted).

In the Kruskall diagram with coordinates (u, v) the initial slice Σ_0 is the $v = 0$ slice in region I and III. Σ_0 is nonstationary and its 3+1 time-evolution depends on the choice of the lapse. Any spacelike slice, in particular, can be evolved into a time-independent slice if lapse and shift are choosen such that $t^a = \alpha n^a + \beta^a$ coincides with the timelike vector field of the spacetime.

Remark 9.3.1. *The choice of shift does not affect the slicing. The shift determines how spatial coordinates are carried from one slice to the next one. In a simulation, in which space is discretized by a grid, the shift tells how the grid points change from the current to the next slice.*

Considering the directions of the future-pointing timelike Killing vector in the Kuskall diagram, one realizes that, if $\alpha > 0$, it is not possible to construct a foliation that is (i) stationary (ii) extends from region I to III, fig (Cf. discussion in Chap. 8 about CST solution for one BH).

Questions:

(i) How does Σ_0 evolve with 1+log slicing?
(ii) Does Σ_0 evolves to the trumpet slice of Example 9.1.6?
(iii) What is the role of shift during a simulation? (In particular for zero shift and Γ-driver cases)

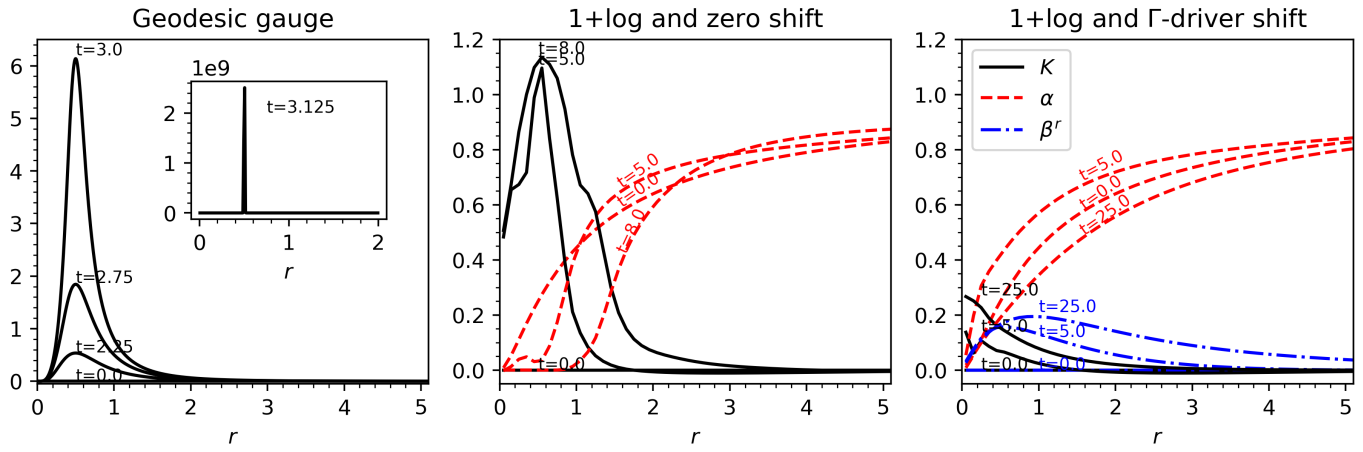

Figure 9.1: Evolution of a single puncture of ADM mass $M = 1$ with different gauges and the Z4c scheme. The left panel show the trace of the curvature blowing up as the observer at $M/2$ approaches the singularity. The middle panel show the lapse collapse; the simulation crashes shortly after $t = 8$. The right panel demonstrates stable evolutions; the fields at $t \approx 25$ reach a stationary state. Grid resolution is $h = 0.005$ for geodesic gauge and $h = 0.1$ otherwise. The initial 1+log lapse is taken as $\alpha = \Psi^{-2}$.

Zero shift case. Observations:

(a) Σ_0 is symmetric under reflections about the v, i.e. the metric γ_{ij} is invariant under $u \mapsto -u$.
(b) The spatial geometry in region III is identical to the one in region I
(c) If one chooses a symmetric lapse $\alpha(t = 0)$, then the geometry must remain symmetric during the time evolution

From the above considerations one would concludes that Σ_0 cannot evolve to the trumpet geometry, as shown in Fig. 9.2.

Problem: numerical experiments suggest Σ_0 evolutions with 1+log and Γ-driver shift asymptotically reach to (i) a quasi-stationary state (ii) very close to trumpet soluton, e.g. (Hannam et al., 2007).

Γ-driver shift case. Consider the numerical experiments of Brown (2008); Hannam et al. (2008) and imagine the space covered by an uniform radial grid. Observations:

(a) Initially the grid points are not uniformly distributed in u, but they are uniform in the radial coordinate r. The shift is initially zero $\beta^r = 0$.
(b) During the evolution the curvature and β^r get large value close to the puncture $r \sim 0$; thus, the Γ-driver pushes the coordinate points from region III to region I of the Kruskall diagram. Since

$$\dot{\beta}^r \sim \mu_S \tilde{\Gamma}^r \ , \tag{9.37}$$

that can happen very quickly if one chooses $\mu_S = 1$ (speed of light) or a faster function for $\alpha \to 0$ (superluminal).
(c) Σ_0 evolves quickly to a slice that in region I and II is close, but different, to the stationary slice. However, the shift evolution pushes the grid points from region III to region II; region III is not anymore resolved after some evolution time.

The experiments are illustrated in Fig. (9.2). During the numerical evolution the spacetime inside the horizon is not resolved, the slice is effectively covered by grid points only in region II and I. Comparing to numerical techniques that excise the inner region of the BH, the puncture gauge choice is simpler and effective; sometimes it is refreed as *natural excision* (see also discussion in (Alcubierre et al., 2003)).

9.3.2 Gravitational collapse

Consider now gravitational collapse in spherical symmetry. That is a different situation from above since the initial slice does not extend from region III to region I: it is a regular slice from $r = 0$ to the matter radius and Schwarzschild in the exterior of the matter distribution. However, the role of the 1+log lapse and Γ-driver shift is similar to the puncture and crucial for successful simulations.

As the collapse proceeds $\alpha \to 0$ and when the horizon is formed ($\alpha \approx 0.3$) the shift vector pushes the grid points to larger proper radii effectively underresolving region II. The simulation reaches a stationary slice identical to the numerical trumpet of Sec. 9.3.1 in region II and I.

This behaviour also explain why in puncture gauge simulations the matter is observed to "disappear" once the horizon forms. The rest-mass is a conserved quantity and cannot change even if the matter flows into the horizon (See Chap. 11). However, if the shift removes grid points from region II, the matter is unresolved on the grid.

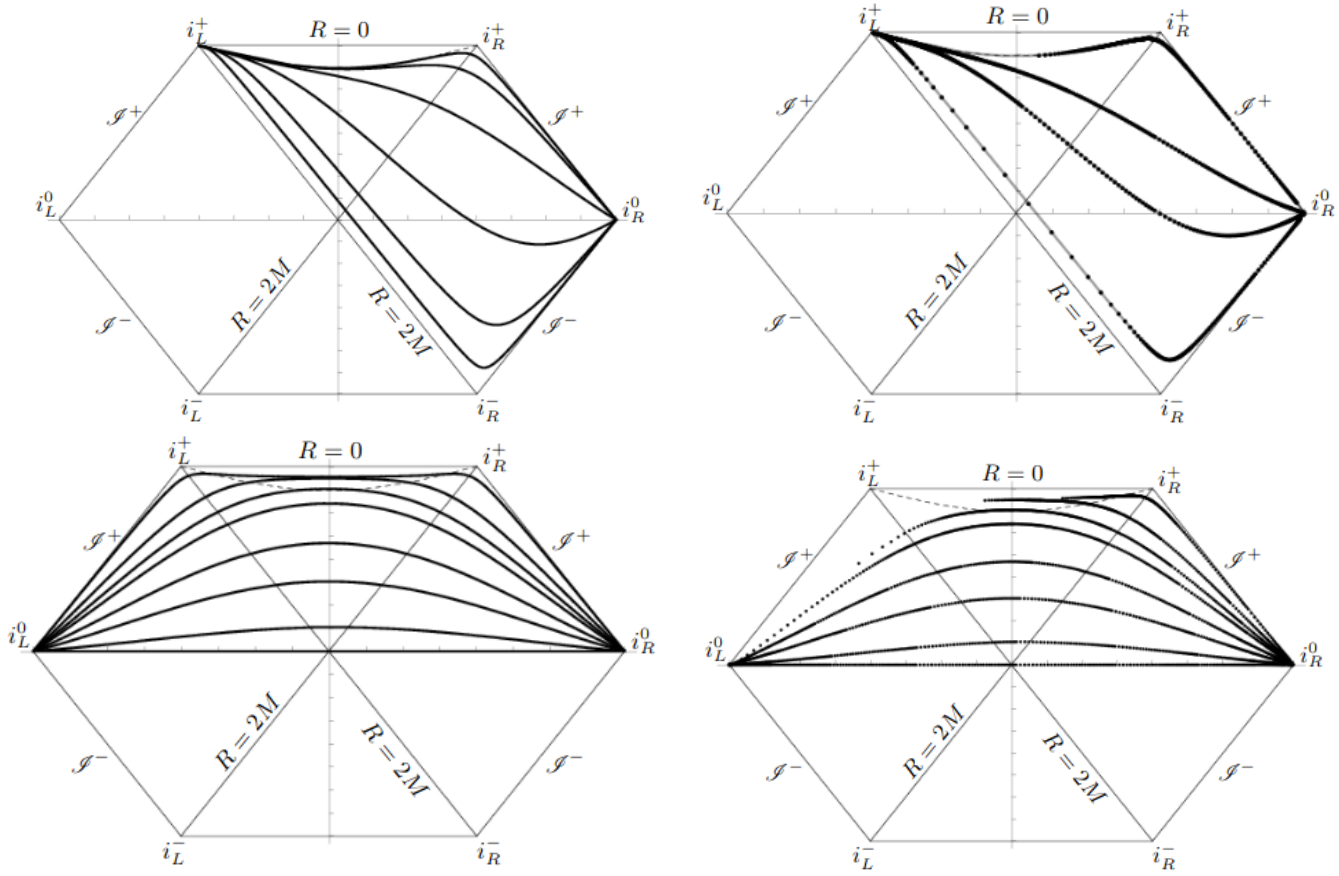

Figure 9.2: Penrose diagram for Schwarzschild with different slicings. Top-Left: analytical stationary 1+log slices of Example 9.1.6 with trumpet $R \approx 1.31M$. Top-Right: analytical stationary 1+log slices of Example 9.1.6 and numerical evolution starting at t=-40M. Bottom-Left: numerical evolution with 1+log and $\beta \equiv 0$. The numerical slicing is different from the stationary 1+log slice, in particular it is symmetric about v. Bottom-Right: numerical evolution with 1+log and Γ-driver shift. The slicing is the same as the one on the left but grid points cover only part of it. Figures from Hannam et al. (2007).

The experiments are illustrated in Fig. (9.2), see (Thierfelder et al., 2011; Dietrich and Bernuzzi, 2015) for more discussions. Note that zero shift $\beta^r \equiv 0$ is not sufficiently robust to simulate the star collapse and the subquent black hole evolution, even in spherical symmetry.

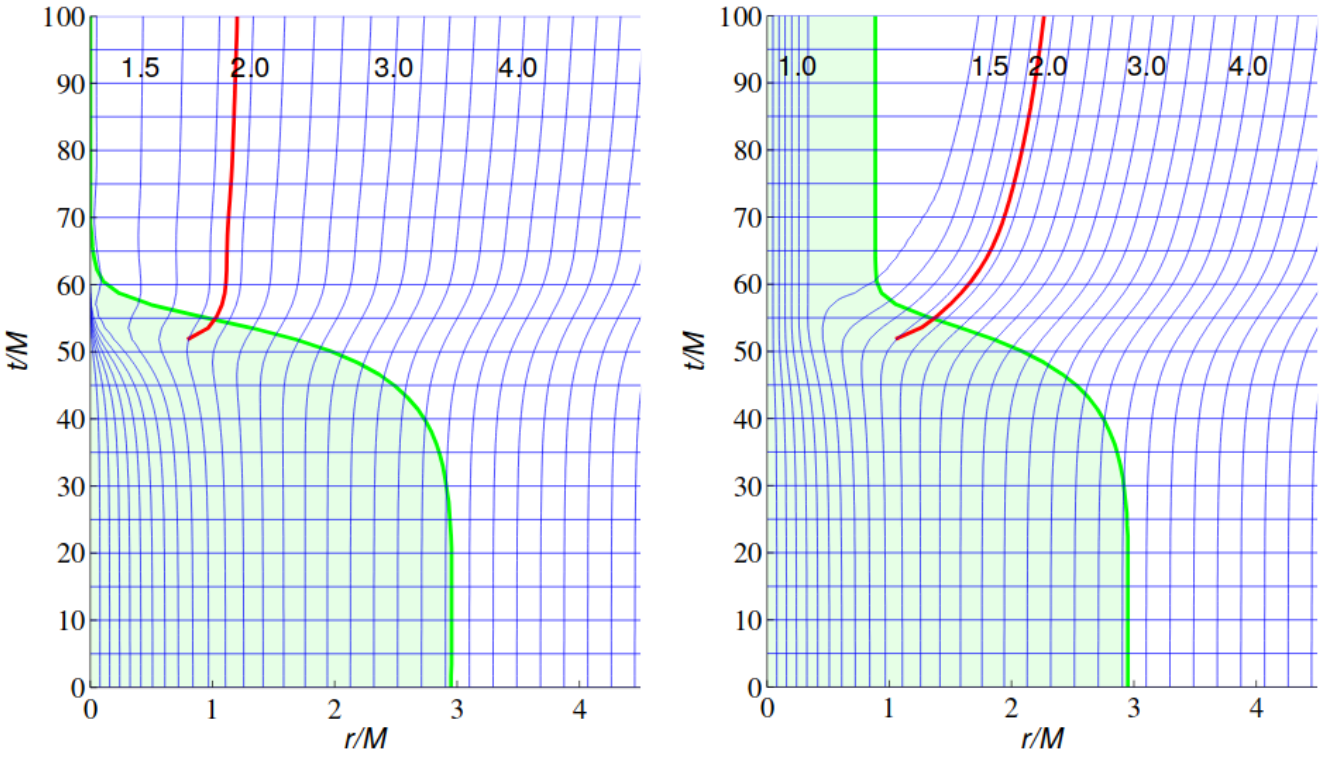

Figure 9.3: Spacetime diagram for a spherically symmetric collapsing star in moving puncture spherical coordinates. Γ-driver parameters are $\mu_S = 1$ (Left) $\mu_S = \alpha^2$ (Right). The second choice makes the shift slower but the simulations crashes shortly after. The horizontal blue lines are lines of constant coordinate time. The thick red line denotes the apparent horizon.The vertical blue lines are lines of constant Schwarzschild radius $R = const$ which values are on top of the lines. The shaded green area bounded by the thick green lines shows the region of the matter; note that the rest-mass is conserved if region II is better resolved. Figure from Thierfelder et al. (2011).

10. Hyperbolic free-evolution schemes

In this lecture the two most popular free-evolution scheme for EFE employed in astrophysical applications are described. Focus is on the reduction of the equations to strongly hyperbolic form, the condition under which the Cauchy problem is well-posed. The concept of hyperbolicity and its relation with well-posedness of the Cauchy problem are summarized in Appendix A.

Suggested readings. *Chap. 2.6-2.9 of Alcubierre's book; Chap. 4 of Baumgarte's lecture notes (Book's Chap. 2, 11); Chap. 10 of Gourgoulhon's lecture notes.*

10.1 Free-evolution schemes for EFE

The most common approach for (3+1)D simulations is free-evolutions: once specified the initial slice at $t = 0$ by solving the constraints, one solves the Cauchy problem associated to the 3+1 evolution EFE in order to compute the spacetime at successive times. The approach is justified since, up to numerical errors, the constrains remain satisfied at $t > 0$.

The free-evolution approach requires to develop 3+1 schemes for EFE that admit a well-posed Cauchy problem or IVP. To this aim the evolution equations must be written in symmetric or strongly hyperbolic form in order to exploit the following

Theorem 10.1.1. *A strongly hyperbolic PDE system admits a well-posed Cauchy problem (IVP).*

See Chap. 3 for our operative/generic definition of well-posedness and Appendix A for a short review of hyperbolic equations and well-posedness of the Cauchy problem. For the time being, the operative definition of strong hyperbolicity that we adopt is:

Definition 10.1.1. *A second-order system of PDEs is strongly hyperbolic iff the principal part (highest derivatives) is in the form* $\Box_g u \simeq 0$.

We discuss below two formulations for free-evolutions: the generalized hamornic gauge (GHG) and the BSSNOK scheme. Those are the schemes in use for most of the astrophysical applications, in particular

- The GHG scheme with constraint damping terms was used by Pretorius (2005) for the binary black hole (BBH) breaktrhough.
- The GHG in first-order symmetric hyperbolic form is currently the preferred scheme for implementations based on pseudo spectral methods (`SpEC` code - SXS collaboration, `bamps` code - Jena/CoRe collaboration).
- The BSSNOK scheme was used for the moving puncture BBH breaktrhough (Baker et al., 2006; Campanelli et al., 2006) and it is the standard scheme employed for black hole evolutions with that technique (1+log and gamma-driver gauge) and finite-differencing–based numerical techniques.
- The BSSNOK scheme with 1+log and gamma-driver gauge is also the most popular scheme for simulations of compact binaries with matter or gravitational collapse (supernovae explosion).
- Closely related to the BSSNOK, the Z4c scheme proposed by Bernuzzi and Hilditch (2010); Hilditch et al. (2013) based on the Z4 formulation improves the Hamiltonian constraint violation by using an additional equation that propagates and damps the constraint ($\dot{\theta} = ...$ in Eq. (5.39c)). Thanks to this property, Z4c is prefereed to BSSNOK for matter evolutions, e.g. (Reisswig et al., 2013; Hotokezaka et al., 2013)

Remark 10.1.1. *There exist other approaches to the evolution problem in GR. One possibility is to consider the spacetime foliated by* null hypersurfaces *(instead of spacelike). This approach, also known as* characteristic approach*, is optimal for the description of radiation and asymptotic fields (e.g. boundary conditions at null infinity) but brings in difficulties in the description of the strong-field region (caustics). See Winicour (2009) for a review. A second possibility is to consider spacetime foliations that are spatial everywhere but reach null infinity; they are called* hyperboloidal hypersurfaces*. Adopting a conformal decomposition of the 4-metric,* $g_{ab} = \Omega^2 \tilde{g}_{ab}$ *in which* $\Omega = 0$ *represents null-infinity, Friedrich (1986); Friedrich and Nagy (1999) has derived regular and symmetric hyperbolic equations scheme for the conformal variables defining a well-posed IVP (*conformal approach*, see also Zenginoğlu (2008)). The*

hyperboloidal approach has several advantages w.r.t the spacelike approach (boundary considtions, extraction of radiation, etc) but astrophysical applications in (3+1)D are not yet possible due to the limited developments/knowledge of gauge conditions, scri-fixing techniques, and initial data.

10.2 Generalized Harmonic Gauge (GHG) scheme

EFE in vacuum are $R_{ab}=0$ with the Ricci tensor given by

$$R_{ab} = \underbrace{-\frac{1}{2}g^{cd}\partial_c\partial_d g_{ab} + \nabla_{(a}\Gamma_{b)}}_{\text{principal part}} + g^{cd}g^{ef}(\partial_e g_{ca}\partial_f g_{db} - \Gamma_{ace}\Gamma_{bdf}) \ , \tag{10.1}$$

where

$$\Gamma_a := g^{bc}\Gamma_{abc} \ , \quad \nabla_a\Gamma_b = \partial_a\Gamma_b - g^{cd}\Gamma_{cab}\Gamma_d \ . \tag{10.2}$$

Enforcing the condition

$$\Gamma_\alpha \equiv 0 \ , \quad \text{(Harmonic gauge, HG)} \tag{10.3}$$

leads to a manifestly symmetric hyperbolic system of 10 eqs and the 4 constraints:

$$\Box_g g_{\alpha\beta} := g^{\gamma\delta}\partial_\gamma\partial_\delta g_{\alpha\beta} = 2g^{\gamma\delta}g^{\sigma\rho}(\partial_\sigma g_{\gamma\alpha}\partial_\rho g_{\delta\beta} - \Gamma_{\alpha\gamma\sigma}\Gamma_{\beta\delta\rho}) \quad \text{(HG scheme)} \tag{10.4a}$$

$$\mathcal{C}_\alpha := (R_{\alpha\beta} - \frac{1}{2}g_{\alpha\beta}R)n^\beta = 0 \quad \text{(HG constraints)} \tag{10.4b}$$

Verify the condition above corresponds to a harmonic choice of the coordinates:

$$0 = \Box x^\mu = g^{\alpha\beta}\nabla_\alpha\nabla_\beta x^\mu = g^{\alpha\beta}\nabla_\alpha(\partial_\beta x^\mu) = g^{\alpha\beta}[\partial_\alpha(\underbrace{\partial_\beta x^\mu}_{\delta^\mu_\beta}) - \underbrace{\partial_\gamma x^\mu}_{\delta^\mu_\gamma}\Gamma^\gamma_{\alpha\beta}] = 0 - g^{\alpha\beta}\Gamma^\mu_{\alpha\beta} = -\Gamma^\mu \ . \tag{10.5}$$

In the *generalized harmoinic gauge* formulation (Friedrich, 1985; Garfinkle, 2002) one introduces the 4 functions

$$\Gamma_a \equiv H_a \ , \quad \text{(Generalized harmoinic gauge, GHG)} \tag{10.6}$$

that are either prescribed or the solution of some symmetric hyperbolic gauge equations. Also in this case the resulting evolution system is manifestly symmetric hyperbolic. Taking H_a as a given function, one can define the algebraic constraint

$$Z_a := H_a - \Gamma_a \ , \tag{10.7}$$

and write the EFE as the equivalent system:

$$\bar{R}_{ab} := R_{ab} - \nabla_{(a}Z_{b)} = 0 \ , \quad \text{and} \quad Z_a = 0 \ . \tag{10.8}$$

The Bianchi identities guarantees that GHG gauge is maintained along the evolution if initially $Z_a = \dot{Z}_a \equiv 0$ because the algebraic constraint evolves according to a linear wave equation:

$$\bar{R} := g^{ab}(R_{ab} - \nabla_{(a}Z_{b)}) = R - \nabla_d Z^d = 0 \tag{10.9a}$$

$$0 = \nabla^a(\bar{R}_{ab} - \frac{1}{2}\bar{R}g_{ab}) = \underbrace{\nabla^a R_{ab} - \frac{1}{2}g_{ab}\nabla^a R}_{=0 \text{ Bianchi identities}} - \frac{1}{2}\nabla_a\nabla^a Z_b + \frac{1}{2}\underbrace{(-\nabla^a\nabla_b Z_a)}_{=+\nabla_b\nabla^a Z_a - R^c_b Z_c} + \frac{1}{2}g_{ab}\nabla^a\nabla^d Z_d \tag{10.9b}$$

$$= -\frac{1}{2}\nabla_a\nabla^a Z_b + \cancel{\frac{1}{2}\nabla_b\nabla^a Z_a} + \frac{1}{2}R_{bc}Z^c - \cancel{\frac{1}{2}\nabla_b\nabla^a Z_a} \tag{10.9c}$$

$$= \cancel{\frac{1}{2}}\nabla_a\nabla^a Z_b + \cancel{\frac{1}{2}}R_{bc}Z^c = \Box_g Z_b + R_{bc}Z^c \ . \tag{10.9d}$$

The above eq is the same as the Z4 system. Indeed the Z4 system is equivalent to GHG if the Z_a is specified as in Eq. (10.7), i.e. the algebraic constraint enforcing the condition Eq. (10.6). In general, the vector Z^a can be evolved in the Z4 scheme and one can add further equations for the lapse and shift.

A first order GHG formulation was proposed by Alvi (2002); Lindblom et al. (2008). Using 3+1 adapted coordinates, it reads

$$\Pi_{\alpha\beta} := -n^\sigma\partial_\sigma g_{\alpha\beta} \ , \quad \Phi_{i\alpha\beta} := \partial_i g_{\alpha\beta} \ , \quad u := (g_{\alpha\beta}, \Phi_{i\alpha\beta}, \Pi_{\alpha\beta}) \tag{10.10a}$$

$$\partial_t u + A^k(u)\partial_k u = s(u) \tag{10.10b}$$

Principal part:

$$\begin{cases} \partial_t g_{\alpha\beta} - \beta^k \partial_k g_{\alpha\beta} & \simeq 0 \\ \partial_t \Pi_{\alpha\beta} - \beta^k \partial_k \Pi_{\alpha\beta} & \simeq 0 \\ \partial_t \Phi_{i\alpha\beta} - \beta^k \partial_k \Phi_{i\alpha\beta} + \alpha \partial_i \Pi_{\alpha\beta} & \simeq 0 \end{cases} \tag{10.10c}$$

Note the symbol "$\simeq$" used for "principal part"; it will be used again below with the same meaning.

Remark 10.2.1. *The GHG first order formulation of Alvi (2002) can produce shocks since is not a* linearly degenerate *hyperbolic system. For example the* $(0i)$*-component is*

$$\partial_t \beta^i - \beta^k \partial_k \beta^i \simeq 0 \ , \tag{10.11}$$

which is a Burger-like eq. Moreover the constraint

$$\mathcal{C}_{i\alpha\beta} := \partial_i g_{\alpha\beta} - \Phi_{i\alpha\beta} \tag{10.12}$$

drives some numerical instability. The formulation by Lindblom et al. (2008) is linearly degenerate and improves the stability of the constraint $\mathcal{C}_{i\alpha\beta}$*. It is obtained by adding the constraint* $\mathcal{C}_{iab}$ *in a way proportional to free parameters* γ_i $i = 1, 2, 3$ *and carefully choosing the latter.*

10.3 ADMY to BSSNOK

The evolution ADMY equations (Eq. (4.30) and Eq. (5.15)) are a strongly hyperbolic system under the conditions
(i) the shift is a prescribed
(ii) the lapse belongs to the Bona-Masso family or the densitized lapse $\bar{\alpha} = \alpha/\sqrt{\gamma}$ is prescribed
(iii) the momentum constraint is identically satisfied along the evolution.
The result above can be found by explicit constructing the eigenfields (rather than a symmetrizer, see Appendix A) as discussed in detail in Alcubierre's book. While the possibility of specifying the gauge, at least in a certain class, is a desiderable property of the ADMY scheme (the GHG scheme does not have this possibility), the conditions above are too restrictive to guarantee well-posedness of a free-evolution scheme. In particular, it is unclear how to enforce the condition (iii) in numerical applications. If (iii) is dropped the ADMY scheme is weakly hyperbolic (has real eigenvalues but no well-posedness results apply).

Strongly hyperbolic formulations based on ADMY can be found following similar ideas to those presented for HG (Shibata and Nakamura, 1995; Baumgarte et al., 1999). Combine Eq. (4.30) with Eq. (5.15) (or Eq. (5.34a) with Eq. (5.34b)) and consider the principal part of the differential operator (say in Cartesian coordinates):

$$\partial_{tt}\gamma_{ij} \ \simeq \ -2\alpha R_{ij} \ \simeq \ \Delta\gamma_{ij} + \gamma_{ik}\partial_j\partial_l\gamma^{kl} + \gamma_{jk}\partial_i\partial_l\gamma^{kl} \ ; \tag{10.13}$$

without the blue terms the r.h.s. would reduce to the Laplace operator and hyperbolicity would be manifest. A way to proceed is to define the auxiliary variable

$$f^k := \partial_l \gamma^{kl} \ , \tag{10.14}$$

and find an evolution equation for f^k without specifying the gauge. Considering that

$$\partial_t f^k = \partial_t\partial_l\gamma^{kl} = \partial_l\partial_t\gamma^{kl} \simeq \partial_l K^{kl} \sim \mathcal{C}^k \ , \tag{10.15}$$

the natural way to obtain the new equation is to use the momentum constraint. The time derivative of the auxliary variable becomes then proportional to the momentum constraint. Note the similarity to the Z4 formulation and in particular to Eq. (5.39d). The approach discussed above is essentially the one started in Nakamura et al. (1987) and employed by various authors, including the scheme of Nagy et al. (2004) (NOR).

The BSSNOK (Shibata and Nakamura, 1995; Baumgarte et al., 1999) scheme apply this idea to the conformal ADMY equations. The conformal Ricci is

$$\tilde{R}_{ij} = \mathcal{D}_k\tilde{C}^k_{ij} - \tilde{C}^k_{il}\tilde{C}^l_{kj} \simeq -\frac{1}{2}\tilde{\gamma}^{kl}\left(\mathcal{D}_k\mathcal{D}_l\tilde{\gamma}_{ij} + \tilde{\gamma}_{ik}\mathcal{D}_j\mathcal{D}_l\tilde{\gamma}^{kl} + \tilde{\gamma}_{jk}\mathcal{D}_i\mathcal{D}_l\tilde{\gamma}^{kl}\right) \tag{10.16}$$

$$\text{with} \quad \tilde{C}^k_{ij} := \tilde{\Gamma}^k_{ij} - F^k_{ij} = \frac{1}{2}\tilde{\gamma}^{kl}\left(\mathcal{D}_i\tilde{\gamma}_{lj} + \mathcal{D}_j\tilde{\gamma}_{il} - \mathcal{D}_l\tilde{\gamma}_{ij}\right) \ . \tag{10.17}$$

Suggesting the definition of the *auxiliary conformal variables*

$$\tilde{\Gamma}^i := -\mathcal{D}_j\tilde{\gamma}^{ij} = (\tilde{\Gamma}^i_{jk} - F^i_{jk})\tilde{\gamma}^{jk} \ . \tag{10.18}$$

Note this is precisely the variable of gamma-freezing gauge and drivers. An equation for $\tilde{\Gamma}^i$ can be found be taking the divergence of the $\partial_t \tilde{\gamma}_{ij}$ equation and combining it (blue term) with the momentum constraint (blue equation):

$$-\partial_t \tilde{\Gamma}^j = \partial_t(\mathcal{D}_i \tilde{\gamma}^{ij}) = \mathcal{D}_i(\partial_t \tilde{\gamma}^{ij}) = \mathcal{D}_i(-2\alpha \tilde{A}^{ij} - \frac{2}{3}\tilde{D}_k \beta^k \tilde{\gamma}^{ij}) - \mathcal{D}_i(\mathcal{L}_\beta \tilde{\gamma}^{ij}) \tag{10.19a}$$

$$= -2\alpha \mathcal{D}_i \tilde{A}^{ij} - 2\tilde{A}^{ij}\mathcal{D}_i\alpha - \frac{2}{3}\tilde{D}_k\beta^k \underbrace{\mathcal{D}_i \tilde{\gamma}^{ij}}_{=-\tilde{\Gamma}^j} - \frac{2}{3}\tilde{\gamma}^{ij}\mathcal{D}_i(\tilde{D}_k\beta^k) - \mathcal{D}_i(\mathcal{L}_\beta \tilde{\gamma}^{ij}) \Rightarrow \tag{10.19b}$$

$$\mathcal{L}_m \tilde{\Gamma}^i = \frac{2}{3}\tilde{D}_k\beta^k\Gamma^i + \tilde{\gamma}^{jk}\mathcal{D}_j\mathcal{D}_k\beta^i + \frac{1}{3}\tilde{\gamma}^{ij}\mathcal{D}_j\mathcal{D}_k\beta^k - 2(\alpha \mathcal{D}_j \tilde{A}^{ij} + \tilde{A}^{ij}\mathcal{D}_j\alpha) \tag{10.19c}$$

$$\mathcal{D}_j \tilde{A}^{ij} = -\tilde{C}^i_{jk}\tilde{A}^{jk} - 6\tilde{A}^{ij}\tilde{D}_j \ln\Psi + \frac{2}{3}\tilde{D}^i K + 8\pi\Psi^4 P^i \quad \text{(Mom.constraint)} \tag{10.19d}$$

Collecting together all the equations [cf. Eq. (6.22),Eq. (6.23),Eq. (6.40a),Eq. (6.40c)]

BSSNOK evolution eqs:

$$\mathcal{L}_m \Psi = \frac{1}{6}\Psi\left(\tilde{D}_i\beta^i - \alpha K\right) \tag{10.20a}$$

$$\mathcal{L}_m \tilde{\gamma}_{ij} = -2\alpha\tilde{A}_{ij} - \frac{2}{3}\tilde{D}_k\beta^k\tilde{\gamma}_{ij} \tag{10.20b}$$

$$\mathcal{L}_m K = -\Psi^{-4}\left(\tilde{D}_i\tilde{D}^i\alpha + 2\tilde{D}_i \ln\Psi \tilde{D}^i\alpha\right) + \alpha\left[4\pi(E+S) + \tilde{A}^{ij}\tilde{A}_{ij} + \frac{K^2}{3}\right] \tag{10.20c}$$

$$\mathcal{L}_m \tilde{A}_{ij} = \text{ [... as in Eq. (6.40c) ...]} \tag{10.20d}$$

$$\mathcal{L}_m \Gamma^i = \frac{2}{3}\mathcal{D}_k\beta^k\tilde{\Gamma}^i + \tilde{\gamma}^{jk}\mathcal{D}_j\mathcal{D}_k\beta^i + \frac{1}{3}\tilde{\gamma}^{ij}\mathcal{D}_j\mathcal{D}_k\beta^k - 2\tilde{A}^{ij}\mathcal{D}_j\alpha \tag{10.20e}$$

$$- 2\alpha\left(8\pi\Psi^4 P^i - \tilde{A}^{jk}\tilde{C}^i_{jk} - 6\tilde{A}^{ij}\mathcal{D}_j \ln\Psi + \frac{2}{3}\tilde{\gamma}^{ij}\mathcal{D}_j K\right)$$

Algebraic constraints:

$$d := \gamma - f = 0\ , \quad \tilde{A} := \tilde{\gamma}^{ij}\tilde{A}_{ij} = 0\ , \quad \mathcal{A}^i := \tilde{\Gamma}^i + \mathcal{D}_j\tilde{\gamma}^{ij} = 0 \tag{10.20f}$$

Constraints:

$$\tilde{D}_i\tilde{D}^i\Psi - \frac{1}{8}\tilde{R}\Psi + \left(\frac{1}{8}\tilde{A}^{ij}\tilde{A}_{ij} - \frac{K^2}{12} + 2\pi E\right)\Psi^5 = 0 \tag{10.20g}$$

$$\tilde{D}^j\tilde{A}_{ij} + 6\tilde{A}_{ij}\tilde{D}^j \ln\Psi - \frac{2}{3}\tilde{D}_i K - 8\pi P_i = 0 \tag{10.20h}$$

Equations (or a prescription) for the lapse and shift must be added to the BSSNOK eqs. Gundlach and Martin-Garcia (2006) have proven strong hyperbolicity for a class of gauges that include 1+log lapse and gamma-driver shift (excluding certain values of the parameters entering those equations).

Note that

$$\tilde{\gamma} = f \quad \Rightarrow \quad \tilde{C}^k_{ik} = \frac{1}{2}\partial_i \ln\tilde{\gamma} - \frac{1}{2}\partial_i \ln f = 0\ , \tag{10.21}$$

$$\tilde{R} \simeq \mathcal{D}_k\tilde{\Gamma}^k \tag{10.22}$$

In cartesian coordinates the expressions simplify significantly since

$$F^k_{ij} \equiv 0\ , \quad \tilde{C}^k_{ij} = \tilde{\Gamma}^k_{ij}\ , \quad \mathcal{D}_i = \partial_i\ . \tag{10.23}$$

Remark 10.3.1. *For applications involving punctures (either movement or formation) the conformal factor Ψ is often substituted with the variables $\phi = \ln\Psi$ or $\chi = \Psi^{-4} = \exp(-4\phi)$ or $W = \exp(-2\phi)$, because $\Psi \sim 1/r$ is singular* at *the puncture. The new variables have weaker or no singularity at the puncture; but the new equations are in some cases singular, e.g. they contain terms $\propto \chi^{-1}$. In the simulations these terms are experimentally found to be not problematic, a floor is sometimes applied in the implementations.*

11. Relativistic hydrodynamics

This lecture introduces general relativistic hydrodynamics focusing on the properties of perfect fluids, their symmetries and on the conservative formulation of the equations.

Suggested readings. *Gourgoulhon (2006)'s introduction on relativistic hydrodynamics; Chap. 7 of Alcubierre's book; Chap. 10 of Baumgarte's lecture notes (Book's Chap. 5,15); Marti and Müller (1999) and Font (2007) Living Review Relativity.*

11.1 3+1 decomposition of local energy conservation

Bianchi identities imply the local (divergence form) conservation law for the stress-energy tensor

$$\nabla_a T^{ab} = 0 \ . \tag{11.1}$$

Given the 3+1 decomposition of the spacetime the stress-energy tensor is decomposed as (Sec. 5)

$$T_{ab} = S_{ab} + 2n_{(a}P_{b)} + En_a n_b = S_{ij}\gamma^i_a\gamma^i_b + n_a\gamma^i_b P_i + n_b\gamma^i_a P_i + En_a n_b \ , \tag{11.2}$$

where

E matter energy density measured by the Eulerian observers;
P_a matter momentum density measuredby the Eulerian observers;
S_{ab} matter stress-energy projection onto the Σ_t.

Projections of Eq. (11.1):

$$n^b\nabla_a T^a_b = 0 \quad \Rightarrow \quad \mathcal{L}_m E = -\alpha(D_i P^i - KE - K_{ij}S^{ij}) - 2P^i D_i\alpha \tag{11.3a}$$

$$\gamma^c_a\nabla_b T^b_c = 0 \quad \Rightarrow \quad \mathcal{L}_m P_i = -\alpha D_j S^j_i - S_{ij}D^i\alpha + \alpha K P_i - ED_i\alpha \ . \tag{11.3b}$$

The above eqs express energy and momentum conservation as observed by Eulerian frames. They can be easily derived by inserting Eq. (11.2), writing explicitely the projectors, and considering (i) orthogonality conditions, (ii) definitions of Lie derivative and extrinsic curvature (and notably Eq. (4.27) and Eq. (4.34)). For example the divergence and derivative of a spatial vector (tangent to Σ_t) is

$$D_a P^a = \gamma^a_b\gamma^b_c\nabla_a P^c = \gamma^a_c\nabla_a P^c = (\delta^a_c + n^a n_c)\nabla_a P^c = \nabla_a P^a - P^a n^c\nabla_c n_a = \nabla_a P^a - v^a D_a \ln\alpha \tag{11.4a}$$

$$\gamma^b_a n^c\nabla_c P_b = \alpha^{-1}\gamma^b_a m^c\nabla_c = \alpha^{-1}\gamma^b_a(\mathcal{L}_m P_b - P_d\nabla_b m^d) = \alpha^{-1}\mathcal{L}_m P_a + K_{ad}P^d \tag{11.4b}$$

Similarly, for the spatial tensor S^a_b

$$\begin{aligned} D_b S^b_a &= \gamma^c_e\gamma^e_f\gamma^g_a\nabla_c S^f_g = \gamma^c_f\gamma^g_a\nabla_c S^f_g = \gamma^g_a(\delta^c_f + n^c n_f)\nabla_c S^f_g = \gamma^g_a\nabla_c S^c_g + \gamma^g_a n^c n_f\nabla_c S^f_g \\ &= \gamma^g_a\nabla_c S^c_g - \gamma^g_a S^f_g n^c\nabla_c n_f = \gamma^g_a\nabla_c S^c_g - S^f_a D_f\ln\alpha \end{aligned} \tag{11.5a}$$

$$n^a\nabla_b S^b_a = -S^b_a\nabla_b n^a = S^b_a(K^a_b + D^a\ln\alpha n_b) = K_{ab}S^{ab} \ . \tag{11.5b}$$

The Newtonian limit is taken using

$$\gamma_{ij}\mapsto f_{ij} \ , \quad D_i\mapsto\mathcal{D}_i \ , \quad K_{ij}\mapsto 0 \ , \quad \alpha\mapsto\sqrt{1+2\phi}\approx 1+\phi \ , \quad \beta^i = 0 \ , \quad |S_{ij}|\ll E \ (v^2\ll c^2) \ , \tag{11.6}$$

and gives the conservation of energy-momentum with the gravitational field source term:

$$\partial_t E + \mathcal{D}_i P^i = -2P^i\mathcal{D}_i\phi \tag{11.7a}$$

$$\partial_t P_i + \mathcal{D}_j S^j_i = -E\mathcal{D}_i\phi \ . \tag{11.7b}$$

Note the momentum density P^i in the first equation corresponds to the energy flux.

11.2 Perfect fluid

Consider a continuum medium characterized by
u^a *4-velocity field*, velocity of the fluid element at each point of the spacetime (normalized)
p scalar field describing the isotropic *pressure in the fluid's frame.*
The *perfect fluid* model for the matter is defined by the stress energy tensor

$$T_{ab} = (e+p)u_a u_b + p g_{ab} = e u_a u_b + p(u_a u_b + g_{ab}) \ , \tag{11.8}$$

where

$$T_{ab}u^a u^b = e \underbrace{u_a u_b u^a u^b}_{=(-1)(-1)} + p(\underbrace{u_a u_b u^a u^b + g_{ab}u^a u^b}_{(-1)(-1)+(-1)=0}) = e =: \rho(1+\epsilon) \tag{11.9}$$

is the *energy density in the fluid's frame* usually written in terms of the *rest-mass density* ρ and the *internal energy density* ϵ. A way to understand this notation is to consider the fluid as the continuum limit of some particle species, say baryons. If $m_b^{(A)}$ is the mass of baryon species A and n_A its number density, $e_{\rm int}$ is the internal energy containing the kinetic and potential energy of the particles, then restoring the speed of light c one has

$$e = \underbrace{\sum_A m_b^{(A)} n_A}_{\rho} c^2 + \underbrace{e_{\rm int}}_{\rho\epsilon c^2} \ . \tag{11.10}$$

In the nonrelativistic regime the total energy density reduces to the rest-mass density and the pressure is a smaller contribution than the energy density,

$$e = \rho c^2(1+\epsilon) \approx \rho \quad (v^2 \ll c^2) \tag{11.11a}$$

$$(e + \frac{p}{c^2}) \approx e \quad (v^2 \ll c^2) \ . \tag{11.11b}$$

An important quantity appearing in many equations is

$$h := 1 + \epsilon + \frac{p}{\rho} \quad \text{(specific enthalpy)} \quad \Rightarrow \quad (e+p) = \rho h \ . \tag{11.12}$$

that reduces to $h \to 1$ in the Newtonian limit.

11.3 Conservation of particle number & simple fluid

Considering the fluid as the continuum approximation of a gas made of many particles and species. From the microphysics description one must take into account additional equations describing the conservation of the baryon number, the lepton number, etc. These equations cannot be derived from EFE that do not prescribe the composition of the matter, and must be added to Eq. (11.1).

Definition 11.3.1. *The* simple fluid *is a fluid composed of a single species of baryon with mass m_b.*

A gas can be described using the simple fluid model in the following conditions
- Frozen composition and no chemical reactions. The number densities of each particle species is a given fraction of the total, $n_A = Y_A n$.
- Thermodynamical equilibrium and high reaction rate. The number density of the species are given by the equilibrium distribution, $n_A = Y_A^{\rm eq}(s,n)n$

For a simple fluid, the conservation equation or *continuity equation* for the baryon number n is

$$0 = \nabla_a(n u^a) \ \ \text{(Conservation of particle number, simple fluid)} \ . \tag{11.13}$$

Analogous equations must be added in more complicated situations, eventually taking into account source terms. Since $\rho = m_b n$, an alternative expression is $\nabla_a(\rho u^a) = 0$. For a simple fluid, one further defines the *enthalpy per baryon* (Cf. Eq. (11.12))

$$(e+p) = n\bar{h} \ . \tag{11.14}$$

11.4 Equation of state (EOS)

The perfect fluid is described by the set of fields

$$(u^i, e, p) \ \ \text{or} \ \ (u^i, \rho, \epsilon, p) \ . \tag{11.15}$$

To determine them one must solve the local conservation eqs $\nabla_a T^{ab} = 0$ (4 eqs for 5 unknowns) for the first set of fields, or or the local conservation plus the continuity equation (5 eqs for 6 unknowns) for the second set of fields. The system of equations must be closed with an *equation of state* (EOS) describing the thermodynamical properties of the fluid in the comoving frame.

The fundamental Gibbs equation of thermodynamics

$$\mathcal{E} = \mathcal{E}(S, V, N_A) \ , \tag{11.16}$$

where $\mathcal{E}$ is the energy, S the entropy and N_A the number of particles, contains all the information about the system at equilibrium. The first principle of thermodynamics

$$d\mathcal{E} = TdS - pdV + \sum_A \mu_A dN_A \ , \tag{11.17}$$

defines the temperature, pressure and chemical potentials

$$T := \left.\frac{\partial \mathcal{E}}{\partial S}\right|_{V,N_A} \ , \quad p := -\left.\frac{\partial \mathcal{E}}{\partial V}\right|_{S,N_A} \ , \quad \mu_A := \left.\frac{\partial \mathcal{E}}{\partial N_A}\right|_{V,S,N_{B\neq A}} \ . \tag{11.18}$$

Eq. (11.16) is a homogeneous function of the extensive variables, i.e. given a constant λ

$$\mathcal{E}(\lambda S, \lambda V, \lambda N_A) = \lambda \mathcal{E}(S, V, N_A) \ . \tag{11.19}$$

For a constant volume, the fundamental equation can be expressed interms of densitized variables taking $\lambda = 1/V$,

$$\mathcal{E}(\lambda S, \lambda V, \lambda N_A) = V e(s, n_A) \ , \tag{11.20}$$

where $s := S/V$, $n_A := N_A/V$ and $e(s, n_A) := \mathcal{E}(s, 1, n_A)$.

Further deriving Eq. (11.19) w.r.t λ and then setting $\lambda = 1$ and using Eq. (11.18) one obtains the *Gibbs-Duhem relation*

$$\begin{aligned} \partial_\lambda \mathcal{E}(\lambda S, \lambda V, \lambda N_A) &= \partial_\lambda [\lambda \mathcal{E}(S, V, N_A)] \\ \frac{\partial \mathcal{E}}{\partial S} S + \frac{\partial \mathcal{E}}{\partial V} V + \sum_A \frac{\partial \mathcal{E}}{\partial N_A} N_A &= \mathcal{E}(S, V, N_A) \\ TS - pV + \sum_A \mu_A N_A &= \mathcal{E} \end{aligned} \tag{11.21a}$$

and its densitized version

$$Ts - p + \sum_A \mu_A n_A = e \tag{11.21b}$$

The Gibbs-Duhem relation together with the fundamental equation $e = e(s, n_A)$ and the definitions Eq. (11.18) shows that the pressure field is fully determined by thermodynamics from the set of variables e, s, n_A. The thermodynamics equation specifying the pressure is called the *equation of state (EOS)* of the fluid.

For a simple fluid,

$$e = e(n, s) \quad \text{(Simple fluid)} \tag{11.22}$$

and the Gibbs-Duhem relation simplifies to

$$Ts - p + \mu n = e \ \text{ or } \ T\bar{s} + \mu = \bar{h} \ , \tag{11.23}$$

where $\bar{s}$ is the *entropy per baryon*. The first principle of thermodynamics Eq. (11.17) for a simple fluid and a constant volume is

$$de = Tds + \mu dn \ . \tag{11.24}$$

The simple fluid EOS is often expressed in one of the following equivalent forms

$$p = p(n, s) \ , \quad p = p(\rho, s) \ , \quad p = p(\rho, \epsilon) \ . \tag{11.25}$$

11.5 Equations for relativistic perfect fluids

For a perfect fluid:

$$\nabla_a T^{ab} = 0 \quad \Leftrightarrow \quad [u^b \nabla_b (e + p) + (e + p) \nabla_b u^b] u_a + (e + p) a_a + \nabla_a p = 0 \ , \tag{11.26}$$

where $a_a = u^b \nabla_b u_a$ is the acceleration of the vector field u^a.

Consider the projections of Eq. (11.1) along u^a and perperdicular to u^a. The latter can be carried out with the projector

$$P^a_b = \delta^a_b + u^a u_b \ , \tag{11.27}$$

and in particular $P^a_b a_a = a_b$. One obtains:

$$u_b \nabla_a T^{ab} = 0 \quad \Rightarrow \quad -\nabla_a(h\rho u^a) + u^a \nabla_a p = 0 \tag{11.28a}$$

$$P^c_a \nabla_b T^b_c = 0 \quad \Rightarrow \quad (e+p)a_a + \nabla_a p + u_a u^b \nabla_b p = \rho h u^b \nabla_b u_a + \nabla_a p + u_a u^c \nabla_c p = 0 \ \text{ (Euler equation)} \tag{11.28b}$$

The first equation is immediate from Eq. (11.26) since $a_a u^a = 0$; a direct derivation and different expressions are also given below. The Euler equation is also immediate, and one notices that is of the type "$ma = F$". For a constant pressure fluid $p = const$ the Euler equation reduces to the geodesic equation.

Weak-field limit. Explore the weak-field limit, with metric (again restore c):

$$ds^2 = -(1 + \frac{2\phi}{c^2})\mathrm{d}t^2 + (1 - \frac{2\phi}{c^2}) f_{ij}\mathrm{d}x^i \mathrm{d}x^j \ . \tag{11.29a}$$

The 4-velocity in global inertial coordinates and for $v^2 \ll c^2$ is

$$u^\mu = \frac{1}{c}\frac{dx^\mu}{d\tau} = \frac{1}{c}(\frac{dx^0}{d\tau}, \frac{dx^i}{d\tau}) = (\underbrace{\frac{dt}{d\tau}}_{:=u^0}, \frac{1}{c}\frac{dt}{d\tau}\underbrace{\frac{dx^i}{dt}}_{:=v^i}) = (u^0, u^0 \frac{v^i}{c}) \tag{11.29b}$$

$$u^0 = [\frac{1}{g_{00}}(-1 + v^i v^i g_{ij})]^{1/2} \approx 1 - \frac{\phi}{c^2} + \frac{v_j v^j}{c^2} \ , \tag{11.29c}$$

where the second line is obtained from $-1 = u^\mu u^\nu g_{\mu\nu}$ expanding at first order in $1/c^2$. Hence, using

$$u^\mu \mapsto (1 - \frac{\phi}{c^2} + \frac{v_i v^i}{2c^2}, \frac{v^i}{c}) \ , \quad u_\mu \mapsto (-1 - \frac{\phi}{c^2} - \frac{v_i v^i}{2c^2}, \frac{v^i}{c}) \ , \quad u^b \nabla_b \mapsto \partial_t + v^i \partial_i \ , \quad e \mapsto \rho \ , \quad h \mapsto 1 \ , \tag{11.29d}$$

one obtains the Newtonian equations

$$\partial_t \rho + v^i \partial_i \rho = 0 \tag{11.30a}$$

$$\partial_t v^i + v^k \partial_k v^i + \frac{1}{\rho}\partial_i p + \partial_i p = 0 \ . \tag{11.30b}$$

Direct derivation of the u-projection.

$$0 = u_b \nabla_a T^{ab} = u_b \nabla_a (h\rho u^a u^b + p g^{ab}) = u_b \nabla_a (h\rho) u^a u^b + u_b h\rho \nabla_a (u^a u^b) + u_b g^{ab} \nabla_a p \tag{11.31a}$$

$$= u^a \nabla_a (h\rho) \underbrace{u_b u^b}_{=-1} + h\rho (\underbrace{u_b u^b}_{=-1} \nabla_a u^a + u_b \underbrace{u^a \nabla_a u^b}_{=\frac{1}{2}u^a \nabla_a (u_b u^b) = 0}) + u^a \nabla_a p \tag{11.31b}$$

$$= -u^a \nabla_a (h\rho) - h\rho \nabla_a u^a + u^a \nabla_a p \tag{11.31c}$$

Substituting $h\rho = (e + p)$ one obtains an alternative form:

$$0 = -u^a \nabla_a (e + p) - (e + p)\nabla_a u^a + \cancel{u^a \nabla_a p} = -u^a \nabla_a e - (e + p)\nabla_a u^a \quad \Rightarrow \tag{11.32a}$$

$$u^a \nabla_a e = -(e + p)\nabla_a u^a = -h\rho \nabla_a u^a = +h u^a \nabla_a \rho \ , \tag{11.32b}$$

where in the last passage of the last line the continuity equation was used.

11.5.1 Properties of simple fluids

Two key properties of simple fluids that follows from the equations above are:
(i) The simple fluid evolution is adiabatic.
(ii) The entropy per baryon is conserved along fluid lines.

Property (i) follows from combining the u-projection with the 1st law of thermodynamics and then using the continuity eq:

$$\begin{cases} u^a \nabla_a e & = -\bar{h} n \nabla_a u^a \\ \nabla_a e & = T \nabla_a s + \mu \nabla_a n \\ \nabla_a (n u^a) & = 0 \end{cases} \quad \Rightarrow \quad 0 = T u^a \nabla_a (s u^a) + \mu \underbrace{\nabla_a (n u^a)}_{=0} - \underbrace{(T\bar{s} + \mu - \bar{h})}_{=0} n \nabla_a u^a \quad \Rightarrow \quad u^a \nabla_a (s u^a) = 0 \ . \tag{11.33}$$

Property (ii) is immediate by combining the continuity equations and (i):

$$u^a\nabla_a\bar{s} = u^a\nabla_a\frac{s}{n} = \frac{1}{n}\underbrace{u^a\nabla_a s}_{-s\nabla_a u^a} - \frac{s}{n^2}\underbrace{u^a\nabla_a n}_{-n\nabla_a u^a} = 0 \ . \tag{11.34}$$

If the simple fluid is *barotropic*,

$$e = e(n) \quad \text{(Barotropic simple fluid)} \ , \tag{11.35}$$

the gradient of the pressure and the gradient of the enthalpy satisfy the simple relation

$$dp = nd\bar{h} \ \text{ or } \ \frac{dp}{e+p} = d\ln\bar{h} \tag{11.36}$$

which is immediately found from Eq. (11.24) and $e + p = n\bar{h}$.

Remark 11.5.1. *For a barotropic fluid the $\boldsymbol{u}$-projection (energy) equation and the continuity equation are redundant, Eq. (11.33).*

Example 11.5.1. *Barotropic simple fluids are model for the cold ($T = 0$) degenerate matter in white dwarfs and neutron stars. The above equation is often used to construct neutron star stationary spacetimes in general relativity.*

Cartan-Lichnerowicz equation. Lichnerowicz & Cartan developed an elegant geometrical formalism for hydrodynamics (See Gourgoulhon (2006) an introduction). The key fields entering the formalism are the *momentum 1-form*

$$\boldsymbol{\pi} := \bar{h}\boldsymbol{u} \ , \quad \text{in components: } \ \pi_a = \bar{h}u_a \ , \tag{11.37}$$

and the *vorticity 2-form*

$$\boldsymbol{\omega} := \mathbf{d}\boldsymbol{\pi} \ , \quad \text{in components: } \ \omega_{ab} = \partial_a\pi_b - \partial_b\pi_a = \partial_a(\bar{h}u_b) - \partial_b(\bar{h}u_a) \ . \tag{11.38}$$

The fundamental equation of motion for a simple fluid (equivalent to Euler equation) involving these fields is [1]

$$\boldsymbol{u}\cdot\boldsymbol{\omega} = T\mathbf{d}\bar{s} \quad \text{(Cartan-Lichnerowicz equation)} \tag{11.39a}$$

$$u^b\left[\partial_b(\bar{h}u_a) - \partial_a(\bar{h}u_b)\right] = T\partial_a\bar{s} \quad \text{(components)} \tag{11.39b}$$

If the simple fluid is *barotropic*, then $\bar{s} = const$ and the Cartan-Lichnerowicz equation simplifies to $u^a\omega_{ab} = 0$.

A useful mathematical identity that holds for <u>any</u> p-form $\boldsymbol{\omega}$ and vector $\boldsymbol{u}$ is

$$\mathcal{L}_u\boldsymbol{\omega} = \boldsymbol{u}\cdot\mathbf{d}\boldsymbol{\omega} + \mathbf{d}(\boldsymbol{u}\cdot\boldsymbol{\omega}) \quad \text{(Cartan identity)} \ , \tag{11.40}$$

which is easily shown for $p = 1$ by combining the definitions of Lie and exterior derivatives

$$\begin{cases} \mathcal{L}_u\omega_a &= u^b\partial_b\omega_a - \omega_b\partial_a u^b \\ (\mathbf{d}\boldsymbol{\omega})_{ab} &= \partial_a\omega_b - \partial_b\omega_a \end{cases} \quad \Rightarrow \quad \mathcal{L}_u\omega_a = -u^b(\mathbf{d}\boldsymbol{\omega})_{ab} + u^b\partial_a\omega_b - \omega_b\partial_a u^b = u^b(\mathbf{d}\boldsymbol{\omega})_{ba} + \partial_a(u^b\omega_b) \ . \tag{11.41}$$

11.6 Symmetries of relativistic perfect fluids

If the spacetime and fluid admit a Killing vector K^a,

$$\mathcal{L}_k\boldsymbol{g} = 0 \quad \text{and} \quad \mathcal{L}_k(\text{matter field}) = 0 \ . \tag{11.42}$$

then there exist the following constant of motion:

$$u^a\nabla_a(\bar{h}u_bK^b) = 0 \quad \Rightarrow \quad \bar{h}u_bK^b = const \ , \ \text{ is conserved along fluid lines} \ . \tag{11.43}$$

The above equation is similar to the geodesic equation but contains $\bar{h}$, accounting for the fact that the fluid has pressure.

The result can be easily shown by applying first the Cartan identity to the momentum 1-form $\boldsymbol{\pi} = \bar{h}\boldsymbol{u}$, and then applying the resulting 1-form to the velocity field:

$$0 = \mathcal{L}_k\pi_a = K^b\omega_{ab} + \left[\mathbf{d}(\bar{h}u_bK^b)\right]_a \quad \Rightarrow \tag{11.44a}$$

$$= K^b\omega_{ab}u^a + u^a\nabla_a(\bar{h}u_bK^b) \tag{11.44b}$$

$$= K^b(T\mathbf{d}\bar{s})_b + u^a\nabla_a(\bar{h}u_bK^b) = K^bT\nabla_b\bar{s} + u^a\nabla_a(\bar{h}u_bK^b) \tag{11.44c}$$

$$= T\mathcal{L}_k\bar{s} + u^a\nabla_a(\bar{h}u_bK^b) = 0 + u^a\nabla_a(\bar{h}u_bK^b) \ . \tag{11.44d}$$

[1] See Sec. 6.1, 6.2 and Eq. (6.13), (6.30) of Gourgoulhon (2006).

Example 11.6.1. *In case of* axisymmetric flow *one can take coordinates* (t, r, θ, ϕ) *and write the Killing vector in those adapated coordinates as* $K^\mu = (0, 0, 0, 1)$. *The conserved quantity is thus*

$$const = hu_b k^b = hu_\phi \ . \tag{11.45}$$

Example 11.6.2. *In case of* stationary flow *the Killing vector in adapted coordinates is* $K^\mu = (\boldsymbol{\partial}_t)^\mu = (c^{-1}, 0, 0, 0)$, *and the conserved quantity is*

$$const = hu_b k^b = hu_t \ . \tag{11.46a}$$

For stationary flow, Eq. (11.43) is the relativistic version of the Bernoullli equation

$$hu_t \approx (1 + \epsilon + \frac{p}{\rho})(1 + \phi + \frac{1}{2}v^2) \quad \Rightarrow \tag{11.46b}$$

$$0 = u^a \nabla_a (hu_b K^b) = u^a \partial_a (hu_b K^a) \approx \frac{u^0}{c} \underbrace{\partial_t (hu_b K^b)}_{=0} + \frac{v^i}{c} \partial_i (hu_b K^a) \quad \Rightarrow \tag{11.46c}$$

$$0 = \frac{v^i}{c} \partial_i (\frac{1}{2}v^2 + \phi + \epsilon + \frac{p}{\rho}) \ . \tag{11.46d}$$

11.7 Irrotational flow

Definition 11.7.1. *A flow is* irrotational *iff the vorticity 2-form vanishes* $\boldsymbol{\omega} = \mathbf{d}\boldsymbol{\pi} \equiv 0$.

For an irrotational flow, the momentum 1-form is exact and the velocity field can be obtained from the gradient of a scalar field called *flow potential*:

$$\mathbf{d}\boldsymbol{\pi} = \mathbf{d}(\bar{h}\boldsymbol{u}) = 0 \quad \Rightarrow \quad \boldsymbol{\pi} = \mathbf{d}\Psi \quad \Rightarrow \quad u^a = \bar{h}^{-1} g^{ab} \nabla_b \Psi \ . \tag{11.47}$$

The flow potential satisfies a wave equation

$$\begin{cases} u^a &= \bar{h}^{-1} g^{ab} \nabla_b \Psi \\ 0 &= \nabla_a (n u^a) \end{cases} \quad \Rightarrow \quad \Box_g \Psi + \frac{\bar{h}}{n} \nabla_a \left(\frac{n}{\bar{h}}\right) \nabla^a \Psi = 0 \ . \tag{11.48}$$

Moreover, from the Cartan-Lichnerowicz equation Eq. (11.39a) immediately follows that an irrotational flow is either isentropic or has $T = 0$, since

$$0 = \boldsymbol{u} \cdot \underbrace{\boldsymbol{\omega}}_{=0} = T \mathbf{d}\bar{s} \quad \Rightarrow \quad T = 0 \text{ or } \bar{s} = const \ . \tag{11.49}$$

Irrotational flow in presence of symmetries has the following property

Given a Killing vector K^a, the Cartan identity Eq. (11.44a) in presence of irrotational flow reduces to $\mathcal{L}_k \pi_a = \left[\mathbf{d}(\bar{h} u_b K^b)\right]_a$, and one obtains

$$0 = \mathcal{L}_k \pi_a = \left[\mathbf{d}(\bar{h} u_b K^b)\right]_a \quad \Rightarrow \quad \bar{h} u_b K^b = const \ , \ \text{ is an integral of motion} \tag{11.50}$$

i.e. it is global constant (not only on fluid lines, Cf. Eq. (11.43)).

Example 11.7.1. *The flow in circular neutron stars binaries is often approximated as irrotational. In that context, the helical Killing vector* $K^a = (\partial_t)^a + \Omega(\partial_\phi)^a$ *discussed in Chap. 8 gives the integral of motion used to solve the equations.*

Remark 11.7.1. *The vorticity 3-form can be associated to a* vorticity *vector*

$$w^a := (4\bar{h})^{-1} \epsilon^{abcd} u_b \omega_{cd} = (4\bar{h})^{-1} \epsilon^{abcd} u_b \left[\partial_c (\bar{h} u_d) - \partial_d (\bar{h} u_c)\right] \tag{11.51a}$$

$$= (4\bar{h})^{-1} \bar{h} \epsilon^{abcd} u_b \left(\partial_c u_d - u_c \partial_d u_c\right) + (4\bar{h})^{-1} \epsilon^{abcd} \left(u_b u_d \partial_c \bar{h} - u_b u_c \partial_d \bar{h}\right) \tag{11.51b}$$

$$= \frac{1}{2} \epsilon^{abcd} u_b \partial_c u_d \ , \tag{11.51c}$$

Above ϵ^{abcd} *is the totally antisymmetric tensor associated to the metric. Note that* $w^a u_a = 0$. *The spatial components reduce to the curl of the 3-velocity in the Newtonian limit,* $\vec{w} \approx 1/c \, \nabla \times \vec{v}$. *The vorticity vector thus make the connection with the classical fluid mechanics, circulation theorems etc.*

11.8 Conservative form of general relativistic hydrodynamics

The numerical solution of nonlinear hyperbolic equations is best carried on the equations in *conservative form* (see Appendix A)

$$\partial_t q + \partial_i F^i(q) = s(q) \ , \tag{11.52}$$

where q is a state vector of variables. Euler equations for classical (Newtonian) hydrodynamics hydrpdynamics are typically written in conservative form for applications, e.g. (Toro, 1999; LeVeque, 2002). The conservative form of the relativistic equations is constructed starting from the decomposition Eq. (11.2) of the stress-energy tensor for the Eulerian observers, (Anile, 1990; Marti et al., 1991; Banyuls et al., 1997; Del Zanna et al., 2007). **Note:** In this section P^a of Eq. (11.2) is renamed S^a.

Let us consider the relation between the energy density measured by the Eulerian observers and the fluid variables in the comoving frame

$$E = n^a n^b T_{ab} = n^a n^b (h\rho u_a u_b + p g_{ab}) = h\rho \underbrace{(u^a n_a)}_{=:W}{}^2 - p \ . \tag{11.53}$$

The quantity $W := -u^a n_a$ is the *Lorentz factor* between the Eulerian and fluid frames. To see this, take a fluid element at point $p \in \Sigma_t$, at a successive time $t + \delta t$ the fluid element moves to point $q \in \Sigma_{t\delta t}$ in a proper time in the fluid frame $\delta\tau_{\rm F}$. Let the proper time measured by the Eulerian observers be $\delta\tau_{\rm E}$, the Lorentz factor is defined by the expression

$$\delta\tau_{\rm E} = W \delta\tau_{\rm F} \ . \tag{11.54}$$

The two vectors $\delta\tau_{\rm F}\boldsymbol{u}$ and $\delta\tau_{\rm E}\boldsymbol{n}$ join the point p with $q \in \Sigma_{t+\delta t}$ and $q' \in \Sigma_{t+\delta t}$ respectively; their difference is the spatial vector $\boldsymbol{\delta s} = \overrightarrow{qq'}$,

$$\delta\tau_{\rm F} u^a = \delta\tau_{\rm E} n^a + (\delta s)^a \ . \tag{11.55}$$

From the equation above one immediately identifies the Lorentz factor by contracting with $\boldsymbol{u}$

$$\underbrace{u_a u^a}_{=-1} \delta\tau_{\rm F} = \underbrace{u_a n^a}_{=-W} \delta\tau_{\rm E} + \underbrace{u_a (\delta s)^a}_{=0} \ . \tag{11.56}$$

Morever one obtains that the fluid 4-velocity decomposes in terms of the vector n^a and of a vector v^a tangent to Σ_t (spatial) as follows:

$$u^a = W(n^a + v^a) \quad \text{(3+1 split of fluid 4-velocity)} \tag{11.57}$$

$$v^i := \frac{ds^i}{d\tau_{\rm E}} = \frac{u^i}{W} + \frac{\beta^i}{\alpha} \quad \text{(Fluid's velocity relative to the Eulerian observer)} \tag{11.58}$$

Note that

$$-1 = u_a u^a = W^2 (\underbrace{n_a n^a}_{=-1} + 2 \underbrace{u_a v^a}_{=0} + v_a v^a) \quad \Rightarrow \quad W = 1/\sqrt{1 - v^i v_i} = \alpha u^0 \ . \tag{11.59}$$

Finally, the components of the strees-energy tensor in terms of the fluid quantities in the comoving frame are:

$$E := n^a n^b T_{ab} = h\rho W^2 - p \tag{11.60a}$$

$$S_i := -\gamma^b_i n^c T_{bc} = (e + p) W^2 v_i = h\rho W^2 v_i \tag{11.60b}$$

$$S_{ij} := \gamma^c_i \gamma^d_j T_{cd} = h\rho W^2 v_i v_j + p\gamma_{ij} \ . \tag{11.60c}$$

11.8.1 Continuity equation

Eq. (11.13) in 3+1 language reads

$$0 = \nabla_a(\rho u^a) = (-g)^{-1/2} \partial_a [(-g)^{1/2} \rho u^a] = (-g)^{-1/2} \partial_t [\gamma^{1/2} \underbrace{\alpha u^0}_{=W} \rho] + (-g)^{-1/2} \partial_i [\gamma^{1/2} \alpha u^i \rho] \tag{11.61a}$$

$$= (-g)^{-1/2} \partial_t [\gamma^{1/2} \underbrace{\rho W}_{=:D}] + (-g)^{-1/2} \partial_i [\gamma^{1/2} \underbrace{\alpha u^0}_{=W} \rho \underbrace{(\alpha v^i - \beta^i)}_{=:\tilde{v}^i}] \tag{11.61b}$$

The field $D := \rho W$ is the rest-mass measured by Eulerian observers; the final form is

$$\partial_t(\sqrt{\gamma} D) + \partial_i(\sqrt{\gamma} D \tilde{v}^i) = 0 \quad \text{(Continuity equation)} \tag{11.61c}$$

Remark 11.8.1. *The continuity equation directly implies the conservation of the rest-mass*

$$M_b = \int_\Sigma \mathrm{d}^3x\sqrt{\gamma}D \ . \tag{11.62}$$

11.8.2 Energy & Momentum equations

The energy equation is derived from the projection of the local conservation law along $\boldsymbol{n}$ and using Eq. (11.2):

$$0 = n_a\nabla_b T^{ab} = \nabla_b(\underbrace{n_a T^{ab}}_{=-En^b-S^a}) - T^{ab}\nabla_b n_a = (-g)^{-1/2}\partial_a[(-g)^{1/2}n_b T^{ab}] - T^{ab}\nabla_b n_a \quad \Rightarrow \tag{11.63a}$$

$$0 = \partial_t(\gamma^{1/2}E) + \partial_i[\gamma^{1/2}(\alpha S^i - E\beta^i)] - \alpha\gamma^{1/2}T^{ab}\nabla_b n_a \tag{11.63b}$$

$$= \partial_t(\gamma^{1/2}E) + \partial_i[\gamma^{1/2}(\alpha S^i - E\beta^i)] - \alpha\gamma^{1/2}(K_{ij}S^{ij} - S^k\partial_k\ln\alpha) \tag{11.63c}$$

where in the last line one uses Eq. (4.27) and Eq. (4.34).

$$\partial_t(\gamma^{1/2}E) + \partial_i[\gamma^{1/2}(\alpha S^i - E\beta^i)] = \alpha\gamma^{1/2}(K_{ij}S^{ij} - S^k\partial_k\ln\alpha) \ \text{(Energy equation)} \tag{11.63d}$$

The momentum equation calculation follows from the spatial projection:

$$0 = \gamma^b_j\nabla_a T^a_b = (-g)^{-1/2}\partial_a[(-g)^{1/2}T^a_j] - \frac{1}{2}T^{ab}\partial_j g_{ab} \quad \Rightarrow \tag{11.64a}$$

$$0 = \partial_a[(-g)^{1/2}(n^a S_j + \gamma^{qi}S_{ij})] - \frac{1}{2}S^{ik}\partial_j\gamma_{ik} + \alpha^{-1}S_i\partial_j\beta^i - E\partial_j\ln\alpha \tag{11.64b}$$

which results in

$$\partial_t(\gamma^{1/2}S_j) + \partial_i[\gamma^{1/2}(S_j\tilde{v}^i + p\delta^i_j)] = \gamma^{1/2}(\frac{1}{2}\alpha S^{ik}\partial_j\gamma_{ik} + S_i\partial_j\beta^i - S\partial_j\alpha) \ \text{(Momentum equation)} \tag{11.64c}$$

Note the source terms do not contain time derivatives of the 3-metric.

Remark 11.8.2. *The energy equation is often substituted by an equation for the field $\tau := E - D$. The Newtonian limit of this variable is*

$$\tau = E - D = \rho h W^2 - p - \rho W \approx \rho\epsilon + \frac{1}{2}\rho v^2 \ . \tag{11.65}$$

Recall that for a barotropic fluid the energy equation and the continuity equation are redundant.

11.8.3 Conservative variables & Hyperbolicity

The system composed of Eq. (11.61c), Eq. (11.63d), Eq. (11.64c) is in conservative form with

$$q := \sqrt{\gamma}(D, S_i, \tau) \tag{11.66a}$$

$$F^i := (D\tilde{v}^i, S_j\tilde{v}^i + p\delta^i_j, \tau\tilde{v}^i + pv^i) \tag{11.66b}$$

$$s(q) := (0, \alpha\gamma^{1/2}(K_{ij}S^{ij} - S^k\partial_k\ln\alpha), \gamma^{1/2}(\frac{1}{2}\alpha S^{ik}\partial_j\gamma_{ik} + S_i\partial_j\beta^i - S\partial_j\alpha)) \tag{11.66c}$$

The system is closed by an EOS in the form $p = p(\rho, \epsilon)$.

There exist two distinct set of fields:

- *conservatives* $q = \sqrt{\gamma}(D, S_i, \tau)$
- *primitives* $w = (\rho, v^i, \epsilon, p)$

Primitives must be calculated numerically from conservatives during the evolution. A common approach valid for a generic EOS is to search for the root the function $f(p)$ defined by

$$f(p) := p(\rho, \epsilon) - p \ , \tag{11.67a}$$

where the EOS is evaluated on $\rho(q, p)$ and $\epsilon(q, p)$ computed from

$$v^i = \frac{S^i}{\tau + p} \ , \quad W = \sqrt{1 - v^i v_i} \tag{11.67b}$$

$$\rho = \frac{D}{W} \tag{11.67c}$$

$$\epsilon = \frac{\tau - DW + p(1 - W^2)}{DW} \ . \tag{11.67d}$$

Note that the derivative of f is a simple expression of the velocity and sound speed c_s^2:

$$f'(p) = v^2 c_s^2 - 1 \ . \tag{11.67e}$$

The system is strongly hyperbolic for causal EOS,

$$c_s^2 = \frac{\partial p}{\partial e} < 1 \ . \tag{11.68}$$

The calculation of characterstic fields, i.e. the diagonalization of the matrices $A^i = \partial F^i/\partial q$, is nontrivial due to the presence of the two sets of fields (primitive/conservative) and of the EOS as closure relation (Anile, 1990; Banyuls et al., 1997). In Cartesian coordinates and in 1D

$$\lambda_0 = \tilde{v}^x = \alpha v^x - \beta^x \quad \text{(triple)} \tag{11.69a}$$

$$\lambda_\pm = \frac{\alpha}{1-v^2c_s^2}\left[v^x\left(1-c_s^2\right) \pm c_s\sqrt{(1-v^2)[\gamma^{xx}(1-v^2c_s^2) - v^x v^x(1-c_s^2)]}\right] - \beta^x \ . \tag{11.69b}$$

The eigenvalues in the other directions are obtained by indexes permutation. Expressions for the eigenvectors can be found in e.g. Font et al. (2000); Font (2007).

Special relativistic limit The special relativity limit is easily obtained taking

$$\alpha \mapsto 1 \ , \quad \beta^i \mapsto 0 \ , \quad \tilde{v}^i \mapsto v^i \ , \quad \gamma_{ij} \mapsto f_{ij} \ , \tag{11.70}$$

and one finds a system in conservative form with

$$q := (D, S_i, \tau) \tag{11.71a}$$

$$F^i := (Dv^i, S_j v^i + p\delta^i_j, \tau v^i + pv^i) \tag{11.71b}$$

$$s(q) := 0 \ . \tag{11.71c}$$

Weak-field limit The Newtonian limit of the special relativsitc equation is obtained taking

$$v \ll c \ , \quad W \mapsto 1 + \frac{1}{2}v^2 \ , \quad h \mapsto 1 \ , \quad e \mapsto \rho\epsilon + \frac{1}{2}\rho v^2 \ , \tag{11.72}$$

In presence of weak gravity the conservative form is the well-known system (Toro, 1999)

$$q := (\rho, \rho v_j, e) \tag{11.73a}$$

$$F^i := (\rho v^i, \rho v^i v_j + p\delta^i_j, (e+p)v^i) \tag{11.73b}$$

$$s(q) := (0, -\rho\partial_j\phi, -\rho v^i \partial_i \phi) \ . \tag{11.73c}$$

Note source terms are given by the gradients of the gravitational potential. The conservative-to-primitive conversion is trivial in this case.

A. Hyperbolicity and well-posedness

Short review of hyperbolic equations and well-posedness of the Cauchy problem.

Suggested readings. *Chap. 5.1-5.3 of Alcubierre's book; Hilditch's lecture notes; Evans (1998).*

A.1 Hyperbolic equations

Hyperbolic eqs naturally appears in Cauchy (or *initial value*, IVP) problems associated to causal theories. The basic model is the wave equation in second-order form with initial and boundary (if the domain is finite) data specified:

$$\partial_{tt}\phi - c^2\Delta\phi = 0 \ , \quad x \in \Omega \tag{A.1a}$$
$$\phi(t=0,x) = b(x) \ , \quad x \in \Omega \tag{A.1b}$$
$$\phi(t,x) = f(t,x) \ , \quad x \in \partial\Omega \ . \tag{A.1c}$$

The second-order wave equation can be written as a first-order-in-time and second-order-in-space system

$$\partial_t\phi = \Pi \tag{A.2a}$$
$$\partial_t\Pi = c^2\Delta\phi \ , \tag{A.2b}$$

where the first equation defines a new variable. This is the form of the 3+1 EFE, as discussed in Sec. 5. The first-order form of the wave eq is obtained by introducing other variables,

$$\partial_t\phi = \Pi \tag{A.3a}$$
$$\partial_t\chi_i = c\partial_i\Pi \tag{A.3b}$$
$$\partial_t\Pi = c\partial_i\chi^i \ , \tag{A.3c}$$

where $\chi_i := c\partial_i\phi$; note this definition introduces a constraint. The general (matrix) form for the above system is

$$\partial_t u + A^i(u)\partial_i u = s(u) \ , \tag{A.4}$$

where $u = (u_A)$ $A = 1, 2, ..., N$ is a state vector for the N fields and $A^i(u) = (A^i_{AB})$ some matrices, that in general depend on the state vector. Source terms are also introduced. The generalized harmonic system discussed in Sec. 10 can be written in this form.

Example A.1.1. *In 1D and assuming a costant coefficient and diagonalizable matrix $A \sim \Lambda = \mathrm{diag}\lambda_A$ (as in the wave equation), the first order system can be separated in N* advection equations *for the N* characteristic fields *w_A,*

$$\partial_t w - \lambda\partial_x w = 0 \ . \tag{A.5}$$

The solution of each equation is simply a translation (advection) of the initial profile $w_0(x)$ along the characteristics *curves $dx/dt = \lambda$, i.e. $w(t,x) = w_0(x - \lambda t)$. The original solution is given by projecting back the characteristic waves with the left eigenvetors of A: $u_A = L_{AB}w^B$ ($LAR = R^{-1}AR = \Lambda$). For the wave equation there are two characteristics: the left and right elementary waves with characteristic speeds $\lambda = \pm c$.*

In general, one can study high-frequency plane waves (Fourier mode) solutions for Eq. (A.4), setting

$$u = \tilde{u}_k \exp\left(-\mathrm{i}(\omega t - x\cdot k)\right) = \tilde{u}_k \exp\left(\mathrm{i}k(x\cdot\hat{n} - vt)\right) \ , \tag{A.6}$$

with $v := \omega/k$, and plugging into the equation to find the eigenvalues problem:

$$(-\mathrm{i}kv)\tilde{u}_k + (\mathrm{i}k)A^j n_j \tilde{u}_k = s \quad \Rightarrow \quad -v\tilde{u}_k + A^j n_j \tilde{u}_k = \frac{s}{\mathrm{i}k} \quad \Rightarrow \quad (A^j n_j)\tilde{u}_k = v\tilde{u}_k \quad (k\to\infty) \ . \tag{A.7}$$

The system of equations is called *strongly hyperbolic* if there exists a complete set of eigenvectors and eigenvalues $\lambda = v \in \mathbb{R}$. There exists different concepts of hyperbolicity; the hyperibolicity properties directly relate to the well-posedness of the IVP.

The hyperbolic system Eq. (A.4) can be often written in *conservative form*

$$\partial_t u + \partial_i F^i(u) = s(u) \ , \tag{A.8}$$

where $F^i = \partial A^i(u)/\partial u$ are the *fluxes* related to the matrices above by the jacobians $A^i_{AB} = \partial F^i_A/\partial u_B$. In absence of source terms, the conservative form highlights the conservation of mass (or charge) constained in a volume V (volume integral of the density u) related to the mass flux trhough the closed surface S around V:

$$\dot{m} := \frac{d}{dt}\int_V u = \int_V \partial_i F^i(u) = \oint_S F^i(u) n_i \ . \tag{A.9}$$

Hydrodynamics equations, both Newtonian and relativistic ones, are often written in conservative form. The latter is the most suitable form to apply numerical methods that captures correctly the weak (generalized, integral) solutions describing shocks and other physical discontinuities (Lax and Wendroff, 1960; Anile, 1990; Evans, 1998). Nonlinear hyperbolic equations like those of hydrodynamics have in general characteristics speeds that depend on the solution u itself. A (1+1)D prototype model is the Burger eq with $F(u) = u^2$,

$$0 = \partial_t u + \partial_x F(u) = \partial_t u + u\partial_x u \ , \tag{A.10}$$

which is the limit of Euler equation for pressureless fluid (dust). Similarly to the linear problem, the solution is constant along characteristics, but differently from that the characteristics can now cross, thus forming a discontinuous solution ("shock"). If a discontinuity forms, then the differential eq is not applicable, and one must study generalized (weak) solutions: integral solutions weighted by test functions. Weak solutions have physical meaning, but are not unique. For example, for Euler equations, they might represent the propagation of sound waves in the inviscid fluid; the physical solution can be selected among the weak solutions as the zero-viscosity limit that guarantees that entropy does not decreases (*entropy conditions*). In general, a characteristic field w_A associated to the eigenvalue λ_A and eigenvector r_A is said *linearly degenerate* if $\partial\lambda_A/\partial u \cdot r_A = 0$ (eigenvalue is constant along the integral curves of the eigentvector). For linearly degenerate fields, an initial discontinuity simply moves along the characteristic line, and it is called a contact discontinuity. If $\partial\lambda_A/\partial u \cdot r_A \neq 0$, then the field is called *genuinely nonlinear* and the discontinuity is either a shock wave (characteristics converge at the discontinuity) or a rarefraction waves (characteristics diverge).

A.2 Well-posedness

The operative definition of well-posedness in Sec. 3 says that a well-posed IVP has a unique solution that depends continuously on the boundary data. A more formal definition is

Definition A.2.1. Well-posed IVP *iff exists a norm* $||.||$ *in which the solution is "bounded" in time by all (or a certain class) of the initial data according to the expression:*

$$||u(t,x)|| \leq K \exp(\alpha t)||u(0,x)|| \ , \tag{A.11}$$

with K, α *independent on the initial data* $u(0,x)$.

Note that well-posed IVP can have solutions exponentially growing in time. From the discussion in Sec. A.1, it should be clear that the IVP for the wave equation is well-posed.

Example A.2.1. *Consider the IVP for the "inverse" heat equation (note the "wrong" sign in front of the spatial second derivative):*

$$\begin{cases} \partial_t u & = -\partial_{xx} u \\ u(0,x) & = \exp(\mathrm{i}kx) \end{cases} \tag{A.12}$$

Looking for Fourier mode solutions $u(t,x) = \tilde{u}_k \exp(\sigma t + \mathrm{i}kx)$*, one finds*

$$\sigma \exp(...)\tilde{u}_k = -(\mathrm{i}k)^2 \exp(...)\tilde{u}_k \quad \Rightarrow \quad \sigma = k^2 \ , \tag{A.13}$$

the solution grow exponentially $u(t,x) \sim \mathrm{e}^{k^2 t + ikx}$ *in a way that depends on the Fourier mode. This IVP is ill-posed.*

Example A.2.2. *The IVP for the heat equation (now with correct sign)*

$$\begin{cases} \partial_t u & = +\partial_{xx} u \\ u(0,x) & = \exp(\mathrm{i}kx) \ , \end{cases} \tag{A.14}$$

is instead well-posed since the same calculation as above gives $\sigma = -k^2$*, and every nonzero frequency Fourier mode is damped in time.*

Example A.2.3. *Consider the IVP for the "inverse" wave equation $\partial_{tt}u = -\partial_{xx}u$ (note the wrong sign in front of the spatial derivatives). The equation correspond to the Laplace equation in which one dimension is taken as "time". In first order form $(u_0, u_1) := (\partial_t u, \partial_x u)$ and omitting the $\partial_t u = u_0$ equation:*

$$\partial_t \begin{pmatrix} u_0 \\ u_1 \end{pmatrix} = \begin{pmatrix} 0 & -1 \\ 1 & 0 \end{pmatrix} \partial_x \begin{pmatrix} u_0 \\ u_1 \end{pmatrix} \ . \tag{A.15}$$

The Fourier mode $u(t,x) = \tilde{u}_k \exp(\sigma t + \mathrm{i}kx)$ evolves as $(u, u_0, u_1) = \tilde{u}_k(1, k, k\mathrm{i})\exp(kt + \mathrm{i}kx)$, hence the problem is ill-posed.

Example A.2.4. *The IVP for the first order system*

$$\partial_t \begin{pmatrix} u_0 \\ u_1 \end{pmatrix} = \begin{pmatrix} 1 & \lambda \\ 0 & 1 \end{pmatrix} \partial_x \begin{pmatrix} u_0 \\ u_1 \end{pmatrix} \tag{A.16}$$

reduces to two advection equations for $\lambda = 0$ and thus it is well-posed for that value. However, for $\lambda \neq 0$ the system is coupled and the matrix A cannot be diagonalized. The evolution of a Fourier mode

$$u_0 = \left(\mathrm{i}k\lambda\tilde{u}_k^{(1)}t + \tilde{u}_k^{(0)}\right)\exp\left(\mathrm{i}k(t+x)\right) \tag{A.17}$$

$$u_1 = \tilde{u}_k^{(1)}\exp\left(\mathrm{i}k(t+x)\right) \tag{A.18}$$

and grows in time in a frequency-dependent way, hence the IVP is ill-posed.

A.3 Hyperbolicity

Given the hyperbolic equation Eq. (A.4) and identified a direction n^i, hyperbolicity is characterized according to the *principal symbol*

$$P(n^i) := M^i n_i \quad \text{(Principal symbol)} \tag{A.19}$$

The system in Eq. (A.4) is called

Definition A.3.1. Weakly hyperbolic *iff P has real eigenvalues for every n^i but does not have a complete set of eigenvectors.*

Definition A.3.2. Strongly hyperbolic *iff P has real eigenvalues and a complete set of eigenvectors for every n^i.*

The principle symbol of a a strongly hyperbolic system satisfies $PR = \Lambda R$, where R is the right eigenvectors matrix and $\Lambda = \mathrm{diag}\lambda_A$. For a strongly hyperbolic system one can define the *symmetrizer*

$$H := (R^{-1})^\dagger R^{-1} \quad \text{(Symmetrizer)} \ , \tag{A.20}$$

with properties

(i) Symmetric (Hermitian) and positive definite
(ii) HP is also symmetric: $HP = (R^{-1})^\dagger R^{-1}P = (R^{-1})^\dagger \Lambda R^{-1} = ((R^{-1})^\dagger \Lambda R^{-1})^\dagger$.
(iii) $HP = P^\dagger H^\dagger = P^\dagger H$
(iv) Not unique as R and λ depend on normalization.

The system in Eq. (A.4) is called

Definition A.3.3. Symmetric hyperbolic *iff H is independent on n^i (all A^i are symmetric).*

Note that

$$\text{Symmetric hyperbolic} \ \subset \ \text{Strongly hyperbolic} \ \subset \ \text{Weakly hyperbolic} \ .$$

Example A.3.1. *The ADMY scheme is weakly hyperbolic with prescribed shift and for a large class of singularity avoiding slicing conditions, e.g. (Alcubierre, 2008). The BSSN scheme is strongly hyperbolic under the same conditions of ADMY and also for Γ-driver shift (except for certain values of the shift eq parameters), (Sarbach et al., 2002; Gundlach and Martin-Garcia, 2006). The generalized harmonic scheme is symmetric hyperbolic, e.g. (Choquet-Bruhat and Geroch, 1969; Friedrich, 1983). The GRHD equations in conservative form are strongly hyperbolic (Banyuls et al., 1997).*

A.4 Well-posedness of symmetric hyperbolic systems

For symmetric and strongly hyperbolic formulations it is possible to construct an *energy norm* from which one proves the well-posedness of the IVP.

The inner product and the norm are defined as

$$\langle u, v\rangle := u^\dagger H v \ , \quad ||u||^2 := \langle u, u\rangle = u^\dagger H u \ . \tag{A.21}$$

Consider a Fourier mode solution $u(t,x) = \tilde{u}_k(t)\exp(\mathrm{i}kx\cdot n)$; from Eq. (A.4) one gets

$$\partial_t u = \mathrm{e}^{\mathrm{i}kx\cdot n}\partial_t \tilde{u}_k \tag{A.22a}$$

$$= A^j\partial_j = A^j(\tilde{u}_k\partial_j \mathrm{e}^{\mathrm{i}kx\cdot n} = \tilde{u}_k(\mathrm{i}k)A^j n_j)\mathrm{e}^{\mathrm{i}kx\cdot n} = (\mathrm{i}k)P\tilde{u}_k\mathrm{e}^{\mathrm{i}kx\cdot n} \ . \tag{A.22b}$$

Hence, the evolution of the norm is conserved independently on the initial data:

$$\partial_t||u||^2 = \partial_t(u^\dagger H u) = \partial_t(u^\dagger)Hu + u^\dagger H\partial_t u = \mathrm{i}k\tilde{u}_k^\dagger P^\dagger H\tilde{u}_k - \mathrm{i}k\tilde{u}_k^\dagger HP\tilde{u}_k = \mathrm{i}k\tilde{u}_k^\dagger(P^\dagger H - HP)\tilde{u}_k = 0 \ . \tag{A.23}$$

The energy norm and symmetrizer can be constructed for both symmetric and strongly PDEs; the difference is that for strongly hyperbolic system P and H will in general depend on the particular direction one chooses. We have thus proven:

Theorem A.4.1. *The IVP for symmetric and strongly hyperbolic PDE is well-posed.*

Remark A.4.1. *The above discussion assume A^i is a costant coefficient matrix. In the general case $A^i(u)$ and one needs to linearize the equations around a given solution u_0. As a consequence, well-posedeness can be proven only in a local sense.*

The problem of interest for numerical application is the initial-boundary-value problem (IBVP) in which data on the spatial boundary $\partial\Omega$ are also specified. In the IVBP case, boundary data must be included into the norm and the analysis is more complex and different notion of well-posedness apply. Roughly, the result of the theorem still holds but building well-posed boundary conditions for symmetric hyperbolic system is technically easier than strongly hyperbolic ones.

Bibliography

Alcubierre, M. (2008). *Introduction to 3+1 Numerical Relativity*. Oxford University Press.

Alcubierre, M. and Brügmann, B. (2001). Simple excision of a black hole in 3+1 numerical relativity. *Phys. Rev.*, D63:104006.

Alcubierre, M., Brügmann, B., Diener, P., Koppitz, M., Pollney, D., et al. (2003). Gauge conditions for long term numerical black hole evolutions without excision. *Phys.Rev.*, D67:084023.

Alcubierre, M. et al. (2000). Towards a stable numerical evolution of strongly gravitating systems in general relativity: The conformal treatments. *Phys. Rev.*, D62:044034.

Alvi, K. (2002). First order symmetrizable hyperbolic formulations of Einstein's equations including lapse and shift as dynamical fields. *Class. Quant. Grav.*, 19:5153–5162.

Anile, A. M. (1990). *Relativistic Fluids and Magneto-fluids*.

Anninos, P., Camarda, K., Masso, J., Seidel, E., Suen, W.-M., and Towns, J. (1995). Three-dimensional numerical relativity: The Evolution of black holes. *Phys. Rev.*, D52:2059–2082.

Arnowitt, R., Deser, S., and Misner, C. W. (1960). Energy and the Criteria for Radiation in General Relativity. *Phys. Rev.*, 118:1100–1104.

Arnowitt, R. L., Deser, S., and Misner, C. W. (1959). Dynamical Structure and Definition of Energy in General Relativity. *Phys. Rev.*, 116:1322–1330.

Ashtekar, A. and Hansen, R. O. (1978). A unified treatment of null and spatial infinity in general relativity. I - Universal structure, asymptotic symmetries, and conserved quantities at spatial infinity. *J. Math. Phys.*, 19:1542–1566.

Baer, C., Ginoux, N., and Pfaeffle, F. (2008). Wave Equations on Lorentzian Manifolds and Quantization. *arXiv e-prints*, page arXiv:0806.1036.

Baker, J. G., Centrella, J., Choi, D.-I., Koppitz, M., and van Meter, J. (2006). Gravitational wave extraction from an inspiraling configuration of merging black holes. *Phys. Rev. Lett.*, 96:111102.

Balakrishna, J., Daues, G., Seidel, E., Suen, W.-m., Tobias, M., and Wang, E. (1996). Coordinate conditions and their implementation in 3-D numerical relativity. *Class. Quant. Grav.*, 13:L135–L142.

Banyuls, F., Font, J. A., Ibanez, J. M. A., Marti, J. M. A., and Miralles, J. A. (1997). Numerical 3+1 General Relativistic Hydrodynamics: A Local Characteristic Approach. *Astrophys. J.*, 476:221.

Bartnik, R. and Isenberg, J. (2002). The Constraint equations. In *50 Years of the Cauchy Problem in General Relativity: Summer School on Mathematical Relativity and Global Properties of Solutions of Einstein's Equations Cargese, Corsica, France, 29 July - August 10 2002*.

Baumgarte, T. W., Hughes, S. A., and Shapiro, S. L. (1999). Evolving Einstein's field equations with matter: The 'hydro without hydro' test. *Phys. Rev.*, D60:087501.

Baumgarte, T. W., Murchadha, N. O., and Pfeiffer, H. P. (2007). The Einstein constraints: Uniqueness and non-uniqueness in the conformal thin sandwich approach. *Phys. Rev.*, D75:044009.

Baumgarte, T. W. and Shapiro, S. L. (1999). On the numerical integration of Einstein's field equations. *Phys. Rev.*, D59:024007.

Beig, R. and O'Murchadha, N. (1998). Late time behavior of the maximal slicing of the Schwarzschild black hole. *Phys. Rev.*, D57:4728–4737.

Bernuzzi, S. and Hilditch, D. (2010). Constraint violation in free evolution schemes: comparing BSSNOK with a conformal decomposition of Z4. *Phys. Rev.*, D81:084003.

Bona, C., Ledvinka, T., Palenzuela, C., and Zacek, M. (2003). General-covariant evolution formalism for Numerical Relativity. *Phys. Rev.*, D67:104005.

Bona, C. and Masso, J. (1988). HARMONIC SYNCHRONIZATIONS OF SPACE-TIME. *Phys. Rev.*, D38:2419–2422.

Bona, C., Massó, J., Stela, J., and Seidel, E. (1996). A class of hyperbolic gauge conditions. In Jantzen, R. T., Keiser, G. M., and Ruffini, R., editors, *The Seventh Marcel Grossmann Meeting: On Recent Developments in Theoretical and Experimental General Relativity, Gravitation, and Relativistic Field Theories*, Singapore. World Scientific.

Bonazzola, S., Gourgoulhon, E., Grandclement, P., and Novak, J. (2004). A constrained scheme for Einstein equations based on Dirac gauge and spherical coordinates. *Phys. Rev.*, D70:104007.

Bowen, J. M. and York, Jr., J. W. (1980). Time asymmetric initial data for black holes and black hole collisions. *Phys. Rev.*, D21:2047–2056.

Brandt, S. and Brügmann, B. (1997). A Simple construction of initial data for multiple black holes. *Phys. Rev. Lett.*, 78:3606–3609.

Brown, J. D. (2008). Puncture Evolution of Schwarzschild Black Holes. *Phys. Rev.*, D77:044018.

Brügmann, B. (1996). Adaptive mesh and geodesically sliced Schwarzschild spacetime in 3+1 dimensions. *Phys. Rev.*, D54:7361–7372.

Campanelli, M., Lousto, C. O., Marronetti, P., and Zlochower, Y. (2006). Accurate Evolutions of Orbiting Black-Hole Binaries Without Excision. *Phys. Rev. Lett.*, 96:111101.

Cantor, M. (1977). The Existence of Nontrivial Asymptotically Flat Initial Data for Vacuum Space-Times. *Commun. Math. Phys.*, 57:83–96.

Cantor, M. (1979). Some problems of global analysis on asymptotically simple manifolds. *Compositio Mathematica*, 38(1):3–35.

Choquet-Bruhat, Y. and Geroch, R. P. (1969). Global aspects of the Cauchy problem in general relativity. *Commun. Math. Phys.*, 14:329–335.

Choquet-Bruhat, Y. and York, Jr., J. W. (1980). The Cauchy problem. In *Measurement of the Spin Dependent Total Cross Section $\Delta\sigma_L$ in pp Collisions Between 200 and 600 MeV*, pages 99–172.

Choquet-Bruhat, Y. and York, Jr., J. W. (1996). Well posed reduced systems for the Einstein equations.

Cook, G. B. (1991). Initial data for axisymmetric black-hole collisions. *Phys. Rev.*, D44(10):2983.

Cook, G. B., Choptuik, M. W., Dubal, M. R., Klasky, S., Matzner, R. A., and Oliveira, S. R. (1993). Three-dimensional initial data for the collision of two black holes. *Phys. Rev.*, D47:1471–1490.

Cook, G. B. and Scheel, M. A. (1997). Well behaved harmonic time slices of a charged, rotating, boosted black hole. *Phys. Rev.*, D56:4775–4781.

Dedner, A., Kemm, F., Kröner, D., Munz, C.-D., Schnitzer, T., and Wesenberg, M. (2002). Hyperbolic Divergence Cleaning for the MHD Equations. *Journal of Computational Physics*, 175:645–673.

Del Zanna, L., Zanotti, O., Bucciantini, N., and Londrillo, P. (2007). ECHO: an Eulerian Conservative High Order scheme for general relativistic magnetohydrodynamics and magnetodynamics. *Astron. Astrophys.*, 473:11–30.

Dietrich, T. and Bernuzzi, S. (2015). Simulations of rotating neutron star collapse with the puncture gauge: end state and gravitational waveforms. *Phys.Rev.*, D91(4):044039.

Dimmelmeier, H., Font, J. A., and Müller, E. (2002). Relativistic simulations of rotational core collapse. I. Methods, initial models, and code tests. *Astron. Astrophys.*, 388:917–935.

Evans, L. C. (1998). *Partial Differential Equation*. Graduate Studies in Mathematics. American Mathematical Society, Providence, Rhode Island, 2nd edition.

Font, J. A. (2007). Numerical hydrodynamics and magnetohydrodynamics in general relativity. *Living Rev. Rel.*, 11:7.

Font, J. A., Miller, M. A., Suen, W.-M., and Tobias, M. (2000). Three Dimensional Numerical General Relativistic Hydrodynamics I: Formulations, Methods, and Code Tests. *Phys. Rev.*, D61:044011.

Friedrich, H. (1983). Cauchy problems for the conformal vacuum field equations in general relativity. *Comm. Math. Phys.*, 91:445–472.

Friedrich, H. (1985). On the hyperbolicity of einstein's and other gauge field equations. *Communications in Mathematical Physics*, 100(4):525–543.

Friedrich, H. (1986). On the existence of n-geodesically complete or future complete solutions of Einstein's field equations with smooth asymptotic structure. *Comm. Math. Phys.*, 107:587–609.

Friedrich, H. and Nagy, G. (1999). The initial boundary value problem for Einstein's vacuum field equations. *Comm. Math. Phys.*, 201:619–655.

Frittelli, S. and Reula, O. A. (1996). First order symmetric hyperbolic Einstein equations with arbitrary fixed gauge. *Phys.Rev.Lett.*, 76:4667–4670.

Frittelli, S. and Reula, O. A. (1999). Well posed forms of the (3+1) conformally decomposed Einstein equations. *J.Math.Phys.*, 40:5143–5156.

Garat, A. and Price, R. H. (2000). Nonexistence of conformally flat slices of the Kerr space-time. *Phys. Rev.*, D61:124011.

Garfinkle, D. (2002). Harmonic coordinate method for simulating generic singularities. *Phys.Rev.*, D65:044029.

Geyer, A. and Herold, H. (1995). Slicing the Schwarzschild spacetime: Harmonic versus maximal slicing. *Phys. Rev. D*, 52(10):6182–6185.

Giulini, D. (1999). The Generalized thin sandwich problem and its local solvability. *J. Math. Phys.*, 40:2470–2482.

Gourgoulhon, E. (2006). An introduction to relativistic hydrodynamics. *EAS Publ. Ser.*, 21:43.

Gourgoulhon, E., Grandclement, P., and Bonazzola, S. (2002). Binary black holes in circular orbits. 1. A Global space-time approach. *Phys. Rev.*, D65:044020.

Gundlach, C. and Martin-Garcia, J. M. (2006). Well-posedness of formulations of the Einstein equations with dynamical lapse and shift conditions. *Phys.Rev.*, D74:024016.

Hannam, M., Husa, S., Ohme, F., Brügmann, B., and O'Murchadha, N. (2008). Wormholes and trumpets: The Schwarzschild spacetime for the moving-puncture generation. *Phys.Rev.*, D78:064020.

Hannam, M., Husa, S., Pollney, D., Brügmann, B., and O'Murchadha, N. (2007). Geometry and Regularity of Moving Punctures. *Phys. Rev. Lett.*, 99:241102.

Hannam, M. D., Evans, C. R., Cook, G. B., and Baumgarte, T. W. (2003). Can a combination of the conformal thin sandwich and puncture methods yield binary black hole solutions in quasiequilibrium? *Phys. Rev.*, D68:064003.

Hawking, S. W. and Ellis, G. F. R. (2011). *The Large Scale Structure of Space-Time*. Cambridge Monographs on Mathematical Physics. Cambridge University Press.

Hilditch, D., Bernuzzi, S., Thierfelder, M., Cao, Z., Tichy, W., and Bruegmann, B. (2013). Compact binary evolutions with the Z4c formulation. *Phys. Rev.*, D88:084057.

Hotokezaka, K., Kyutoku, K., and Shibata, M. (2013). Exploring tidal effects of coalescing binary neutron stars in numerical relativity. *Phys.Rev.*, D87(4):044001.

Husa, S., Hannam, M., Gonzalez, J. A., Sperhake, U., and Brügmann, B. (2008). Reducing eccentricity in black-hole binary evolutions with initial parameters from post-Newtonian inspiral. *Phys.Rev.*, D77:044037.

Isenberg, J. (1995). Constant mean curvature solutions of the einstein constraint equations on closed manifolds. *Classical and Quantum Gravity*, 12(9):2249–2274.

Lax, P. and Wendroff, B. (1960). Sistem of conservation law. *Commun. Pure Appl. Math.*, 13:217–237.

Le Tiec, A. (2012). Spacetime Symmetries and Kepler's Third Law. *Class. Quant. Grav.*, 29:217002.

LeVeque, R. J. (2002). *Finite Volume Methods for Hyperbolic Problems*. Cambridge University Press.

Lichnerowicz, A. (1944). L'integration des equations de la gravitation relativiste et le probleme des n corps. *J. Math. Pures Appl.*, 23:37.

Lindblom, L., Matthews, K. D., Rinne, O., and Scheel, M. A. (2008). Gauge Drivers for the Generalized Harmonic Einstein Equations. *Phys.Rev.*, D77:084001.

Marti, J. M., Ibanez, J. M., and Miralles, J. A. (1991). Numerical relativistic hydrodynamics: Local characteristic approach. *Phys. Rev.*, D43:3794–3801.

Marti, J. M. and Müller, E. (1999). Numerical hydrodynamics in special relativity. *Living Rev. Rel.*, 2:3.

Nagy, G., Ortiz, O. E., and Reula, O. A. (2004). Strongly hyperbolic second order Einstein's evolution equations. *Phys. Rev.*, D70:044012.

Nakamura, T., Oohara, K., and Kojima, Y. (1987). General Relativistic Collapse to Black Holes and Gravitational Waves from Black Holes. *Prog. Theor. Phys. Suppl.*, 90:1–218.

Oechslin, R., Rosswog, S., and Thielemann, F. K. (2002). Conformally Flat Smoothed Particle Hydrodynamics: Application to Neutron Star Mergers. *Phys. Rev.*, D65:103005.

Penrose, R. (1965). Gravitational collapse and space-time singularities. *Phys. Rev. Lett.*, 14:57–59.

Penrose, R. (1969). Gravitational collapse: The role of general relativity. *Riv. Nuovo Cim.*, 1:252–276. [Gen. Rel. Grav.34,1141(2002)].

Pfeiffer, H. P. and York, Jr., J. W. (2003). Extrinsic curvature and the Einstein constraints. *Phys. Rev.*, D67:044022.

Pfeiffer, H. P. and York, Jr., J. W. (2005). Uniqueness and non-uniqueness in the Einstein constraints. *Phys. Rev. Lett.*, 95:091101.

Pretorius, F. (2005). Evolution of binary black hole spacetimes. *Phys. Rev. Lett.*, 95:121101.

Reimann, B. and Bruegmann, B. (2004). Maximal slicing for puncture evolutions of Schwarzschild and Reissner-Nordstrom black holes. *Phys. Rev.*, D69:044006.

Reisswig, C., Ott, C., Abdikamalov, E., Haas, R., Mösta, P., et al. (2013). Formation and Coalescence of Cosmological Supermassive Black Hole Binaries in Supermassive Star Collapse. *Phys.Rev.Lett.*, 111:151101.

Sarbach, O., Calabrese, G., Pullin, J., and Tiglio, M. (2002). Hyperbolicity of the BSSN system of Einstein evolution equations. *Phys. Rev.*, D66:064002.

Schoen, R. and Yau, S.-T. (1979). Positivity of the Total Mass of a General Space-Time. *Phys. Rev. Lett.*, 43:1457–1459.

Schon, R. and Yau, S.-T. (1981). Proof of the positive mass theorem. 2. *Commun. Math. Phys.*, 79:231–260.

Shibata, M. (1999). Fully general relativistic simulation of coalescing binary neutron stars: Preparatory tests. *Phys. Rev.*, D60:104052.

Shibata, M. and Nakamura, T. (1995). Evolution of three-dimensional gravitational waves: Harmonic slicing case. *Phys. Rev.*, D52:5428–5444.

Shibata, M. and Uryu, K. (2000). Simulation of merging binary neutron stars in full general relativity: $\Gamma = 2$ case. *Phys. Rev.*, D61:064001.

Smarr, L. and York, James W., J. (1978a). Kinematical conditions in the construction of space-time. *Phys.Rev.*, D17:2529–2551.

Smarr, L. and York, Jr., J. W. (1978b). Radiation gauge in general relativity. *Phys. Rev.*, D17(8):1945–1956.

Thierfelder, M., Bernuzzi, S., Hilditch, D., Brügmann, B., and Rezzolla, L. (2011). The trumpet solution from spherical gravitational collapse with puncture gauges. *Phys.Rev.*, D83:064022.

Toro, E. F. (1999). *Riemann Solvers and Numerical Methods for Fluid Dynamics*. Springer-Verlag, 2$^{\text{nd}}$ edition.

van Meter, J. R., Baker, J. G., Koppitz, M., and Choi, D.-I. (2006). How to move a black hole without excision: gauge conditions for the numerical evolution of a moving puncture. *Phys. Rev.*, D73:124011.

Wilson, J., Mathews, G., and Marronetti, P. (1996). Relativistic numerical model for close neutron star binaries. *Phys.Rev.*, D54:1317–1331.

Winicour, J. (2009). Characteristic Evolution and Matching. *Living Rev. Rel.*, 12:3.

Witten, E. (1981). A Simple Proof of the Positive Energy Theorem. *Commun. Math. Phys.*, 80:381.

York, James W., J. (1971). Gravitational degrees of freedom and the initial-value problem. *Phys.Rev.Lett.*, 26:1656–1658.

York, James W., J. (1972). Role of conformal three geometry in the dynamics of gravitation. *Phys.Rev.Lett.*, 28:1082–1085.

York, James W., J. (1999). Conformal 'thin sandwich' data for the initial-value problem. *Phys.Rev.Lett.*, 82:1350–1353.

York, Jr., J. W. (1973). Conformatlly invariant orthogonal decomposition of symmetric tensors on Riemannian manifolds and the initial value problem of general relativity. *J. Math. Phys.*, 14:456–464.

Zenginoğlu, A. (2008). Hyperboloidal foliations and scri-fixing. *Class. Quant. Grav.*, 25:145002.